DEVELOPMENT OF ALUMINUM METAL MATRIX COMPOSITES REINFORCED WITH MICRO/ NANO REINFORCEMENTS BY FRICTION STIR PROCESSING

Thesis Submitted for the Award of the Degree of Ph.D. in Mechanical Engineering

DOCTOR OF PHILOSOPHY
in
MECHANICAL ENGINEERING

By

GAGANDEEP SINGH RAHEJA

(41500115)

<table>
<tr><td>Supervised by</td><td>Co-Supervised by</td></tr>
<tr><td>Dr. Chander Prakash</td><td>Dr. Shankar Sehgal</td></tr>
<tr><td>Professor and Associate Dean</td><td>Associate Professor in Mech. Engg.</td></tr>
<tr><td>School of Mechanical Engineering and</td><td>UIET, Panjab University</td></tr>
<tr><td>Division of Research and Development, LPU</td><td>Chandigarh, India</td></tr>
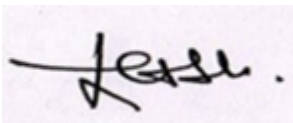</table>

LOVELY PROFESSIONAL UNIVERSITY

PUNJAB

2023

DECLARATION/ CERTIFICATE

I declare that the thesis entitled "DEVELOPMENT OF ALUMINUM METAL MATRIX COMPOSITES REINFORCED WITH MICRO/ NANO REINFORCEMENTS BY FRICTION STIR PROCESSING" has been prepared by me under the guidance of **Dr. Chander Prakash**, Associate Dean & Professor of School of Mechanical Engineering, Lovely Professional University and **Dr Shankar Sehgal** Associate Professor (Dept. of Mechanical Engineering, UIET) P.U Chandigarh**.** No part of this thesis has formed the basis for the award of any degree or fellowship previously.

Gagandeep Singh Raheja
School of Mechanical Engineering**,**
Lovely Professional University
Jalandhar-Delhi G.T. Road (NH-1), Phagwara
Punjab, (India) - 144411
DATE : 22-11-2023

Dr. Chander Prakash   **Dr. Shankar Sehgal**

Signature of Guide   **Signature of Co-Guide**

22-11-2023 & 21503   **22-11-2023**

CERTIFICATE OF PUBLICATION OF PAPERS FOR PH.D.

This is to certify that Mr./Ms. GAGANDEEP SINGH RAHEJA _ pursuing Ph.D. (**Part Time**) programme in Department of Mechanical Engineering_ with Registration Number 41500115_ under the Guidance of **Dr. Chander Prakash_** has the following Publications / Letter of Acceptance in the Referred Journals / Conferences mentioned thereby fulfilling the minimum programme requirements as per the UGC.

Sno.	Title of paper with author names	Name of journal / conference	Published date	Issn no/ vol no, issue no	Indexing in Scopus/ Web of Science/UGC-CARE list (*please mention*)
1.	Processing and characterization of Al5086-Gr-SiC hybrid surface composite using friction stir technique	materialstoday: PROCEEDINGS	4 June 2020	Volume 28, Part 3, 2020, Pages 1350-1354	Scopus
2.	Development of hybrid Gr/SiC reinforced AMCs through friction stir processing	materialstoday: PROCEEDINGS	1 July 2020	Volume 50, Part 5, 2022, Pages 539-545	Scopus
3.	Experimental investigation on the synthesis of Al5086-GRN-ηSiC hybrid Surface composite using additive	Indian Journal of Engineering and Materials Sciences (IJEMS)	Accepted	ISSN-0971-4588	Scopus (https://www.scimagojr.com/journalsearch)

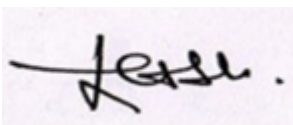|					
	powder fed friction stir processing				
4.	Development of Al5086-GRN-ηSiC hybrid Surface composite using additive powder fed friction stir processing	Metal Science and Heat Treatment	Accepted	ISSN 0026-0673	Scopus (http://mitom.folium.ru/index.php/mitom)
5.	A novel method for maintenance of shafts with solid state stirring.	Patent	Published	Publication no.-36/2020 Application number-202011004574	http://ipindia.nic.in/index.htm

22-11-2023

41500115(reg no.), email- gagandeep.raheja@gmail.com

Signature of Candidate with Date, Registration No, Email ID

Dr. Chander Prakash

Signature of Guide

Date (22/11/2023) & UID

21503

Dr. Shankar Sehgal

Signature of Co-Guide

Date - (22/11/2023)

ABSTRACT

Aluminum (Al) has been widely employed in automotive, aerospace, and defense technologies throughout the previous decade. However, because of inferior mechanical qualities like hardness, wear resistance, and tensile strength, Aluminum (Al) wears out and fails quickly, limiting its value in industrial applications. Several Aluminum based alloys and composites have been made employing a variety of production techniques such as casting, powder metallurgy, and friction stir processing. Among these approaches, friction stir processing has been identified as a promising method for developing hybrid metal matrix composites. A hybrid metal matrix composite is a material composed of three or more physically and chemically diverse components that have been treated without compromising the attributes of any constituent portion. The research was made to create a metal matrix composite using the substrate Al5086 and particle reinforcements Graphene and Silicon Carbide. The FSP, which consists of the Al5086 substrate and the graphene, silicon carbide particulate mixture, has been successfully used to form an aluminum metal matrix composite without melting, resulting in uniform distribution of particulate and impingement of required mechanical, microstructural, and chemical properties for the area of interest. The influence of FSP process parameters such rotating speed, traverse speed, and tool geometry on the microstructure and mechanical characteristics (surface hardness, elastic modulus and wear) has been investigated.

Herein, aluminum (Al5086 alloy) based composite has been developed using graphene (GRN) and nano-silicon Carbide (η_{SiC}) reinforcement via friction stir processing (FSP) technique. The effect of FSP process parameters such as tool rotational speed (RS), welding speed (WS) and plunge depth (PD) has been analyzed on external as well as internal defect formation, microstructure, morphology, and mechanical properties of as-synthesized Al5086-GRN-ηSiC hybrid metal matrix composite. The internal defect formation, microstructure, morphology, and elemental composition was investigated by field emission scanning electron microscopy (FE-SEM) coupled with Energy Dispersive X-Ray Spectroscopy (EDS). Microscopic analysis was conducted to

scientifically ascertain the grain size, crystal structure and surface morphology of FSP zone. The mechanical properties such as hardness and elastic modulus were evaluated using nano-indentation and micro-hardness technique. The microstructure and morphological examination revealed that the grain size of Al-matrix was refined from 30 µm to ~6 µm and reinforcements (Gr/nano-SiC) were uniformly distributed in the matrix, which is expected to improve the mechanical properties. The highest hardness of $198HV_{0.3}$ and tensile strength 209 ± 5 MPa (385 ± 5 MPa as an exception with APF FSP) was obtained with trapezoidal shape tool pin geometry, 1800 rpm and 40mm/min traverse speed.

The current study attempted to produce graphene (GRN) and silicon carbide (SiC) reinforced aluminum (Al-5086) metal matrix composite (MMC) utilizing friction stir processes. The influence of FSP process parameters on the microstructure and mechanical characteristics, such as rotating speed, traverse speed, and plunge depth tool shape, has been investigated. The trials were designed using Taguchi's approach and the L27 orthogonal array. The produced composite's microstructure, elemental, and phase composition were investigated using field-emission scanning electron microscopy, energy dispersive spectroscopy, and X-ray diffraction techniques, respectively. The nano-indentation method and tensile testing were used to determine mechanical parameters like hardness and tensile strength. The maximal micro-hardness, tensile strength and elastic modulus of the FSP-processed composite were discovered to be around 198 HV, 209 MPa, 172 GPa.

ACKNOWLEDGEMENT

TABLE OF CONTENTS

Contents	Page No.

LIST OF FIGURES

LIST OF TABLES

<div align="right">**CHAPTER-1**</div>

INTRODUCTION

1.1 History of composite materials

Composite materials have been utilised throughout history, but the contemporary age of composite materials began with the discovery of synthetic polymers in the twentieth century. Bakelite, the first synthetic thermosetting material, was created in the early 1900s. Bakelite was utilised for many different things, including electrical insulators and automobile components. With the emergence of fibreglass reinforced plastics (FRP) and other composite materials during World War II, composites were widely employed in military aircraft. These materials were further developed for commercial purposes after the war. Carbon fibre composites, which gave even more strength and rigidity than fibreglass composites, were launched in the 1960s. Composite materials have since grown in use in a variety of industries, including aerospace, automotive, construction, sports equipment, and many more. Designers and engineers may employ composites to manufacture materials with specified attributes like as strength, stiffness, and durability while simultaneously lowering weight and boosting efficiency. Composite materials are still evolving today, with new materials and manufacturing processes being researched to generate more stronger, lighter, and more durable materials. Composites are likely to become more popular in the future years as sectors strive to increase performance and efficiency while lowering prices and environmental impact [3].

Composite materials have been used for thousands of years, with early civilizations using natural composites like mud bricks reinforced with straw or animal hair. The research and use of contemporary composite materials, on the other hand, began in the twentieth century. Here is a brief history of composite materials [4].

Early Composites: Composite materials have been used since early civilizations. For example, the Egyptians reinforced their construction materials with a mix of straw and mud. The Chinese also invented composite bows, which were constructed of layers of wood, bone, and animal glue. Reinforced concrete was invented in the nineteenth century by the French gardener Joseph Monier, who blended concrete with inserted iron meshes or bars to increase its strength. This was an early application of composite materials in building.

Fibre Reinforced Composites: Fibre reinforced composites were invented in the early twentieth century. Bakelite, the first synthetic plastic bonded with wood fibres, was created in 1908 by Leo Hendrik Baekeland. This was the beginning of polymer matrix composites. Due to military necessity, breakthroughs in composite materials accelerated during World War II. The British created high-strength composite materials such as "Hercules" and "Tuffnol" for a variety of uses such as aeroplane components and randoms.

Glass Fibre Reinforced Plastics (GRP): Glass fibre reinforced plastics, generally known as fibreglass, became a popular composite material in the 1940s. Researchers such Games Slayter and W. Brandt Goldsworthy contributed significantly to the development of fibreglass and its use in a variety of sectors.

Carbon Fibre Composites: Carbon fibre composites gained popularity in the 1950s and 1960s. Carbon fibres were initially pricey and were largely utilised in aircraft applications. However, breakthroughs in production processes and cost reductions have resulted in broader acceptance in areas such as sports equipment, automotive, and construction. Advanced composites, such as aramid (e.g., Kevlar) and high-performance carbon fibre composites, became more common in the later part of the twentieth century. These materials have remarkable strength-to-weight ratios, heat resistance, and impact resistance, making them suited for high-performance applications in aerospace, defence, and sports.

Nanocomposites: The discipline of nanotechnology has had an impact on composite materials in recent decades. Nanocomposites include nanoparticles or nanofillers into the matrix material, which results in higher mechanical strength, electrical conductivity, and thermal stability. Composite materials continue to advance and find uses in a variety of industries today, including aerospace, automotive, marine, wind energy, and sports. Ongoing research focuses on the development of sustainable and bio-based composites, the exploration of new reinforcing materials, and the improvement of production methods in order to make composites more cost-effective and ecologically friendly. The desire for stronger, lighter, and more durable materials in a variety of sectors has led to constant developments and discoveries throughout the history of composite materials.

Composite materials are used by both Nature and Man[1] as:

➢ **Nature**

• Structural components of Plants.

- Structural components of Animals.

➢ **Man**

- In 1300 B.C Egyptians and Mesopotamian uses bricks made up of straws.

- In 400 B.C Laminated writing materials made up of the papyrus plant is used.

- In 1200 A.D the first composite bow is invented by Mongols.

1.2 Introduction to composite materials

An excellent material properties like high specific strength, good thermal properties, stiffness, controllable thermal expansion, abrasion resistance and wear control creates a lot of interest among material engineers towards the development of Al based. In contrast with other metal matrix composites, the low cost of aluminum composites based on metal matrix also increase its domain of use [2]. Matrix and a reinforcement combination in a suitable manner leads to the creation of material which gives properties far superior than that of individual material is called as the composite material. In composite material, fibers are the reinforcement material and it mainly imparts strength and stiffness to the matrix. The alignment of fibers in the matrix greatly affects the resulting properties of the composite. Matrix acts as the shielding for the reinforcement, bonds the reinforcement together and protects it from chemical and environmental attack [3].

The choice of composite material for manufacturing of components is mainly because of considerable weight saving at equivalent strength and stiffness. For example, at one fifth of weight, carbon-fiber reinforced composite are more than five times stronger than that of the 1020 grade of steel. Carbon fiber composite has a density nearly twice that of aluminium and more than five times that of steel. As a result, substituting aluminium with carbon fibre in the same dimensions reduces weight by 42%. When steel is replaced with carbon fiber, the weight is reduced by a factor of five. [4].

As like all other engineering materials composite materials after fabrication also have some advantages as well as disadvantages, which should be properly take care at the initial stage. Composite material is not suitable for each and every application but we can alter the direction of reinforcement in the parent matrix in order to meet the particular demand. For example, if you want to make the composite material which is capable to withstand

fire, then we should focus on the material of matrix which has fire resistance properties. Other Mechanical properties like strength and stiffness can also be adjusted as per the requirements in the developing stage of composite. In order to meet the external environment conditions, many types of paints as well as coatings are available which will be selected as per the need of the particular property[4].

Composite materials made up of metals found application in many areas day-by-day. These are mix of matrix and solid as well as hard fortifying stage. These materials are fabricated by the traditional methods and preparing of metals [5]. Materials such as high carbide content of steel, or cast iron in addition of graphite or and in addition of tungsten carbides, comprising of carbides and binders of metallic compound i.e., cobalt, additionally have a place with this gathering of composite materials. For some specialists the term metal framework composites (MMCs) is frequently compared with the term light metal grid composites (LMCs). Considerable advance in the modification of light metal framework composites has been accomplished in late decades, with the goal that they could be brought into the most essential applications [6]. In building, particularly in the car business, LMCs have been utilized industrially in fiber fortified cylinders and aluminum wrench cases with reinforced barrel surfaces and in addition molecule reinforced brake circles. They have broad enthusiasm from guard, aviation and car businesses and they have turned out to be exceptionally encouraging materials for auxiliary applications as well [7].

For applications of modern development and also in are of material science, these composite materials of metal matrix have unlimited applications. As per the need of application these materials can be customized for both in design as well as for mechanical properties requirement. This technology is capable to compete with other modern technologies for customization of materials like powder metallurgy. These composite materials are only successful when the relationship between the cost of fabrication and performance is justified. These materials are very useful when there is restriction are we can say compulsion of particular properties or profile for the components [8].

Accordingly, the likelihood of joining different material frameworks such as metal – ceramic – non-metal) open door for boundless variety. Properties of the new material fabricated depends upon the properties of the individual materials. Figure 1.1 (Pg. 7)

demonstrates the assignment of the materials made with composites into gatherings of different sorts of materials. The support of metals can have a wide range of objectives [8, 9].

- Due to the possibility of light weight reinforcement in the matrix of metal, it is capable for the application where strength to weight ratio is very important. The main objectives for the development of the light metal composite are as:

- Lightweight: The fundamental goal of producing light metal composites is to minimize material weight while preserving strength and durability. This is especially essential in areas where weight reduction is vital for fuel economy and performance, such as aircraft, automotive, and transportation.

- Light metal composites must be strong and rigid enough to handle the loads and stresses that they will face in their intended use. To obtain the necessary qualities, the metal matrix and reinforcing materials must be carefully selected, as well as the production process optimized.

- In order to keep their qualities at high temperatures, light metal composites must be thermally stable. This is especially true in situations where the material will be subjected to high temperatures, such as engines or exhaust systems.

- Light metal composites must be inexpensive to produce and utilise. This necessitates careful material and production process selection in order to keep prices low while preserving desirable qualities.

- Overall, the desire to increase the performance, efficiency, and sustainability of many industrial applications is driving the development of light metal composites.

Resistance to corrosion: Many light metals, such as aluminum and magnesium, are prone to corrosion. As a result, it is critical to produce corrosion-resistant composites, particularly in hostile settings. In the conclusion part we can say that due to high strength to weight ratio and capable to Optimization techniques, composite materials open up unlimited application for future technologies [10].

1.3 Concept of Composite material

In modern-day applications, reinforcement of particles or Fibers in the other material matrix are the best example for the composite materials which finds its place in mostly structural parts. When the different layers of materials are fabricated to perform specific application, these are called as the Laminates composite. As we know that reinforcements in a material take majority of the load in order to serve the intended purpose. To encourage definition, the complement is frequently moved to the levels at which separation occur as macroscopic or microscopic. On the basis of matrix composites, the matrix fills two foremost needs viz., restricting the support stages set up and misshaping to appropriate the worries among the constituent fortification materials under an applied load. For successful fabrication of composite certain parameters should be accomplished like capable for variations in temperature, sensitive to moisture, electric resistor or conductor etc. Some materials which are of inorganic nature like polymers and metals offers great advantage and applications to be as matrix materials for the structural composites, with great rate of success. With the application of load whether tensile or compressive, these type of materials remain elastic until ultimate point and failure point showed considerable decrease in rate of strain [11].

Contact between the matrix and reinforcement is called as the interface. Wherever the interface exists, it should be between each side of the adjoining component. A few composites give interphases when surfaces divergent constituents cooperate with each other. Decision of creation technique relies on upon framework properties and the impact of lattice on properties of fortifications. One of the prime contemplations in the choice and creation of composites is that the constituents ought to be inert and of chemically non-reactive nature.

1.3.1   Composite material classification

The classification of composite material can be characterized at two levels:

➢ On the basis of Matrix i.e. at the first level, composites can be classified as Composites with matrix as a ceramic material i.e. CMCs, Composites with matrix as a material i.e. MMCs and Organic Matrix Composites i.e. is OMCs. OMCs further includes carbon matrix composites i.e. CMCs or carbon-carbon composite and Polymer Matrix Composites i.e. PMCs.

➢ On the basis of reinforcement i.e. at second level, Composites with fiber reinforcement, laminar type of composites and composites with particulate as a reinforcement. Composites

where fiber as a reinforcing material is used is further classified as Continuous or discontinuous fibers[12].

1.3.2 Group classification of Matrix Composite materials:

Matrix composites are materials that consist of a reinforcement phase embedded within a matrix phase. The matrix acts as a binder, holding the reinforcement together and providing mechanical support, while the reinforcement enhances the material's strength and other properties. Depending on the nature of the matrix and reinforcement materials, there are several types of matrix composites. Here are some common ones:

Polymer Matrix Composites (PMCs): In PMCs, the matrix is a polymer, typically a thermoset (e.g., epoxy) or a thermoplastic (e.g., polyimide). The reinforcement can be fibers, such as glass, carbon, or aramid fibers. These composites are lightweight, corrosion-resistant, and widely used in aerospace, automotive, and sports industries.

Metal Matrix Composites (MMCs): MMCs employ a metal matrix, such as aluminum, titanium, or magnesium, with reinforcement often in the form of ceramic particles or fibers. These composites offer excellent strength, thermal conductivity, and wear resistance, making them suitable for applications in automotive, aerospace, and electronic packaging.

Ceramic Matrix Composites (CMCs): CMCs use a ceramic matrix (e.g., silicon carbide, alumina) combined with ceramic fibers. They possess high-temperature capabilities, thermal shock resistance, and are utilized in aerospace propulsion systems, gas turbines, and nuclear applications.

Carbon-Carbon Composites (C/C): These composites feature a carbon matrix with carbon fibers as reinforcement. C/C composites exhibit exceptional thermal stability, high strength, and low thermal expansion, making them ideal for aerospace components and high-temperature applications.

Glass-Ceramic Matrix Composites: Glass-ceramic matrices, reinforced with ceramic fibers, offer good thermal insulation, mechanical strength, and chemical resistance. They are used in some specialized engineering applications.

Hybrid Composites: Hybrid composites combine two or more types of reinforcements or matrices to leverage the unique properties of each component. For example, carbon-glass hybrid composites may be used to achieve a balance between strength and cost-effectiveness.

Nanocomposites: Nanocomposites incorporate nanoparticles (e.g., carbon nanotubes, graphene) into a matrix to enhance specific properties, such as mechanical strength, electrical conductivity, or barrier properties.

These various types of matrix composites provide a wide range of properties and can be tailored for specific applications based on the choice of materials, manufacturing techniques, and design considerations.
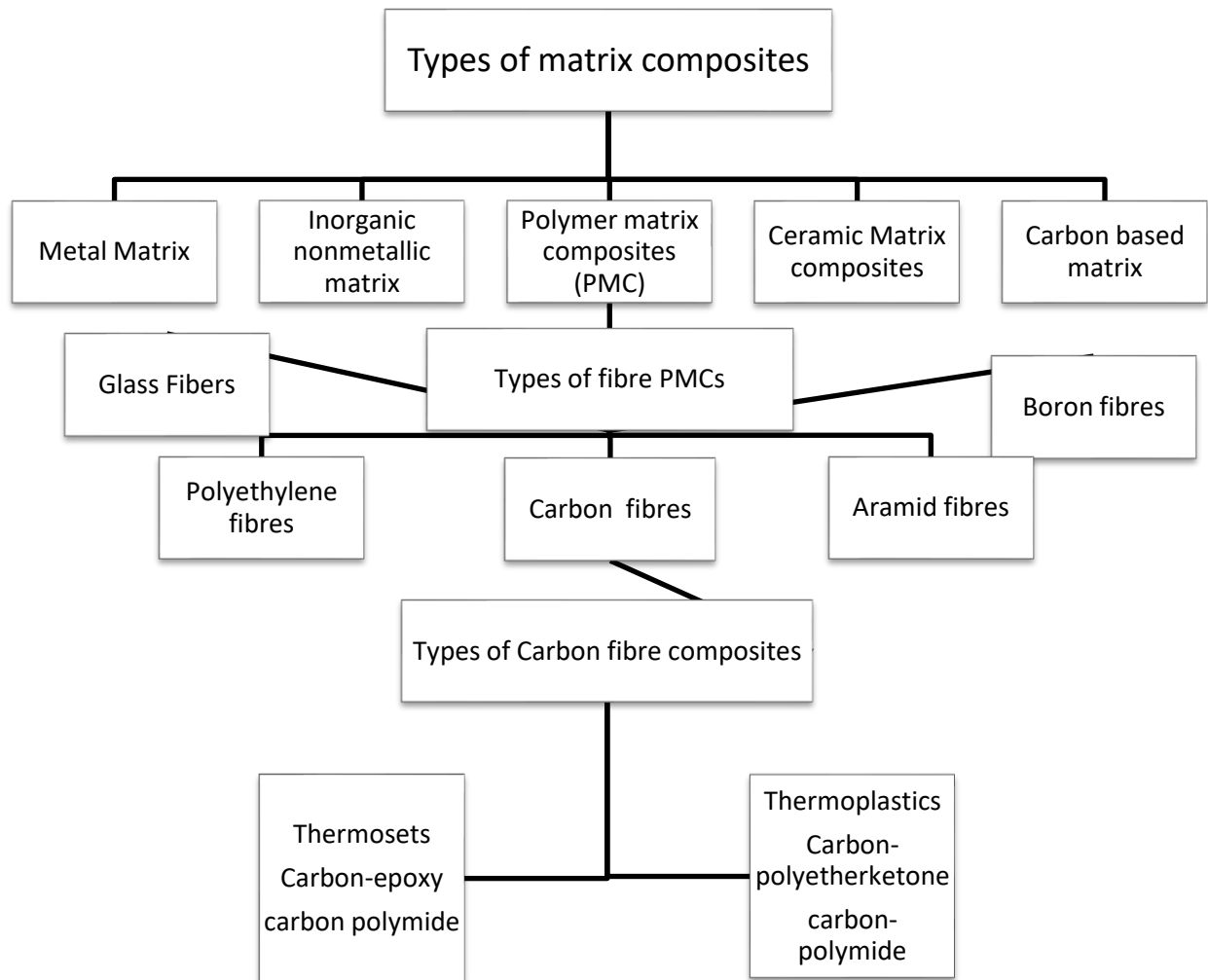
Figure 1.1: Matrix Composite materials classification based on the group of materials [13].

1.4 Classification of Matrices

Composites are materials composed of two or more distinct constituents, each with different physical or chemical properties. When combined, these constituents work together synergistically to create a material with improved or unique characteristics. There

are several types of composites based on the nature of their constituents. Here are some common types:

Ceramic Matrix Composites (CMCs): These composites have a ceramic matrix, typically reinforced with ceramic fibers. CMCs are designed for high-temperature applications due to their excellent thermal and chemical resistance.

Polymer Matrix Composites (PMCs): As mentioned earlier, these composites use a polymer matrix, and they can include fiber-reinforced, particle-reinforced, or laminate composites. PMCs are lightweight and commonly used in various industries.

Metal Matrix Composites (MMCs): In MMCs, a metal matrix is reinforced with ceramic or metallic particles or fibers. They offer high specific strength and stiffness and find applications in the aerospace and automotive sectors.
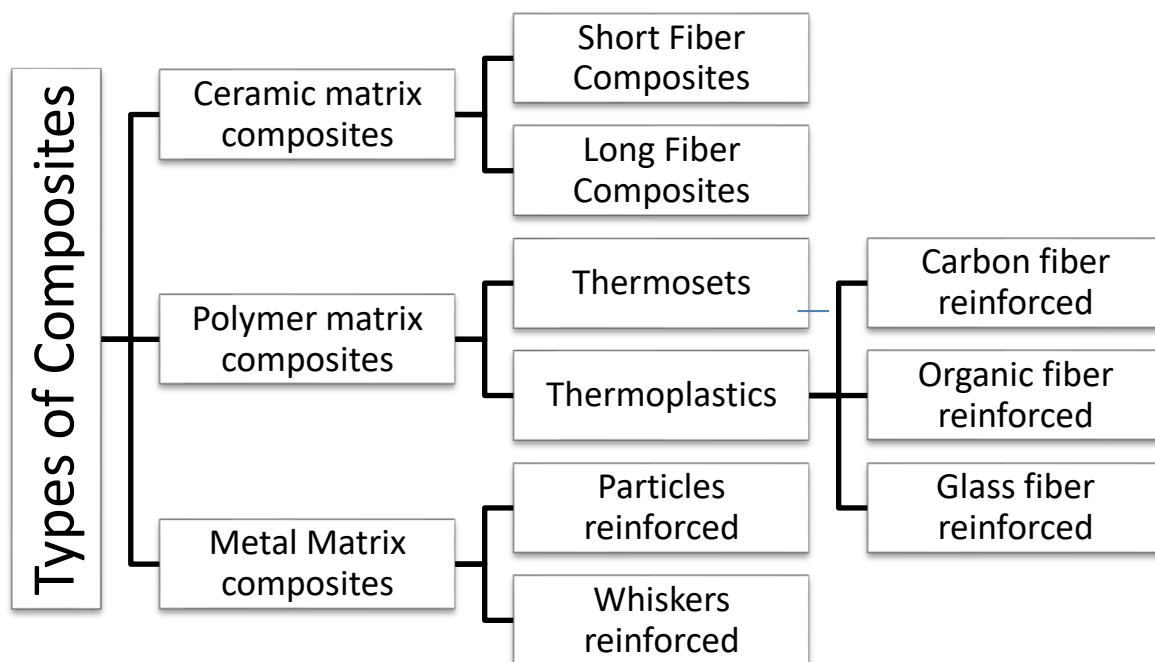
Figure 1.2: Classifications of Matrix Materials [14].

1.4.1 Matrix of Organic Composites

1.4.1.1 Matrix based on Polymer Composites (PMC)/ Matrix based on Carbon Composites or Carbon to Carbon Composites: As in the application of aeronautical sector, where light weight is very necessary, polymers type of composite material is appropriate for the specification. Thermosets and the thermoplastics are two kinds of

polymer. In crystalline thermoplastics, the fortification influences the morphology to an impressive degree, provoking the support to engage nucleation. Figure 1.3 shows sorts of thermoplastics [15].

```
                        SYNTHETIC FIBRES

         ORGANIC                                OTHERS
                              INORGANIC

                POLYAMIDES

                POLYESTERS
                                 GLASS      BICOMPONENT

                POLYVINYL
                DERIVATIVES      CARBON         MULTICOMPONENT

                POLYURETHANE     BORON

                POLYOLEFINS      SILICON
                                 CARBIDE
```
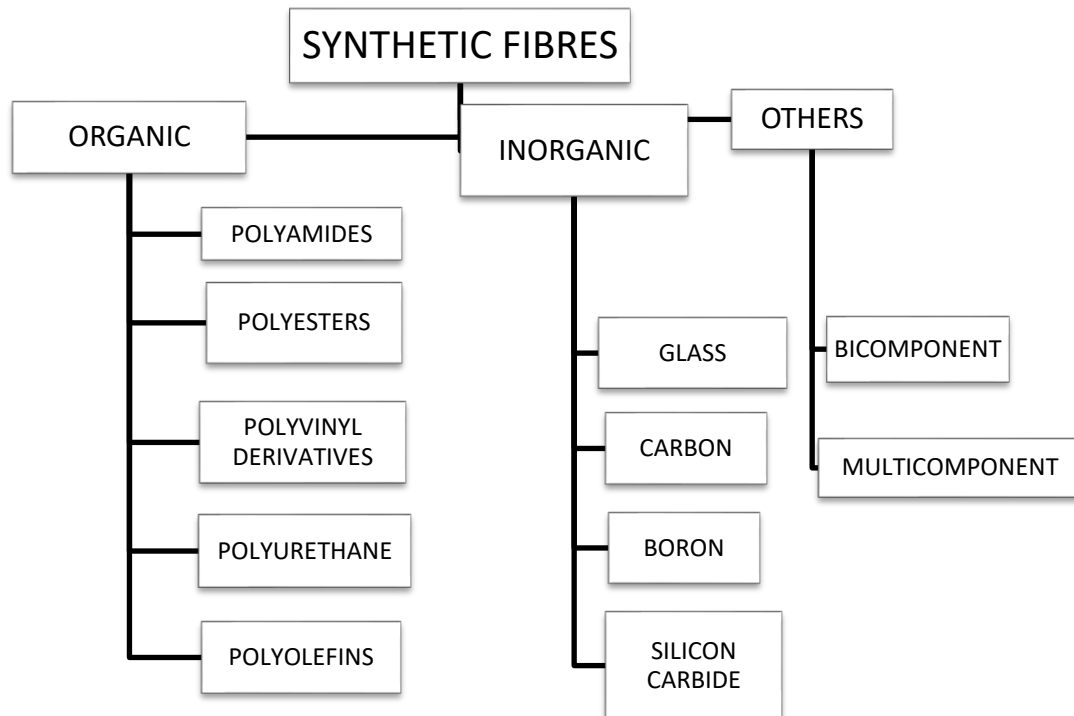
Figure 1.3: Classification of thermoplastics, inorganic and other materials [15]

In the applications like structural engineering field, thermosets can be considered as the most important composite of fiber. In the field of automobile, aerospace parts, defense areas etc., fiber composites are very popular. Materials of epoxy matrix are finds application in the area of printed circuit boards etc. Some thermosets are shown in figure 1.4[16].

```
                        THERMOSETS

                   PHENOLIC
        EPOXY      POLYAMIDE      POLYESTER
                   RESINS
```
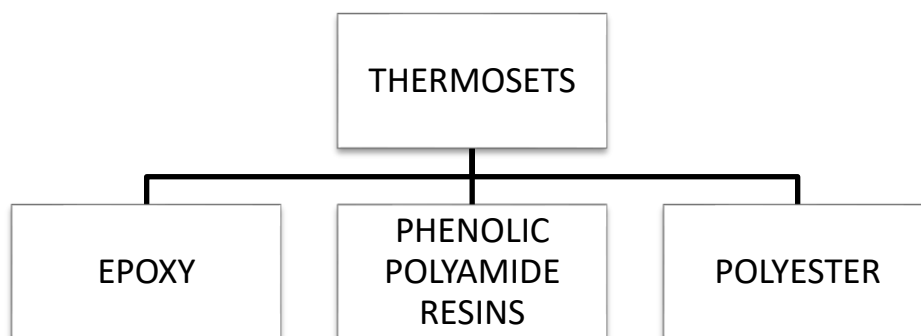
Figure 1.4 Types of thermoset Materials [16]

The cured polyester is generally unbending or adaptable by and large and straightforward. Polyesters withstand the varieties of condition and stable against chemicals. Contingent upon the plan of the tar or administration necessity of utilization, they can be utilized around 75ºC or higher. Different points of interest of polyesters incorporate simple similarity with few glass strands and can be utilized with confirm of strengthened plastic. Sweet-smelling Polyamides are the most looked for after competitors as the frameworks of cutting-edge fiber composites for auxiliary applications requesting long span presentation for consistent administration at around 200-250ºC.

1.4.1.2 Matrix based on ceramic materials (CMM)

Ceramics which can be popularly known for exhibiting the strong bond of ionic nature in general and in some cases covalent bond also. Application where structural materials are the requirement ceramic based composite material are the first choice because of properties like a high point of melting, a corrosion degradation resistance, good stability at high value of temperature and a very good value of strength under compressive loading. High modulus of flexibility and low rate of tensile strain, almost all ceramic have it, consolidated to make the disappointment of endeavors add fortifications to get quality change. This is on the grounds that at the level of stress at which rupture of ceramic takes place, elongation of matrix is not takes place at sufficient level which ultimately restrict the composite to transfer the effective load to the matrix and also to the reinforcement and the composite might be fail if the quantity of the fiber used is not sufficiently high [17].

1.4.1.3 Matrix based on metal Composites (MMC)

Due to strength, property of stiffness and property of toughness of MMCs as compared to polymer matrix, Metal matrix composites is first choice for most of the applications of modern products as well as the for the researcher. As compared with plastic composites, these have the capacity to counter high temperature even at corrosive atmosphere. Particularly for the applications like aircraft, automobile etc. aluminum, titanium and magnesium are important one. If composite of that material can be fabricated, the high strength to weight ratio can be accomplished. Most metals production and composites can be utilized with frameworks of low dissolving point combinations. The selection of fortifications turns out to be more hindered with increment in the softening temperature of matrix materials [18].

1.4.1.4 Classification of Composite based on metal as matrix

Metal network composites can be characterized in different ways as appeared in figure 1.5
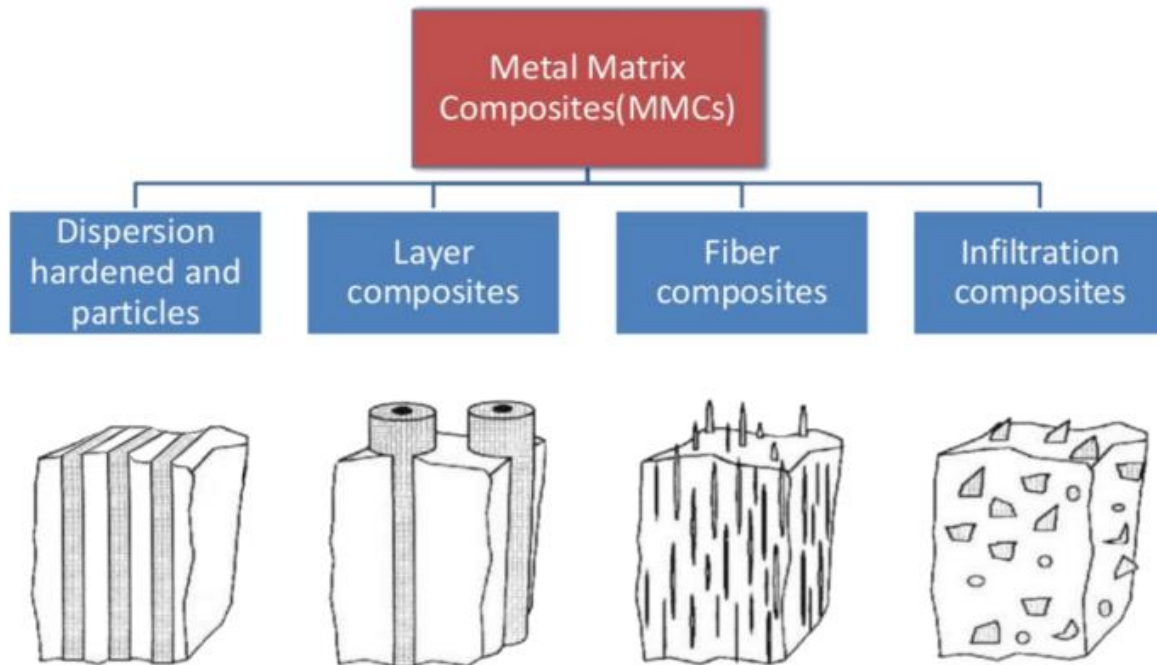
Figure 1.5. Classification of composite materials with metal matrixes.

When the fiber is reinforced in the matrix of metal then it is known as fiber reinforced Composites. The fibers in the matrix should be protected against the effect of bending and buckling [19]. When the layers of the materials are attached together through the matrix then it is known as laminar Composites. Structures which are of sandwich types are come under this types [20]. When the reinforcement is in the form of particles of material then it is called as particulate composites. Particles can be a powder type or may be a flakes[21]. Composite materials where reinforcement is of fiber, particle or filaments can be shown in Figure 1.6 as:
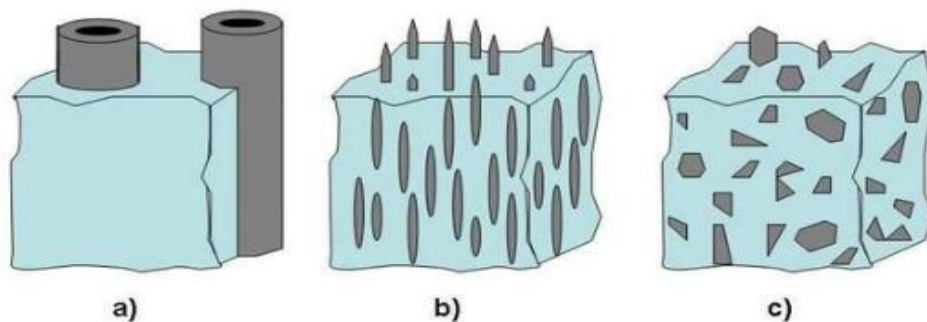
Figure 1.6: Ordered sketch of three types of composite materials based on metal matrix [22].

1.5 Introduction of Reinforcement for matrix

A material which is incorporated in the matrix of base material for the purpose to alter the properties of the original material is called reinforcement. Materials which are used as reinforcement are fibers, ceramics, carbon, glass, whiskers, boron, graphite and even paper is also used. The main point of difference between the filler and the reinforcement is that reinforcement is greatly helps in improving the tensile as well as flexible strength of the material but in case of filler no such properties are increased. For successful fabrication of composite, reinforcement used should be homogeneous in matrix and both must be strongly connected with each other [23]. Some common types of reinforcements which are generally used for fabrication of composite material are shown in figure 1.7 as:
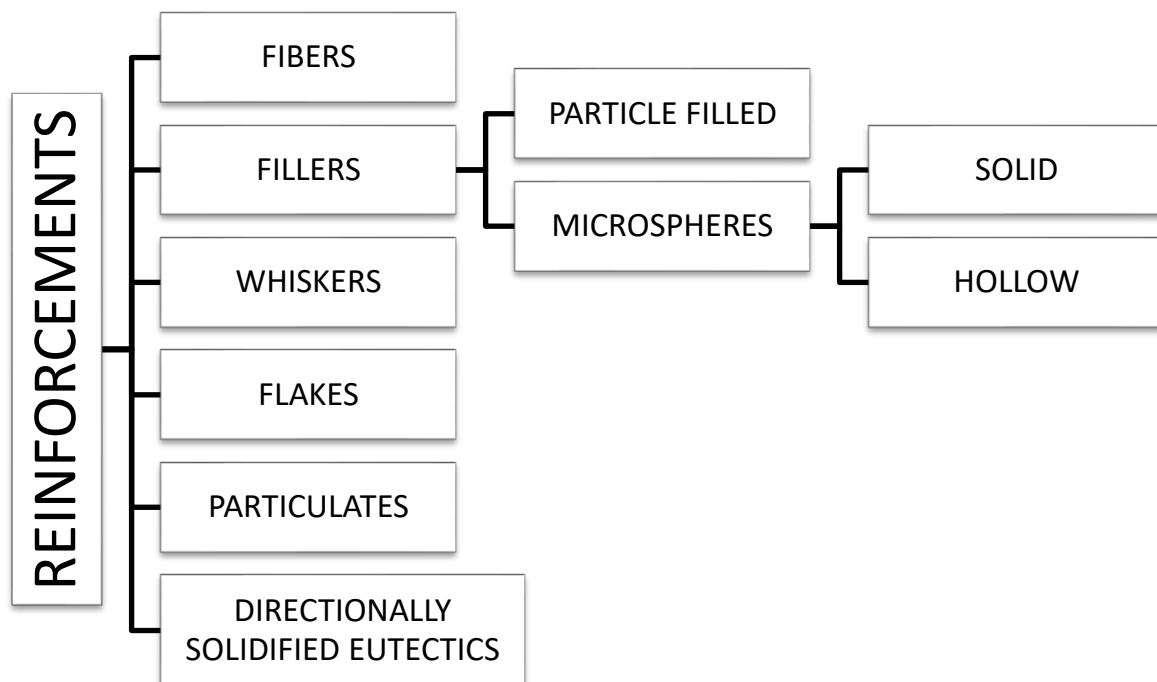
Figure 1.7: Types of Reinforcements.

1.5.1   Fiber Reinforcements

Natural and inorganic filaments are utilized to strengthen▸composite materials. All natural filaments have low thickness, adaptability, and versatility. Silicon carbide, graphite and boron are some of the fibers which has the great potential in the applications of advanced composites [24].

1.5.1.1 Glass Fibers

Time of stacking, temperature, wetness and completely different variables likewise manage the resilience levels of glass filaments and therefore the hurt is in addition intense by the means that the fragility of glass doesn't harden earlier cautioning before the disastrous disappointment. In any case, this could be not entirely obvious in perspective of the means that the intensive form of optical fiber assortment loan themselves pleasantly to manufacture forms like coordinated bite the dirt shaping, fiber twisting lay-up et cetera. Glass strands square measure accessible as mats, tapes, material, consistent and cleaved fibers, roving's and yarns [25]. Expansion of chemicals to oxide sand whereas creating glass yields various varieties of glasses.

1.5.1.2 Metal Fibers

As fortifications, metal filaments have several points of interest. They are square measure effortlessly created utilizing a number of manufacture forms and are additional pliable, other than being not terribly touchy to surface damage and have high qualities and temperature resistance. Be that because it could, their weight and therefore the propensity to reply with one another through alloying instruments square measure important detriments. Steel wire is that the most broadly speaking utilized fortification in most expansive scale metal fiber applications. Wire is employed for its ability to upgrade the rigidity of concrete and consistent metal strands square measure the strengthening constituents in metal and clay composite materials. Discharged strands enhance inconceivably in execution once a fine metal layout is consolidated with unmanageable ceramic ware production by enhancing their heat stun and result resistance properties. Metal wires, of the nonstop kind, in addition fortify plastics like synthetic resin and epoxy. Such blends guarantee top quality, light-weight weight taken care of, not in the slightest degree like glass strands. Higher flexural properties square measure seen in some metal strands strong plastic composites that likewise supply increased quality and weight, than glass filaments [26]. In any case, their poor resilience of high temperatures and therefore the resultant soak form of heat extension constant with the pitches square measure a demoralization that restricts to their applications.

1.5.1.3 Alumina Fibers

Alumina or alumina strands, essentially created to be used in metal grids square measure viewed as a possible tar network composite support. It offers nice compressive quality as critical snap. Its essential property is its high dissolving purpose of around 2000°C and therefore the composite is often effectively utilized at temperatures up to around 1000°C. Metallic element and Al frameworks routinely utilize even within the fluid state. Corundum fiber strong composites as they do not damage the fiber [27].

1.5.1.4 Boron Fibers

They are basically composites, with atomic number 5 which shapes the substrate, usually product of metallic element. Boron- tungsten strands square measure gotten by allowing hot metallic element fiber through a mix of gasses. Atomic number 5 is keep on metallic element and therefore the procedure is proceeded till the desirable thickness is accomplished. The metallic element but stays steady in its thickness. Properties of atomic number 5 filaments by and huge modification with the breadth, in sight of the dynamical proportion of atomic number 5 to metallic element and therefore the surface imperfections that modification as indicated by size. Still, they're illustrious for his or her noteworthy firmness and quality. Their qualities oftentimes distinction and people of glass strands, but their pliable modulus is high, almost four to 5 times that of glass. Atomic number 5 lined carbons square measure significantly more c o s t -effective to c r e a t e than atomic number 5 metallic element fiber. Be that because it could, its low modulus of flexibility often conflicts with it [28].

1.5.1.5 Silicon Carbide Fibers

Silicon carbide is often lined over some metals and their temperature rigid qualities and elastic moduli check those of boron-tungsten. The advantages of semiconductor carbide- tungsten square measure a number of and that they square measure additional engaging than uncoated atomic number 5 metallic elements strands. Hosted temperature execution and therefore the means that they elaborate simply a thirty fifth loss of quality at 1350°C square measure their best qualities. Carbide-tungsten and carbide-carbon have each been believed to own high anxiety break quality at 1100°C and 1300°C. Uncoated boron-tungsten strands have a bent to lose

everything that's in them at temperatures quite 680°C. Carbide filaments do not respond with liquid Al, dissimilar to uncoated atomic number 5 and that they in addition face up to high temperatures utilized. In any case, semiconductor carbide-tungsten filaments square measure thick contrasted with boron-tungsten strands of an analogous distance across. They're inclined to surface damage and wish cautious, fragile managing, notably amid manufacture of the composite. Furthermore, element and carbide, creating it laborious to stay up change in high-temperature framework arrangements. Carbide on 'carbon substrates have a number of focal points, viz. No response at hot temperature, being lighter than carbide metallic element and having elastic qualities and modulus that's square measure often superior to those of semiconductor carbide-tungsten and atomic number 5 strands[29].

1.5.1.6 Quartz and Silica Fibers

The glass-sorts often contain around fifty to seventy-eight oxides. Oxide glass could be a purer optical fiber that may be created by treating covering material during a corrosive shower that evacuates all contaminations while not influencing the oxide. The last item contains ninety-three to ninety-nine oxides. Quartz is far additional immaculate, and quartz strands square measure made mistreatment characteristic quartz precious stones that contain 99% silica, having virtually all of the properties of pure sturdy quartz produced using high silica and also quartz. All network materials that acknowledge fiberglass are amiable to high silica and quartz too. They vary from glass in many components, notwithstanding, particularly in warmth related properties. In spite of the fact that quartz gems are usually accessible, unadulterated precious stones are difficult to find. Then again, high silica originates from an indistinguishable material from glass strands and is effectively available. Be that as it may, quartz compensates for its irregularity with its ability to withstand high temperatures, which silica is unequipped for [30].

1.6 Examples for composite materials
➢ Fiber reinforced plastics
➢ Carbon-carbon Reinforced composite (In the matrix of graphite carbon as a fiber).
➢ Composites in which metal as a matrix i.e. MMCs
  • Laminate of Metal and intermetallic components.
  • Cast iron e.g.: White cast iron.

- Hard metal like carbide in the matrix of metal.
➢ Composites in which carbide as a matrix.
  - Concrete
  - Bone
  - Cermet i.e. blend of metal as well as ceramic[31].

1.7 Important factors to be considered during selection of Matrix

Factors which are taken into consideration during selection of matrix are:

➢ Mechanical strength of the matrix bust be in relation with reinforcement so that both are compatible. If the fiber is of high strength, then the matrix should be of low strength so that the stresses can be transfer effectively.

➢ The chosen matrix should be able to stand with the atmospheric conditions such as external temperature, humidity of the surrounding, ultra-violet, chemical atmosphere, dust particles, etc.

➢ In the fabrication process, the matrix should be used easily.

➢ Requirements of the Smoke.

➢ Expectancy of Life.

➢ At the end the composite should be less in cost.

Before curing into solids, the fibers should be mixed with the liquid resin. Then the solid part acts like a matrix for the material [32].

1.8 Pros, Cons and applications of Composites Materials

1.8.1   Pros of Composites

Some of the pros of composite material are discussed as:

➢ Composite materials behave very good against fatigue loading and corrosion phenomenon.

➢ Composite material offers high strength to weight ratio as compared with the conventional material, composite of the same material is capable of 25% to 45% reduction in weight at similar properties.

➢ Composite materials are highly reliable so very few repairs and inspections are required after their fabrication.

- The reinforcements in the matrix of the material can be altered in any direction as per the need of the mechanical properties required in the whole composite.
- More than one type of properties can be achieved in a single material as there is a possibility to use more than one type of reinforcements in the same matrix.
- Panels made with composite have high capability to sustain dent because they are not as thin as normal gauge of sheet metals.
- Composite have high capacity of load sharing e.g. like in like fiber to fiber path.
- For the higher end profiles like in aerodynamic there are highly useful for drag reduction as Complex parts with double curvature and also of good finish of surface can be formed in a composite material with single operation of manufacturing.
- These materials have sufficient torsional stiffness also. So, they are also useful for high speed of rotation with reduced cost and ease of manufacturing.
- Composite of materials like metals, thermoplastic can be easily made with indefinite shelf life.
- Generally composite materials possess low thermal conductivity because of low thermal coefficient of expansion, so these materials are thermally stable. Composite formed can be altered as per the requirements of design with minimum number of thermal stresses.
- Due to integration of parts fabrication as well as assembly of the composite are simple and cost-effective.
- While machining of these materials nearby tolerance can be possible.
- Due to lightweight and property to dissipate heat like in carbon-carbon composite formed, they find application in aircraft brakes.
- Composite also possess good resistance of friction as well as abrasion due to wear [33].

1.8.2   Cons of Composites

Some of the cons of composites can be discussed as follows:

- Reusability is very less and difficult.
- Bonding of reinforcement and the matrix with homogeneity is difficult.
- After the fabrication of the composite, matrix is weak and majority of load is taken by the reinforcement, so they have low toughness.
- Properties in transverse direction is weak.

➢ Another disadvantage of the composite is that they are brittle than that of the wrought metals so it is more suspect able to damage.

➢ Cost of fabrication as well as raw material is high [34].

1.8.3 Applications of Composite materials

Composite material finds applications in many areas of the today world. Some of the common applications are as:

➢ Due to high strength to weight ratio, these have great potential in aerospace sector, automobile sector and ship building industry too.

➢ Composite material has wide scope in construction work.

➢ It also finds application in medical industry.

➢ Composite have great potential in electrical and electronic industry too.

In a nutshell, we can conclude that composite materials have great potential in future research applicable both for industry as well as academia point of view[35].

1.9 Methods of composite manufacture

Fiber-strengthened polymer composites (FRPs) can be prepared in various courses, contingent on the segments last proposed utilize, and can likewise influence the properties of the part.

1.9.1 Wet lay-up

A form in the state of the last part is required. The support (as a woven texture) is precisely laid into this shape and the grid (gum) is poured on and spread, as a rule with the guide of a roller. This is then left to cure. A gel coat can be added to the form before the fortification is put into it relying upon what surface complete is required (the top surface is the side which is face down in the shape). A discharge specialist can likewise be connected to the form to help with evacuating the part subsequent to curing [36].
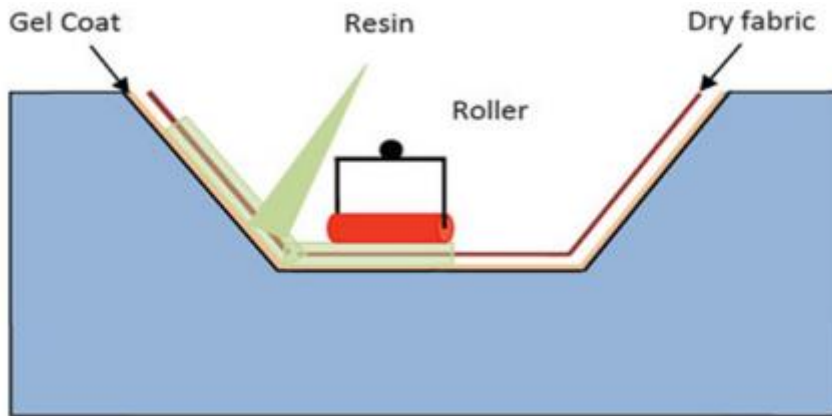
Figure 1.8: Wet lay-up

1.9.2 Filament winding

This procedure is utilized for delivering empty tubes. The support (as strands) is washed up, covering them with the lattice. The get to tar is crushed out by rollers and the fortification filaments are then twisted onto a mandrel to frame the round, empty shape. The heading the filaments are twisted adds to the execution properties required of the completed part [37, 38].
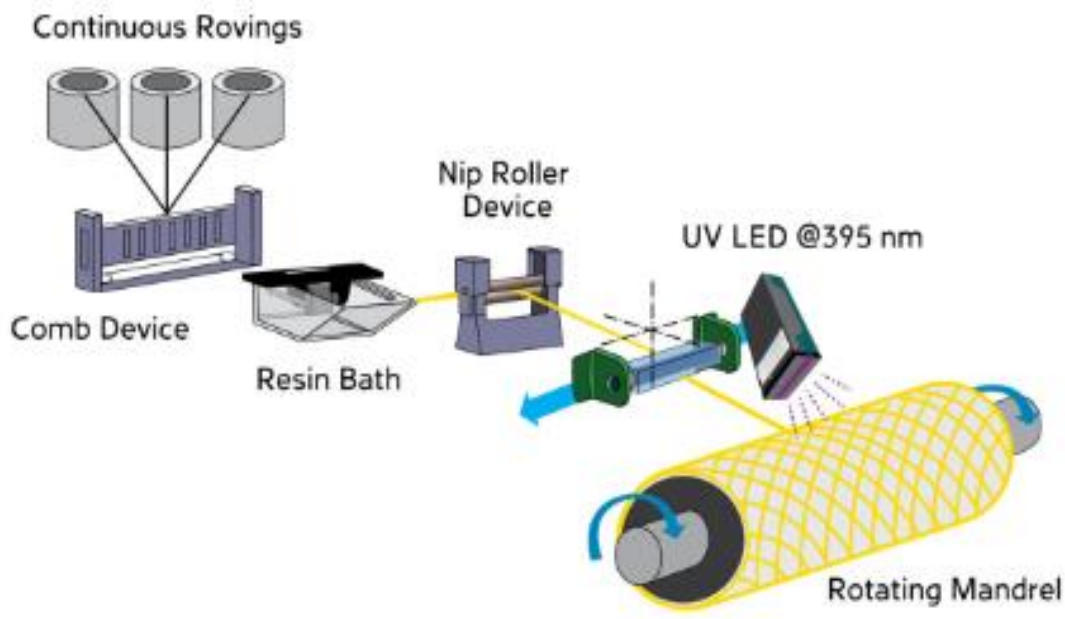
Figure 1.9: Filament winding [POLYMER G]

1.9.3 Compression Molding

Pressure embellishment is regularly utilized with pre-fortification filaments as of now impregnated with tar. The pre filaments is set in an open, warmed female shape. The male form is then put down on to this with the blend of warmth and weight molding and curing the segment. Parts are then permitted to cool before expelling from the

shape [39].

1.9.4 Resin transfer molding

A male and female shape is required. The support (as a woven texture) is set into the female shape as shown in Fig.1.10.
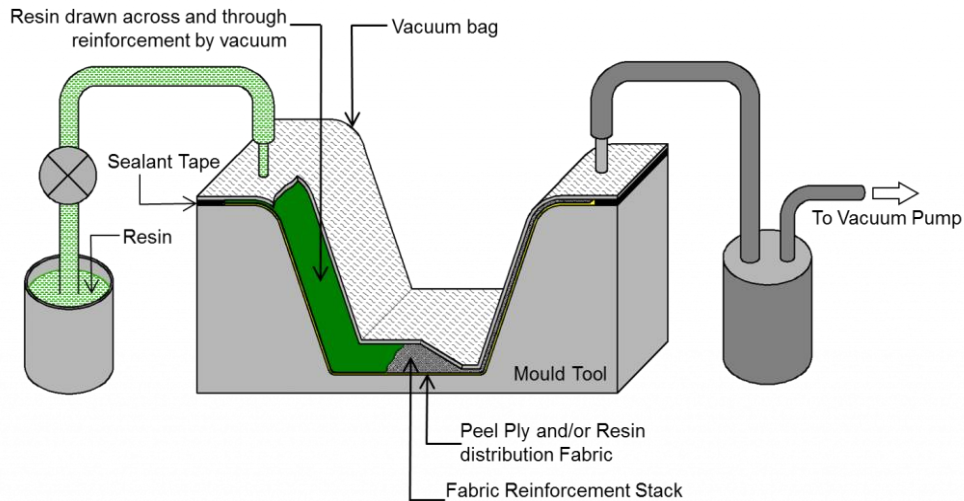
Figure. 1.10: Resin transfer molding [40]

The male form is then pushed downward on this and cinched. Pitch is infused underweight from one side of the form with discretionary vacuum help at the inverse side. This then "wets out" the strands and is then left to cure. On a few events the form is warmed to help the procedure[40].

1.9.5 Vacuum bagging

This procedure can be utilized as an expansion of the wet lay-up method. The support (as woven texture) is set into a shape, which can be pre-covered with a discharge operator or potentially gel coat. The sap is then moved on top. A plastic film is put over this and is completely fixed at the edges. A vacuum then concentrates the air from process combining the part. It guarantees that the gum is uniformly spread [41].
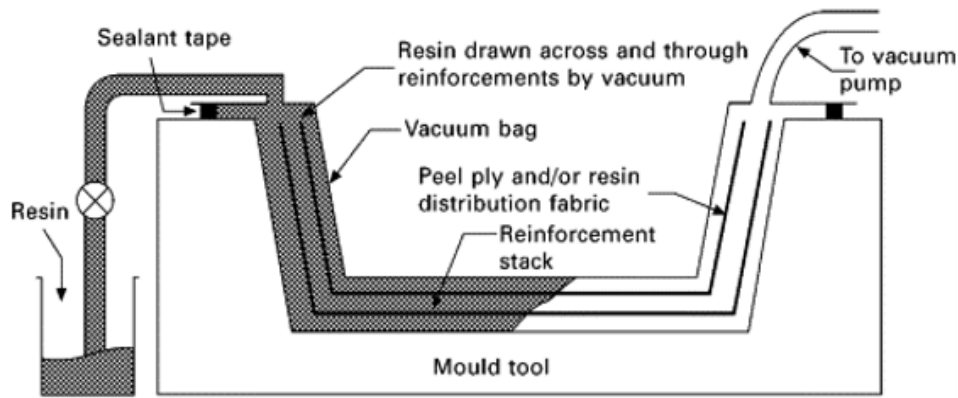
Figure 1.11: Vacuum bagging. [41]

1.9.6 Pultrusion

Pultrusion is a procedure utilized for making long, nonstop parts, for example, link plate (for instance, those utilized as a part of the Channel Burrow). Numerous strands of support filaments are pulled from reels along a transport line sort prepare through aides into a warmer. Amid this warming procedure the strands are covered in tar. The warm, sap covered strands arethen pulled through a trim kick the bucket, framing the last segments shape. It is then sliced to the coveted length with a saw [42].
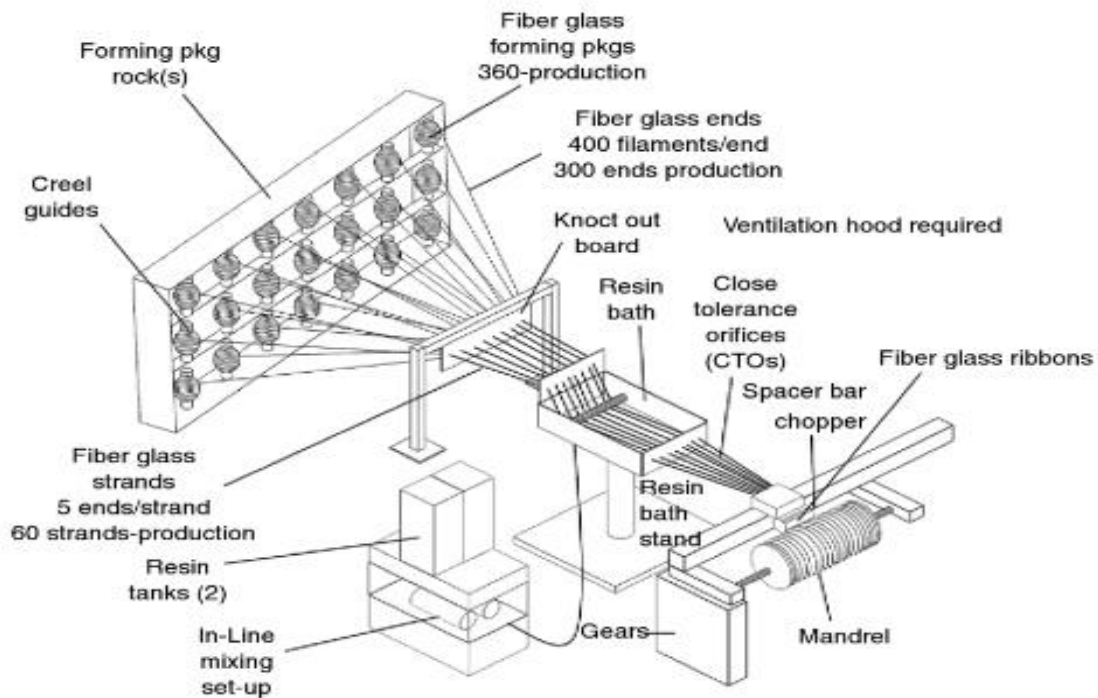
Figure 1.12: Pultrusion [42]

1.10 Types of methods for manufacturing of MMCs reinforced with particulate

The manufacturing of MMCs can be done by two types i.e. solid and liquid [43].

1.10.1 Fabrication methods based on Solid-phase:

1.10.1.1 **Powder Metallurgy i.e., powder blending and consolidation**: Metal in the form of metal and the reinforcements are firstly mixed and after that they are bonded through processes called as thermo-mechanical treatment i.e. extrusion, compacting etc. The basic process can be shown as:
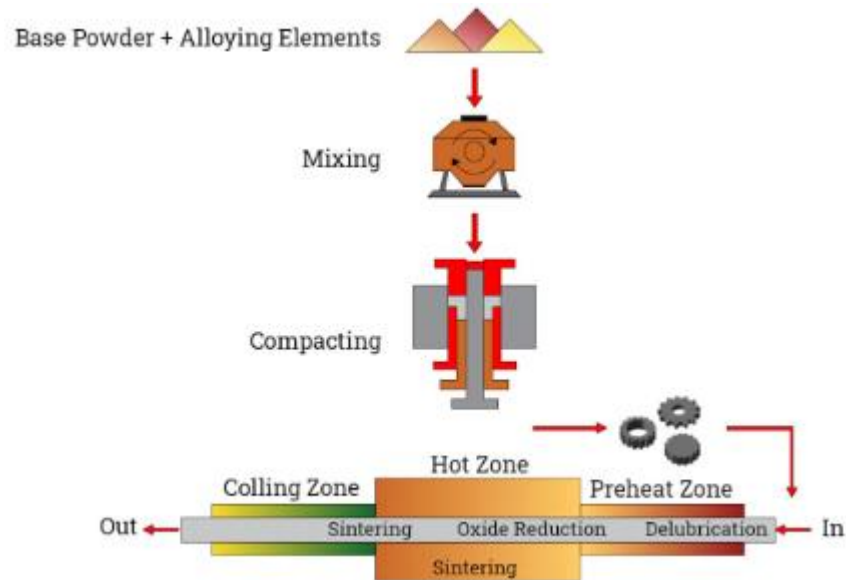
Fig 1.13 Basic process of Powder blending and consolidation [44].

1.10.1.2 **Based on diffusion bonding of foil**: layers of metal are reinforced by long fiber, and after that squeezed through to shape a matrix [45]. The basic process can be shown as:
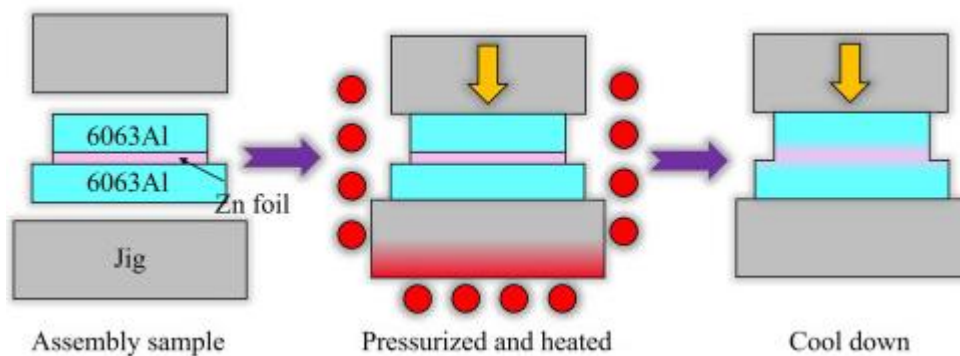
Fig 1.14 Basic process of Foil Diffusion Bonding. [45]

1.10.2 Fabrication methods based on Liquid-phase:

This technique is more useful than that of solid-phase as it is more efficient and needs less time than Solid-phase.

1.10.2.1 **Technique of Electroplating or Electroforming**: In a solution of metal ions as well as particles as reinforcement, they are co-deposited and makes a composite [46].

1.10.2.2 **Technique of Stir casting**: Base metal in molten state and reinforcement particles are mixed in the furnace with rotating stirrer to form composite[47].

1.10.2.3 **Technique of Squeeze casting**: Liquid metal is infused with fibers preplaced inside it [48]. The basic process can be shown as:
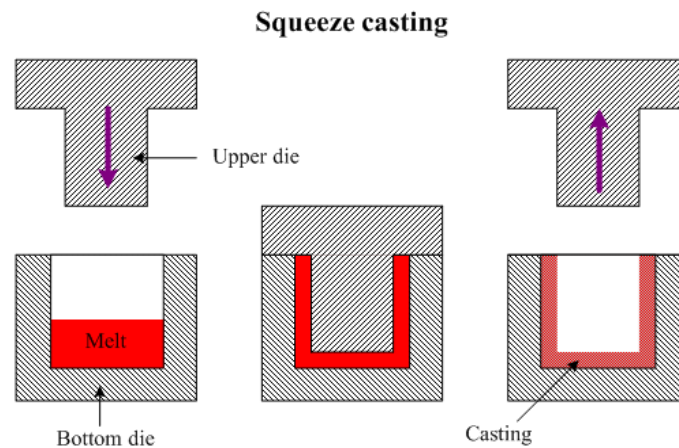
Fig 1.15. Basic process of Squeeze casting. [48]

1.10.2.4 **Technique of Spray deposition**: On the continuous fibers metal in the form of molten state is splashed [49].

1.11 Metal Matrix Composite Fabrication with process as Stir Casting

The setup for stir casting consists of a furnace to heat and a stirrer for mixing. This process is generally used for manufacturing of the composite materials. At first the base material is melted, then the required reinforcements are added to it in order to get the composite material. The stirrer is rotated at various rpm as per the requirements. Figure 1.8 shows for setup for stir casting process.
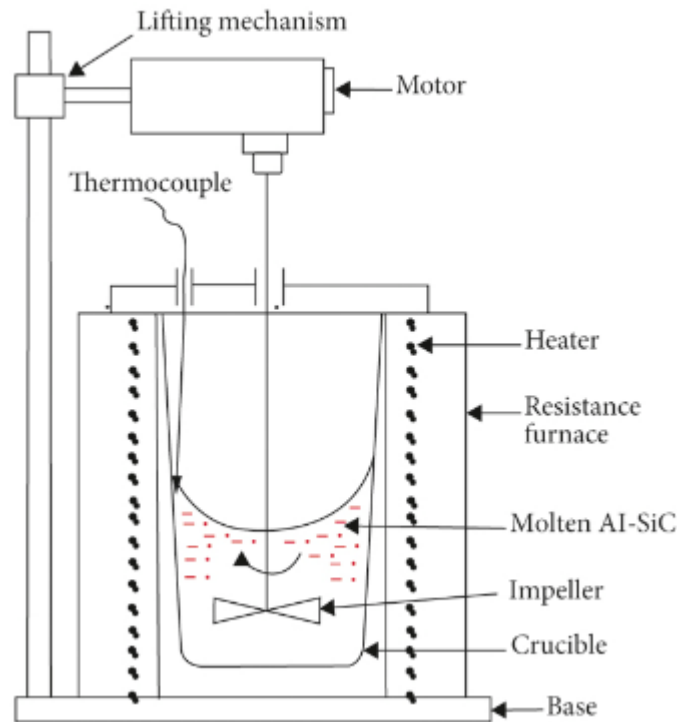
Figure 1.16: Stir casting set up. [50]

Determination of material with explicit properties is the critical in numerous modern applications, particularly in the automotive and aerospace sector. In any case, handling of such composites with explicit properties, similar to high strength, experiences specific limits as far as cost and manufacturing time, although with the decrease of flexibility. Joining of high strength with the high ductility is feasible when the materials are of homogeneous and fine grains microstructure. Consequently, there emerges a need to create a method that would process a material with little grain size that fulfills the necessities of ductility and strength, the expense and the production time. There are different methods of processing the materials like ECAE or we can say Equal Channel Angular Extrusion, FSP or we can say Friction Stir Processing, being created for this reason of the enhancements in conventional methods such as the powder metallurgy Rockwell process strategy etc.

In the year 1991, Friction stir welding i.e. (FSW) grows as an advancement created by The Welding Institute (TWI) in the country called United Kingdom in order to create nearby and surface properties at required areas. Friction stir processing i.e. (FSP) is a recent and interesting thermo-mechanical processing strategy that changes the microstructural as well as the mechanical properties of the material in a sole pass to accomplish greatest performance with minimal creation cost significantly quicker. Current area of study mainly focusing on process called Friction stir processing which is researched as an advanced and potential method of

processing for alloys of aluminum as a result of different benefit it offers over different processes as described previously.

1.12   Friction Stir Processing

A rotating tool of non-consumable is placed on a material of single piece, and then moved over the surface of the base material to be taken in transverse direction. As the work piece touches with the tip of the tool shoulder, it heats up the work piece material is deformed plastically as shown in Fig. 1.17.
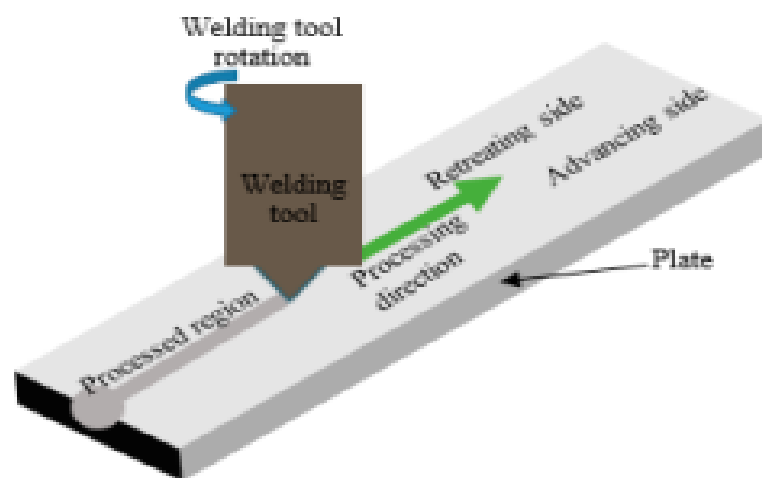
Figure 1.17: Basic setup of FSP. [96]

The force of friction between the tool and the base material to be taken as work pieces, furthermore the plastic distortion of the material produce heat. The rotation of tool and motion of translation, prompts the material development starts from the front end to the rear end of the pin. At first, the process i.e. FSP-Friction stir processing was created by Mishra et al., in order to adjust the microstructural properties [50, 51]. Likewise, FSP has been utilized in the processing of the surface composite of aluminum alloys substrate as well as their composites [52], in the area of MMC's i.e. metal matrix composites, in order to do homogeneity in powder metallurgy process especially for aluminum alloys and for also cast aluminum combinations. FSP has distinct benefits contrasted with other metalwork techniques. To begin with, FSP is an immediate solid state handling procedure that is able to achieve the microstructural adjustment, densification of the grains, and also for the homogenization all the while. Second, improving the design of the tool, process parameters of FSP, and dynamic cooling as well as the heating of the microstructure improve the mechanical properties of the handled area can be exactly

seen. Third, it is difficult to arrive at an alternatively acclimated handled profundity utilizing other manufacturing techniques such as metalworking. In the processed zone, the depth of the material can be alternatively constrained by modifying the pin tool length. Fourth, having a far and wide capacity for the manufacture, handling, and materials synthesis, FSP is a versatile method. Fifth, Friction stir processing is based on the green technology and also it is an energy-proficient procedure without the discharge of any unsafe gases and radiation. Sixth, in Friction stir processing shape as well as the size of the parts to be processed doesn't get adjusted [53].

Friction processing is a wide phrase that incorporates a variety of metal matrix processing processes. Mechanical force and frictional heat are used to affect the structure and characteristics of metal matrix composites in these approaches. Here are a few examples of metal matrix friction processing techniques:

Friction Stir Processing (FSP): Friction Stir Processing (FSP) is a solid-state joining and processing technology that uses a spinning tool to create frictional heat and mechanical force. The tool is inserted into the metal matrix, causing a plasticized area to form. The tool stirs the material as it passes along the processing route, facilitating grain refinement, particle dispersion, and consolidation of the metal matrix composite.

Friction Stir Sintering (FSS): FSS is a process used to generate metal matrix composites by consolidating metal powders and reinforcing particles. It uses a revolving tool to create frictional heat and apply pressure to the powder combination. Heat speeds up the sintering process, causing the metal matrix and reinforcing particles to solidify.

Friction Surfacing: Friction surfacing is a procedure that uses frictional heat and mechanical force to apply a consumable filler material to a substrate. Typically, the filler material takes the shape of a wire or rod. As the spinning tool makes contact with the filler material and the substrate, frictional heat is created, forcing the filler material to melt and bind with the substrate, resulting in the formation of the composite. These friction processing techniques provide benefits such as increased mechanical qualities, microstructural features, and the capacity to treat difficult-to-weld or cast materials. The particular procedure to adopt, however, is determined by the intended product, the kind of metal matrix composite, and the application requirements.

LITERATURE SURVEY

1.1. Historical perspective on Friction Stir Processing

Thomas et.al [54] states that rubbing action between two objects produces friction which ultimately causes heat as known by many centuries back. The similar concept is now popular and forms the basis of processing, technique of surfacing and welding too. As we know the process of friction is a very efficient to reach a plastic state at material on some specific locations so for the processes like welding preparation, extrusion or may be for cladding or surfacing it is very useful for contamination removal. This concept is sustainable and eco-friendly as no fumes are generated and did not consume any filler wire and gas. Friction welding is the concept of production of heat by rubbing action between two points under the action of load as shown in fig. 2.1. On the point of required temperature and the rate of material deformation, force is either static or increased so that a solidification state occurs and bond is created. This concept of friction is very much useful for welding of dissimilar metals have wide range of welding temperature and physical properties.
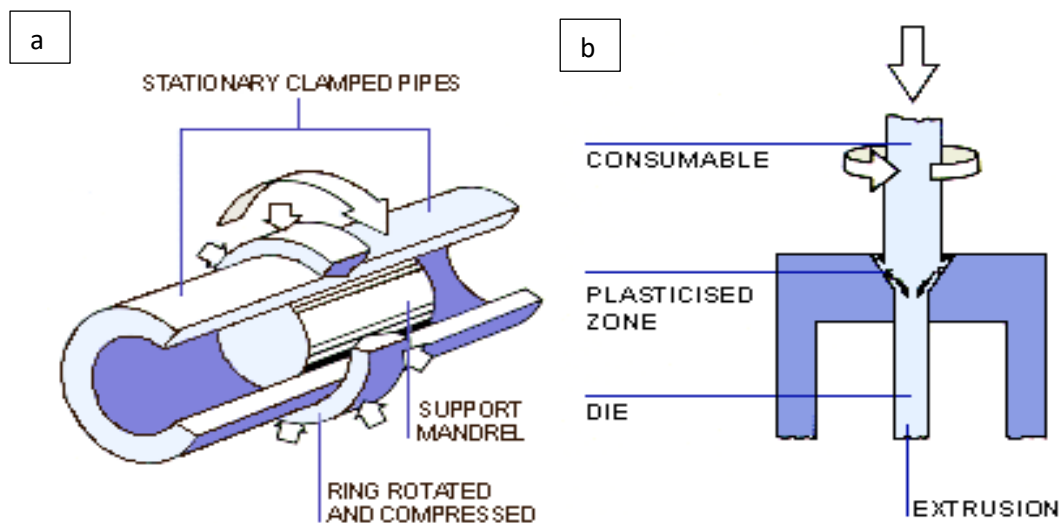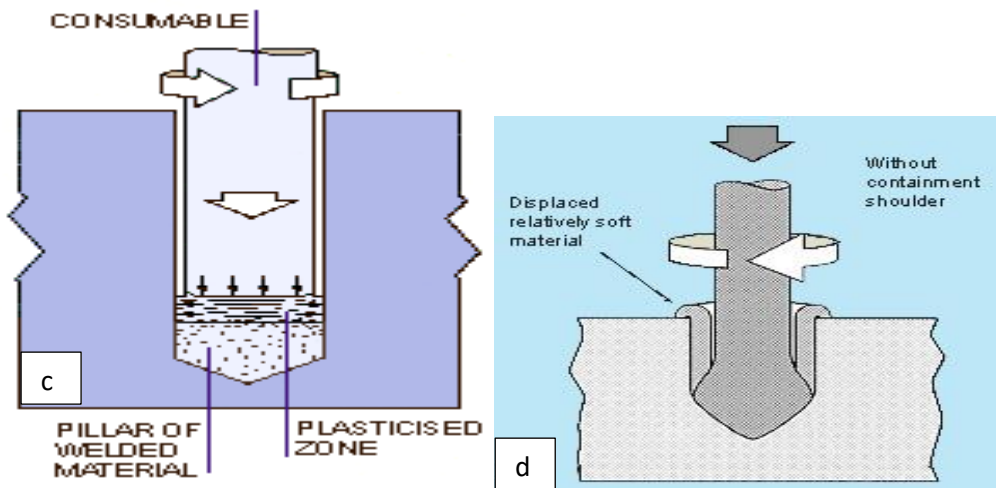
Figure 2.1: Pictorial view of a) friction welding radially, b) extrusion by friction, c) processing through friction by hydro pillar d) without contamination of shoulder a friction plunge welding process. [54]

Thomas et.al [55, 56] Work has exhibited that few elective strategies exist or are being created to meet the prerequisite for steady and solid joining of large-scale manufacturing of aluminum vehicle bodies. Three of these strategies (friction stir welding, mechanical joining and lasers) are probably going to have an effect in modern industries in the upcoming 5 years' time. Process of Friction Stir Welding successfully applied in the production of welds as a straight-line as a minimal expense compare to the process of arc welding (for example in the creation of truck floors). The advancement friction stir welding by robotized the process could broaden the scope of utilizations into complex parts called as 3D parts also.

Mishra et.al [57] takes Al 7075 and Al 5083 alloy and then utilizes the FSW in order to make them super-elastic. Results of the study revealed that grains sizes <5μm which is equi-axed, in the surface it is homogeneous and recrystallized too. They had high points of disorientation ranging to angle from 20^0 to 60^0. In addition of that they had performed elastic testing at high temperature to comprehend the superplastic behavior of friction stir processing on sheets of aluminum alloy.

Mishra et al. [58] tested as well as demonstrated that friction stir processing process can be used for manufacturing of the surface composites. Feasibility study is conducted for Al-Sic surface composites by varying the volume percentage of the reinforcement particles. Ranging from 50μm to 200μm, the thickness of the surface composite are taken. Particles of the Sic were taken for the aluminum matrix. The surface composites have fantastic holding with the

aluminum compound substrate. The micro hardness of the surface composite built up with 27 volume % Sic of 0.7 μm normal molecule size was ~173 HV, practically two times of the 5083Al compound substrate (85 HV). The fine microstructure and solid state processing outcomes are necessary for superior working of surface composites.

Thomas et al. [59] published a review paper on friction technologies for materials like aluminum, stainless steel etc., which are getting far reaching interest. Friction stir welding, plunge welding processing through hydro pillar processing etc. are a portion of these procedures. They saw that this innovation made conceivable the welding of un-weld able alloys of aluminum and stainless steel possible. Utilizing this innovation sheets up to the thickness of 75mm can be welded with small efforts.

Rhodes et.al. [60] takes aluminum alloy as a base material and process it with the help of friction stir processing using extract technique and rotary-tool plunge. Aim of the study is to evolve the fine grain structure of the aluminium alloy. In the start of the process, rotating tool causes the deformation of the grains, also deform the sub grains which are pre-existing. In the starting also, for the freezing of structure, High cooling rate is introduced. In whole of the process, by the rotation of tool, heat is generated and is expressed as the rate of cooling which is applied externally and speed of rotation of the tool also. When speed of the tool is high and rate of cooling is low, then deformed grains of aluminum is recrystallized as shown at rpm levels in fig.2.2. When the new grains are formed after the recrystallization, their size is approximately 25-100 nm, which is smaller than that of pre-existing sub-grains in the initial. After several experiments, it is found that grains which are newly formed can grow up to size of 2-5 μm, which is same as found When aluminum is friction stir processed at range of temperature from 350-450 degree Celsius and time of 1 to 4 minute. It is concluded that grains i.e. 2-5 μm, formed is because of nucleation and when heavily deformed grains grows. Sub-grains rotation is not responsible for this.
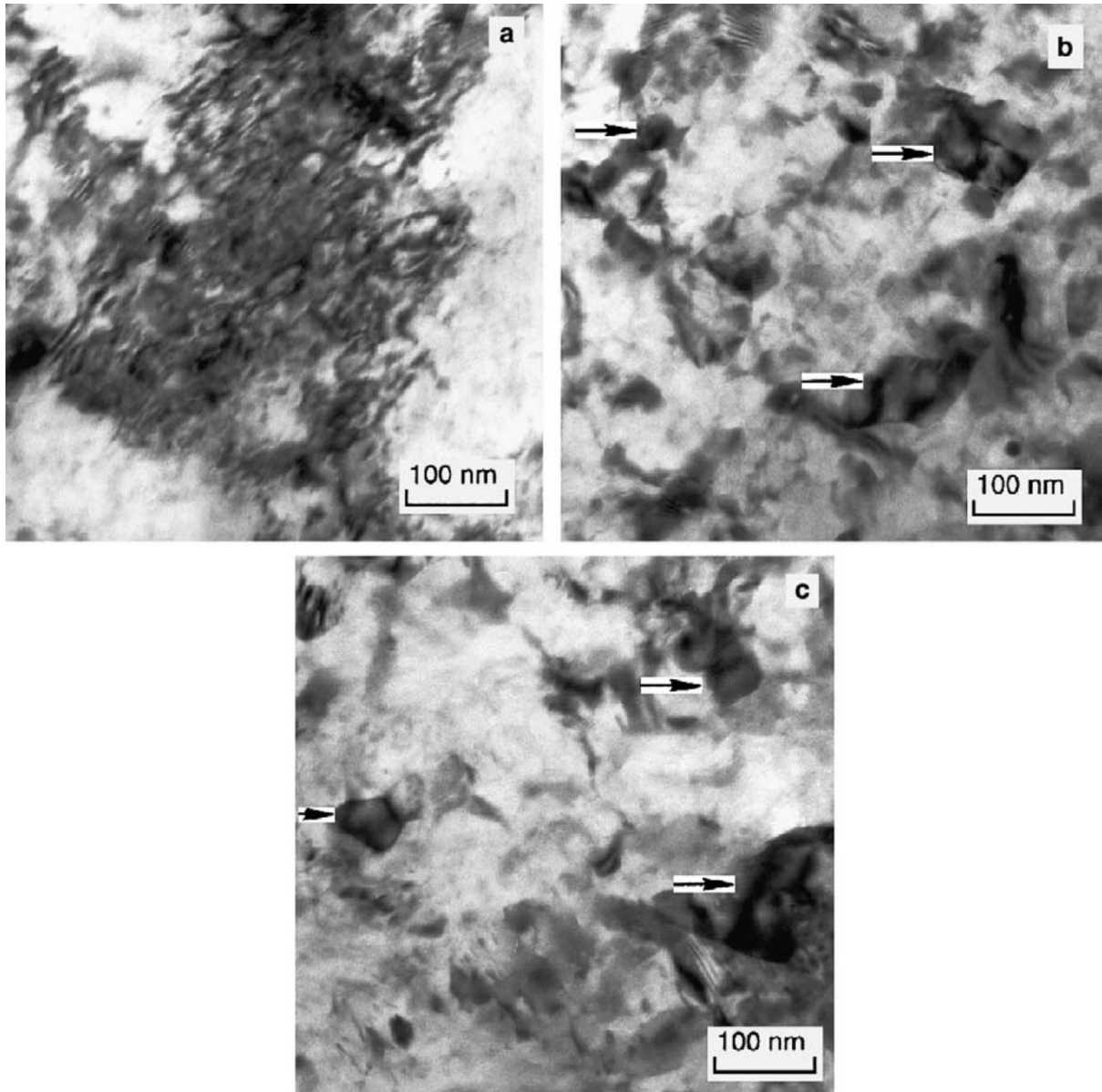
Fig. 2.2. Pictorial view of TEM micrographs of FSP. (a) speed of tool rotation 200 rpm, (b) speed of tool rotation 300 rpm, and (c) speed of tool rotation 500 rpm. [60]

Cabibbo et.al. [61]. joined Al-Si-Mg alloys through friction stir welding process by making butt join. Output parameters for the process are mechanical testing, measurement of hardness, study of metallurgical properties such as microstructure of the specimens. They also try to correlate the microstructure evaluation by TEM with the mechanical properties measured after performing the tests. After the process of the friction stir welding of the joint, it is thermally treated at of temperature 530 degree Celsius after that it is aged at 160 degrees Celsius i.e. (T6) heat treatment. Base material which is heat treated i.e. (T4) and after friction Stir welding heat treatment i.e. (T6) shows that the ductility of the material is reduced considerably after (T6) i.e. about 80 to 90% as cast material.

Sato et.al. [62] takes Al1050 alloy of thickness 1mm which is equal channel angular pressed. After equal channel angular pressing by two passes with the help of dye made up of cell type structure with size of cell is 0.58μm and is nearly 46 HV in hardness. They processed it with friction stir processing process and laser beam. During the laser beam processing process, the microstructure produces is coarse and the grains produced are equiaxed in both fusion and heat affected zone, by which hardness of the material is reduced to less than 30 HV. In contrast to it in case of friction stir processing the microstructure produce is fine because of low amount of generation of heat and plastic strain together. In the area of transition and also in weld zone, the size of grains is less than 1μm, hardness is high in friction stir welding. So, it is concluded that for retaining the strength of alloy, toughness and also for fine grains, FSW is better option.

Reynolds et.al. [63] Selected Al6061 alloy as a base material for friction stir welding. Input parameters for the study are process parameters of friction stir welding and geometry of the tool. They attempted to investigate the force in x-axis and power too with addition of rotational speed and translation speed of the tool. In case of Al6061 alloy, welding per unit length of the weld highest energy is observed. When the force in x-axis increased, then energy of the weld is decreased for all aluminum alloy except Al6061 as this is highly thermal conductive.

Kwon et.al [64] takes Al1050 alloy as a base material and process it with the help of friction stir processing. It is observed that when the speed of rotation of the two decreases, then the properties like hardness as well as the tensile strength increases particularly at the value of 560 rpm the mechanical properties of the sample increases because of the grain refinement of the material.

Charit et.al. [65] Select Al2024 alloy and then process it with friction stir processing. Previously they conduct study on super plasticity of aluminum alloys. To control the growth of grains in an irregular pattern as seen in some alloys of aluminum when processed it with friction stir processing. They develop a new vision by doing optimization of the process, design of the alloy and then finally utilizing it for the FSP in the application of super plasticity in high strain rate. They fixed the speed of transverse at 25.4mm/min, then with speed of rotation of the tool grain size variation are presented. At last they concluded that for speed of rotation greater than 300 rpm and low speed of transverse, irregularity in growth of grain is not observed.

Beron et al. [66]. takes aluminum alloys as Al-Ti-Cu and Al-Ti-Ni, which has very high value of specific strength and then they processed it with the help of friction stir processing. As these techniques are very helpful for imparting the ductility in the material. By friction stir processing of these alloys, good amount of ductility i.e. about 10% and higher value of strength i.e. 650 MPa can be achieved. Because of the homogenization of grains in the microstructure of the samples, improvement in the ductility can be observed. In the present study, authors tries to investigate two processes i.e. one friction stir processing and other one hot isostatic pressing. After that they compare the mechanical properties and the microstructure of Al7075 Alloy in as casted form with the processed one. In case of HIP, the structure is non-homogeneous, ductility is low but strength is high as shown in fig. 2.3. In contrast to it in case of FSP ductility is high in temperature range of 300 to 500 degrees Celsius but strength is low i.e. less than 740Mpa. But in order to improve the strength in case of friction stir processing process, parameters can be optimized to lower the time and temperature. In the conclusion, it can be found that friction stir processing is able to produce aluminum alloys of optimum ductility and high strength. Also, it is found that for are the different types of material to be processed, the key factor is design of tool. In this study many numbers of high-performance tools are also analyzed.
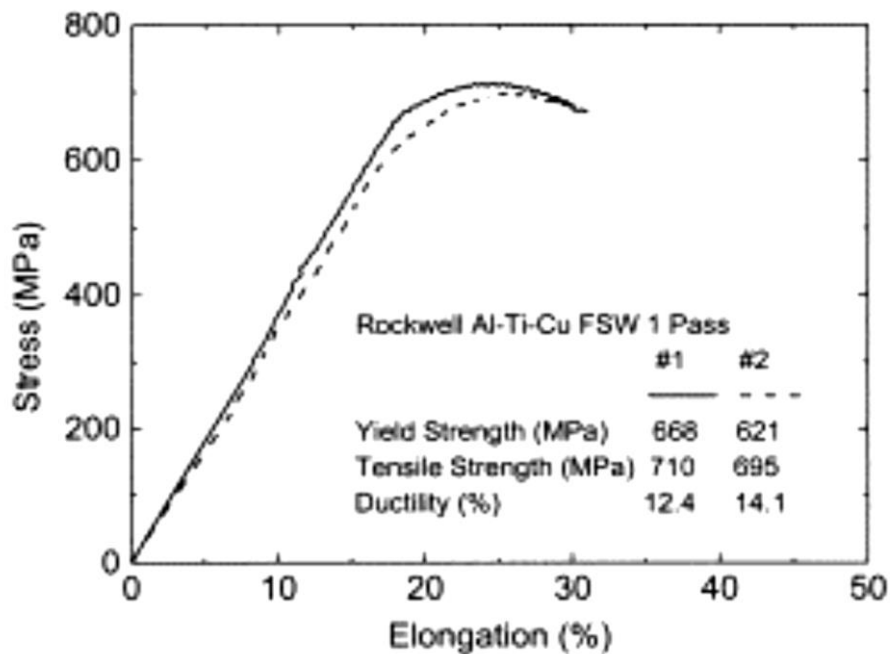
Figure 2.3: Graph of the tensile tests for the FSP material. [66]

Thomas et al. [67] mainly focus on the advancement of tools for the friction stir processing of a ready existing and potential area of materials as well as applications. In the current study, alloys of aluminum with thickness ranging from 1mm to 50mm has been friction Stir welded in one go and also thick Al6082 [T6] plate of 75mm is friction stir welded. Ranging from 6mm to 50mm thickness, number of materials are friction Stir welded with the use of MX Triflute[TM] as shown in fig.2.5 tool in single go. MX Triflute[TM] type of tools reduce the volume to be displaced by 70% and in case of Whorl[TM] it reduces to 60%.

Figure 2.4: Pictorial view of Friction Stir Welded tools Shoulder profile.
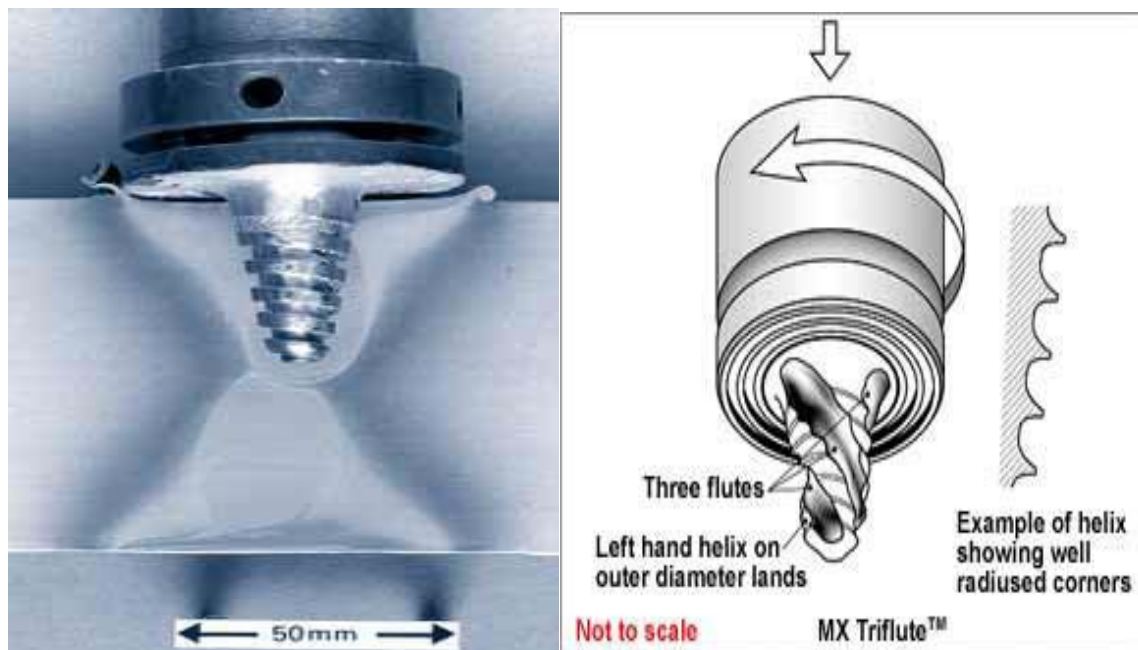
Figure 2.5: i) Prototype of the Whorl[TM] tool. ii) MX Triflute[TM] [67]

Prado et al. [68] studied Al6061 alloy composite with reinforcement of 20% of Al2O3. Tool used is right hand threaded and wear of tool reaches to 0.6%/cm at carbon steel nib, at tool rotation of maximum 1000 rpm in CCW direction. After the 1000 rpm of tool rotation, rate of wear reduces and at 1500 rpm rate of wear is 0.42%/cm and at 2000 rpm, rate of tool wear is 0.56%/cm. It is also found out that, there is zero rate of wear for friction stir welding of same nib which are rotating at 1000 rpm for as cast Al6061 alloy.

Mishra et.al. [69] takes Al7075 alloy as a base material and processed it with the help of friction stir processing and found that super plastic properties increase in great proportion at a temperature of 490°C. There is optimum value of super-plastic strain i.e. 10-2 s-1 and value of elongation is 1000 %, which is maximum. Grain size observed is 3.3±0.4μm in average by using technique called MLIT i.e. mean linear intercept technique and formula for same is grain size is grain size = 1.78 × mean linear intercept.

Ma et.al. [70] Select Al7075 alloy in the form of rolled plates and processed it with friction stir processing. With the variation in process parameters, grain size of about 3.8 and 7.5μm are observed. Also they found that after the heat treatment of the friction stir processed sheets at a temperature of 490°C for time of nearly 1 hour, gives microstructure of fine grains and at high temperature also they are stable. At the temperature of (420-530) °C and rate of stain from 1×10-3–1×10-1 s-1, it is observed when the size of the grains are decreased, then the super-plasticity of alloy is also decreases and this is due to the fact that sliding of the boundaries of the grain as confirmed by the SEM images and also because of shift of low value of temperature of the deformation and high value of rate of strain. It is concluded that at a grain size of 3.8μm of alloy, elongation in super-plastic range is 1250% at temperature of 480°C and range of rate of strain is 3×10-3–3×10-2 s-1. For grain size of 7.5μm, value of ductility is 1042% at temperature of 500°C.

Ma et.al [71] takes Al-4Mg-ZR alloy in the form of extruded bar and then process it with friction stir processing, which results a microstructure with fine grains and size of 1.5μm as compared with the as rolled material as shown in fig.2.6. Rate of strain is ranging from 1×10-3 to 1 s-1 and value of maximum elongation is 1280% at temperature of 525°C, value of super plasticity is 1×10-1 s-1. Also at high value of temperature, thermal stability of fiction stir processed alloy is excellent and flow stresses are also reduced by friction stir processing. At 10-2 s-1 value of rate of strain, 7 (Mpa) flow stress is obtained at a temperature of 450°C and when compared with as-rolled alloy it is almost similar at 550°C.
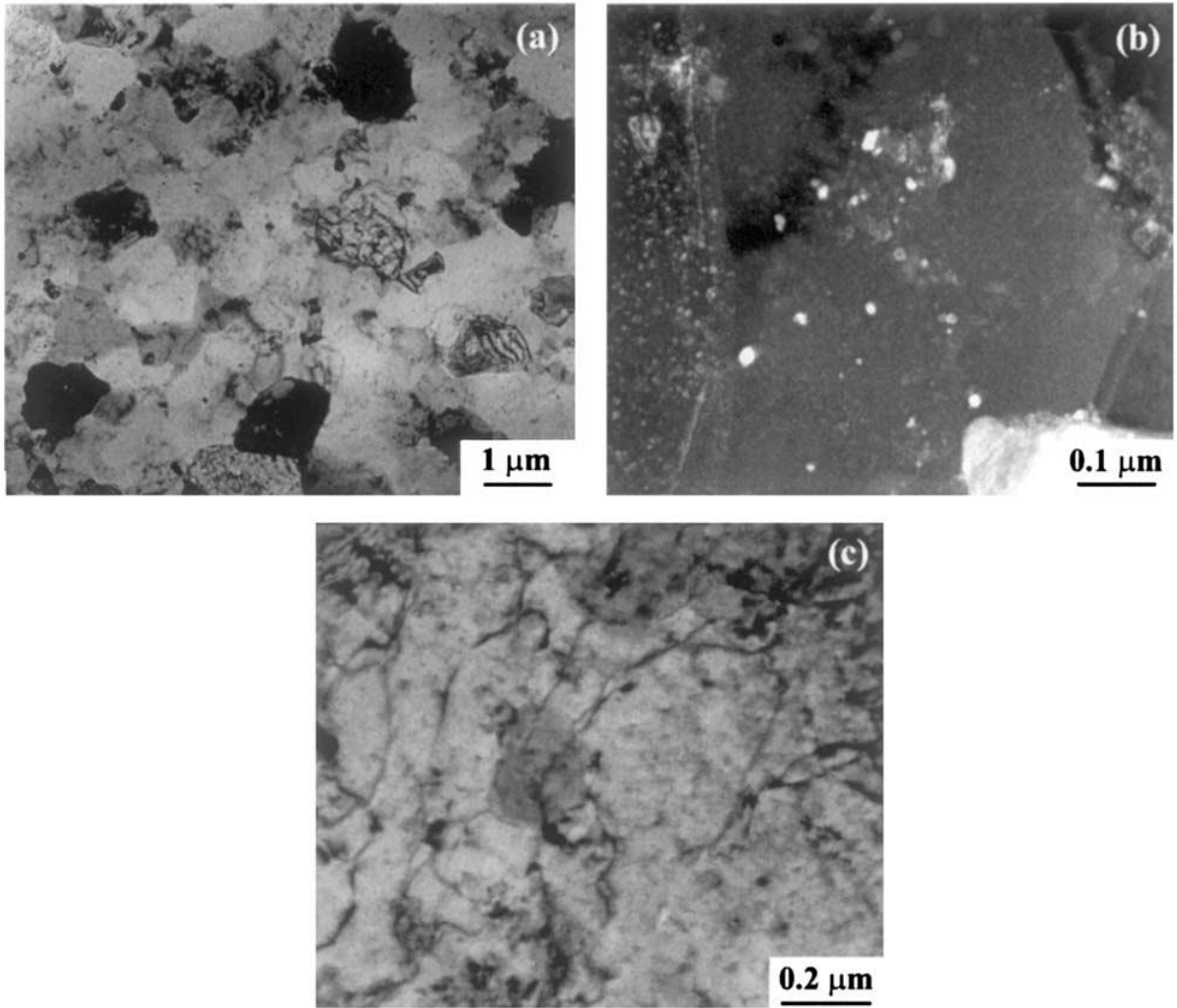
Fig. 2.6. Pictorial view of TEM images (a) fine grains of FSP zone, (b) distribution of Al₃Zr (dark field image), and (c) retained dislocation density in the as FSP condition (bright field image). [71]

Charit et.al [72] takes Al 2024 alloy and then friction stir process it. It is shown that high value of super plasticity can be achieved at the high value of strain rates. While comparing with the as cast material which is non superplastic, high value of ductility can be achieved. At the high rate of stain i.e. 10-2–10-1 s-1, super plasticity can be achieved, earlier in thermo-mechanical processing it is not possible. Maximum elongation obtained is 525% at rate of strain 10-2 s^{-1} and temperature of 430 °C in the current alloy. Mechanism of grain boundary sliding deformation is confirmed by the strain rate sensitivity value of 0.5. If the temperature is increased above 470°C, value of ductility decreases sharply due to uneven grain growth.

Mahoney et.al. [73] takes Al 7050-T651 alloy of thickness greater than 5 mm processed it with friction Stir processing in order to create a microstructure of fine grains. High rate of strain that is greater than 10^{-3} and also super plasticity is observed. Fine grain growth observed even at high rate of strain as compared with the conventional process called thermo-mechanical processing. Although at high rate of strain, high rate of elongation occurs and no diffusion necking occurs.

Chow et.al [74] takes Al5052 as a base material and then apply uniaxial and biaxial type of stress. The main aim of the study is to find the Cavitation behaviour of the tensile specimens. Result revealed that AA5052 available with coarse- grains shows 194% elongation and super-elastic behavior. The prepared samples that is tensile specimens are strained at various temperatures and rate of strains. As compared with Al5083 alloy, in case of Al5052 alloy very low level of growth of Cavitation occurs and also with the increase in strain rate, Cavitation rate also increases.

Chow et.al [75] takes Al5052 alloy as the base material and tries to find the stress state effect that is what is the behavior of the deformation and Cavitation on super plastic type of material. It is found out that in case of Al5052 alloy with coarse grains, deformations starts at optimal temperature i.e. 873K and conditions of stress are biaxial state. Also in the present study, it is found that when the level of strain is increases, number of cavities are also increases.

Essam B. Moustaf et al. [76] utilizes friction stir processing for the fabrication of aluminium-magnesium alloy as Matrix with the reinforcement of silicon carbide particle at nano level and also with aluminium oxide particle at same level. The aim of the work is to increase the resistance of wear and hardness of the specimens. Output parameters are rate of wear, microstructure and hardness of fabricated samples as shown in fig. 2.7. Result of the work shows that the reinforcement of the alloy of aluminium AA5250 with the particles of nano-ceramic causes particle to be more refined. So due to which hardness of the specimen fabricated increases i.e. 90% in case of aluminium oxide reinforcement and 30% in case of silicon carbide (SiC) particles. Resistance to the rate of wear is improved in both for aluminium oxide and silicon carbide reinforcements, but for the silicon carbide fabricated sample it is approximately 5.7 more than that of aluminium oxide particles nanocomposite.
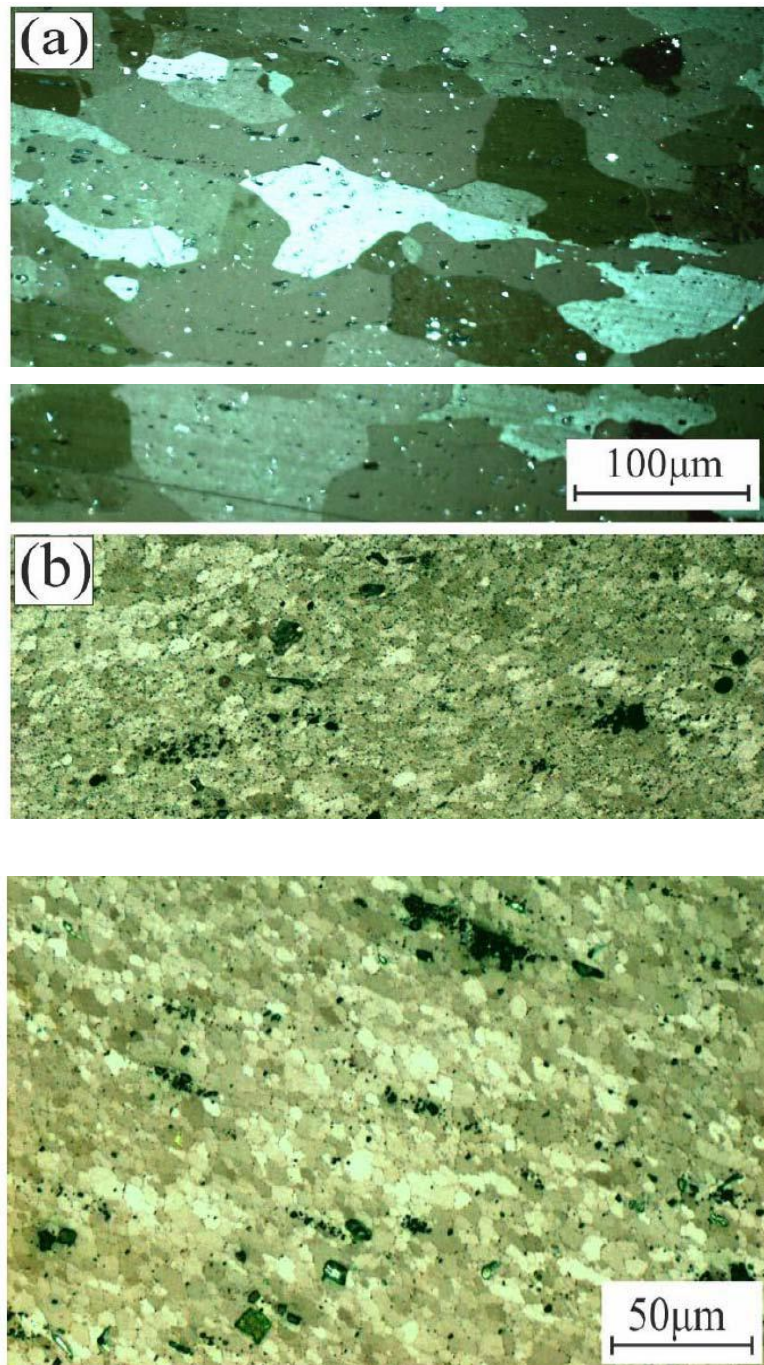
Figure 2.7: Pictorial view of microstructure of (a) AA5250 alloy as base, (b) when reinforced with particles of Al2O3, and (d) when reinforced with particles of SiC. [76]

D. Hari et al. [77] takes Al5083 alloy of aluminum and process it with friction stir processing. Input parameters are speed of rotation and speed of tool travel. Output parameters are microstructure and micro-hardness. Result revealed that ultra-fine refined grains were formed at a speed of rotation of 1000 rpm, because of the alternate rapid solidification cycle and as of high heat input rate. So, because of the grain refinement micro-hardness of the specimens are

38

also increases, very high value of the micro-hardness is found out at the nugget zones due to Ultra level of refinement of grains at that zones.

Ali Ajani et al. [78] did research work mainly in the area of carbon nanotube as reinforcement, in the matrix of ceramics and polymers. In the present study, they taken Al6061 as a base material and then reinforce it with carbon nanotubes with the method of friction stir processing. The output parameters for the study are ultimate tensile strength, ductility and yield strength. For the input of speed of rotation i.e. 1500 rpm and rate of feed i.e. 80mm per minute, strength reaches at 178 MPa. SEM study is also conducted for the fabricated samples in order to find the morphology of the fractured surface and also to get the idea for the ductile failure as shown in fig.2.8. During friction stir processing, maximum temperature rise is 270 degrees Celsius which is below the melting temperature of base material but far above the temperature of the plasticization.
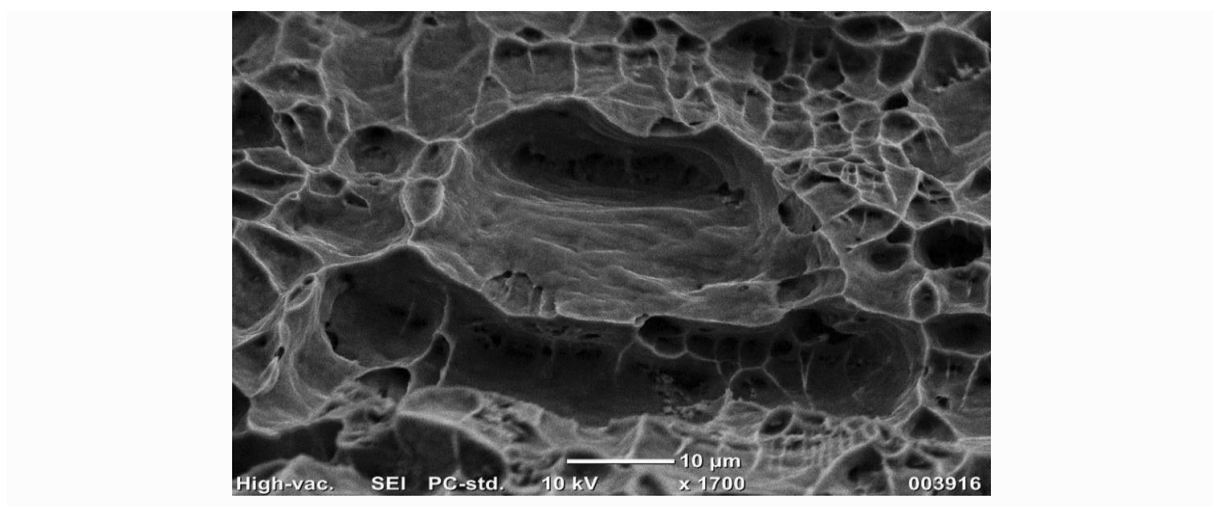
Fig. 2.8. Pictorial view of SEM image for the fracture morphology.[78]

Pabitra Maji et al. [79] choose aluminum 7075 as a base m aterial and fabricated it with particles of MoS2 and CeO2 and then processed it with friction stir processing. After the microstructural study it is found that composite is free of intermetallic compound and uniformly distribution of particles is made (fig.2.9). Then the rate of corrosion and specific wear is interpreted for the fabricated material. Input parameters are speed of transverse, speed of rotation, angle of tilt and the ratio of mixing that is volume percentage of particles reinforced. Method for design of experiment are Taguchi's optimization method and grey relational approach. The main reasons which are responsible for variation are also observed. Along with-it conditions of processing for individual response are also found out.
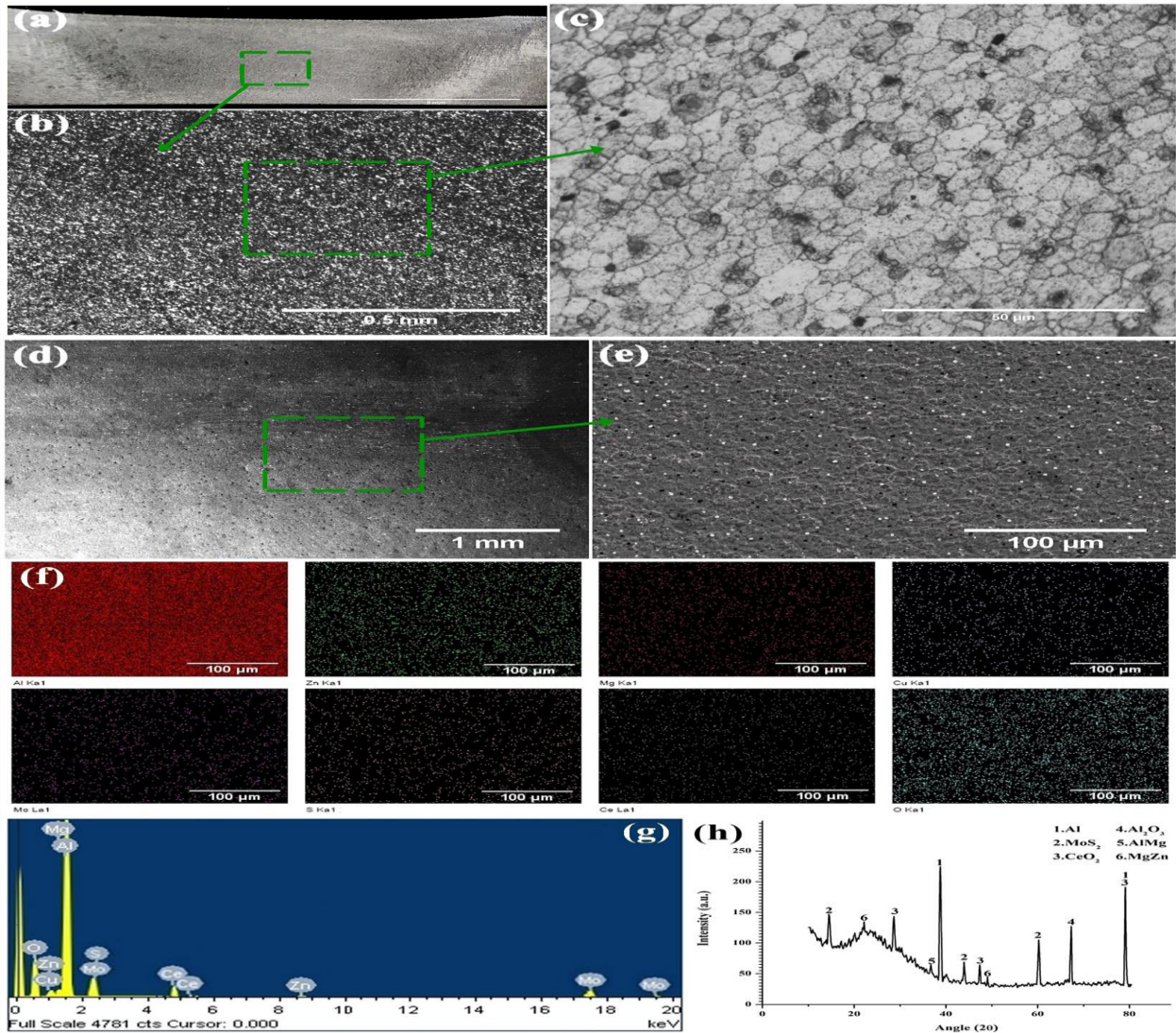
Fig. 2.9 (a–c) Pictorial view of OM images, (d–e) Pictorial view of SEM images, (f) Distribution of elements, (g) EDS spectrum and (h) Pictorial view of XRD graph of Specimen. [79]

Bazani Shaik et al.[80] take aluminium alloy as a base material processed it with friction stir processing. Parameters on which they are working are axial force, angle of tilt, speed of rotation and speed of welding. They used Taguchi's L9 orthogonal array as design of experiment. Output parameters on which they are working are micro-hardness and tensile strength. At speed of welding i.e. 60 mm/min., angle of tilt i.e. 3^0, speed of rotation i.e. 1250 rpm and axial force i.e. 12 KN, the tensile strength obtained is 167 MPa, which is measured as per standard of ASTM. The relation of obtained are very useful for the creation of design for automated systems.

Kia Wai Liew et al. [81] take recycled alloy of aluminum 6063 and processed it with the help of friction stir processing. The main motive of their study is to investigate friction stir processing parameters and geometry of toll pin on the micro-hardness and the roughness of the surface. Varying the geometry of the tool pin greatly affects the output as because of it flow of material changes and heating is localized. In this study mainly two types of tool pin geometry are taken that is taper thread and cylindrical threaded, with the variation of parameters like rate of feed and speed of rotation. After the processing of work piece by friction stir processing, mechanical properties like roughness of the surface, microstructure and micro-hardness are found out. After all the analysis it is concluded that tool of geometry in taper threaded form gives a great improvement in the micro-hardness of the specimen i.e. 63% at lower speed of rotation i.e. 150 RPM and at the rate of feed i.e. 30mm/min. Also at that values microstructure of the sample is finer grains and the distribution of grain is homogeneous and compact as shown in fig.2.10. Again, for the tool of threaded geometry, the surface roughness is quite better than the cylindrical threaded type of tool. But it is noted that in case of cylindrical threaded tool, at rate of speed of 30 mm/min. surface finish is smooth than that of threaded taper tool.
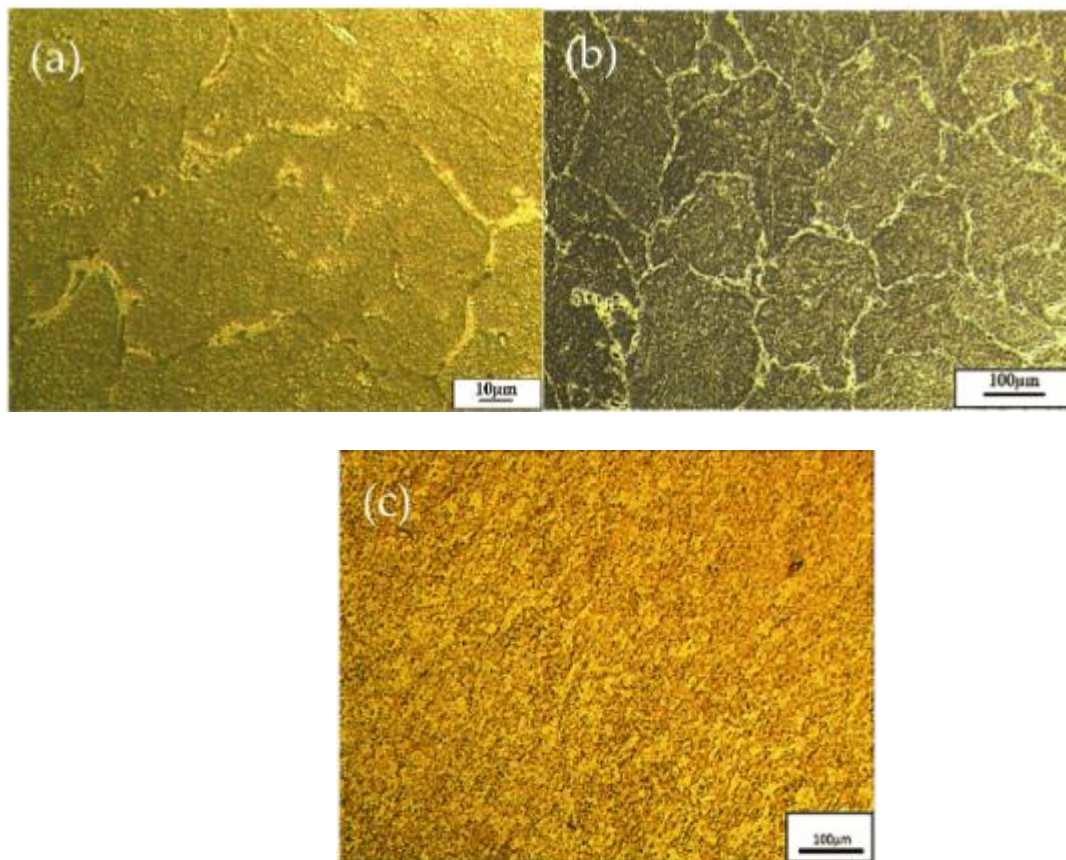
Fig 2.10: Microstructure of AA6063 substrate at magnification of i) 50x ii) 10x iii) stir zone at 10x. [81]

Mostafa Akbari et al. [82] studied aluminium alloy processed by friction stir processing. In-situ cooling effect is investigated during the friction stir processing of the alloy. Parameters like flow of material, resistance to wear, distribution of temperature, axial force, mechanical properties and alloy microstructure is studied. Finite element model is also developed for the study by using the approach of Eulerian and Lagrangian and then the same is verified by history of temperature and experimental force. In situ cooling effect during friction stir processing is observed on the distribution of temperature and flow of material. Experimental tests like hardness, rate of wear and optical microscopy can be done. After that stir zone of both experimental and simulated model with in situ cooling and without of it are compared. It has been observed that with the use of in situ cooling, the flow of material is significant in the area of pin driven as compared to the shoulder zone causing the stir zone conversion from basin to V-type. Stir zone in both simulated and experimental are comparable good. It is also found out that in-Situ cooling process decrease the size of the particles of Si, hence properties like hardness of material, resistance to wear increases. Reduction in size of the Silicon particle is from 10 µm as in base material to the 2.6 µm in air cooled medium and 2µm in water-cooled medium. Also, if we compared with the non-cooled specimens, rate of wear reduces approximately by 28% for air-cooled medium and 40% for water cooled medium, hardness increases 80% for water-cooled specimens and 35% for air-cooled specimens.

Sampath Boopathi et al. [83] studied the fabrication of aluminium alloy with the reinforcement of boron carbide particles by friction stir casting process. The base material selected is Al6061 alloy and the reinforcement particles are B4C. Approach for design of experiment used is Taguchi's L9 Orthogonal array. The variable parameters are volume percentage of particles of boron carbide, speed of rotation, feed rate of travelling. Rate of wear and tensile strength were investigated. The selection of tool is subjected that its travel speed and speed of rotation is Moderate so that optimum response can be observed. The minimum wear obtained is 55 µm and higher tensile obtained is 347Mpa. Optimum parameters are tool travel speed 40mm/min., Speed of rotation is 1400rpm, volume percentage of B4C is 15%.

Vivek Patel et al. [84] select AA7075 aluminium alloy which is of high strength nature and tries to look into the surface topography of the alloy when it is processed through the stationary shoulder friction stir processing process. The shoulder used is of non-rotating nature produces smooth surface finish. They used the unique 3D mapping approach for the surface evaluation by high end digital microscopy in order to find out the quantitative and qualitative nature of

the processed surface. It has been observed that some amount of flash is generated on the surface to be processed and also the technique of the 3D mapping used shows the roughness of the processing zone in both longitudinal and transverse direction. It has been confirmed after examining the roughness value i.e. both peak as well as average that in both longitudinal and transverse direction. Surface finish produced is better in transverse direction and too at high speed of tool rotation and on the other side uniformity is better in longitudinal direction as shown in fig 2.11.
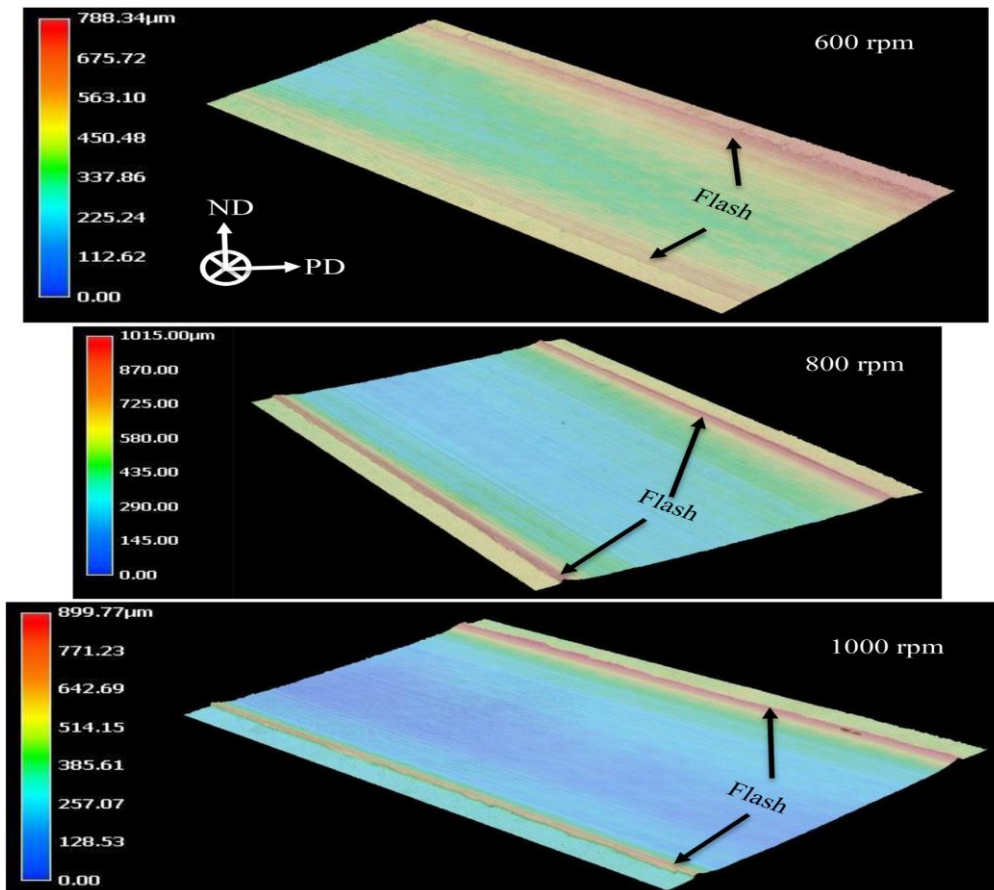
Fig. 2.11. Pictorial view of surface topography in 3D, when processed by FSP, produced at different speeds of rotation of tool. [84]

R. Raja et al. [85] fabricated the Aluminum 6063 composite as a base material with reinforcement of aluminum oxide and particles of zirconium dibromide by the process known as friction stir processing i.e. FSP as shown in fig.2.12. After that the specimens for the testing of the tensile strength is prepared as per the standards according to the ASTM-E8. Then with the help of UTM, tensile strength of the fabricated material is found out. It is confirmed from the results obtained that the tensile strength of the samples reduced when the addition of percentage of volume of the reinforcement in the fabricated material.

Fig. 2.12: A) Pictorial view of Vertical Milling b) Pictorial view of H13 steel tool for FSP.[85]

Fig. 2.13: Pictorial view of Samples after FSP. [85]

M. Mostafavi et al. [86] studied the Al-4.5cCu alloy with content of silicon 1%, 3% and 5% by weight percentage. The main aim of their study is post process aging effect on the mechanical properties as well as the microstructure of alloy, when it is friction stir processed by multiple pass. As per the results obtained, addition of Si increases the content of fluidity and at same time porosity content of decreases. Upto 3% wt% of the Si addition, tensile strength increases, but with further addition of the content of Si i.e. upto 5% wt%, it starts decreasing. Frictions stir processing with first pass, increases both tensile strength by 25% and fracture strain by 125% for an alloy with Si at 3% wt%. After the 2nd and 4th pass, fracture strain of alloy increases but hardness and tensile strength both decreases. Friction stir processing with post processing i.e. aging for time 8 hrs and temperature 180ºC, increases mechanical

44

properties as compared with the as-cast alloy, properties improves as toughness by 310%, Fracture strain by 175%, hardness by 107% and tensile strength by 108%. With the effect of post processing i.e. aging on alloy, fracture morphology of surface is changed. As in cast conditions it is quasi-cleavage mode and after post processing it is ductile-dimple fracture confirmed by fractography results.

Friction Stir Processing (FSP) is a technology for solid-state joining and material processing that is used to improve the microstructure of metals, notably aluminium alloys. It uses a spinning tool to create frictional heat and mechanical deformation in order to change the material without melting it. While FSP is most commonly used for welding or mending, it may also be used to improve the characteristics of aluminium alloys such as aluminium 5086. Aluminium 5086 is a non-heat treated aluminum-magnesium alloy with moderate strength and strong corrosion resistance. The microstructure of Aluminium 5086 may be modified by FSP, leading in improved mechanical characteristics and perhaps higher performance. FSP may efficiently reduce grain size, increase grain refinement, and minimise material flaws.

Among the possible advantages of friction stir treated aluminium 5086 are:Strengthening: FSP may cause grain refinement and the creation of a more homogenous microstructure, which results in enhanced mechanical characteristics such as greater strength and hardness. Enhanced corrosion resistance: The refined microstructure achieved by FSP can contribute to improved corrosion resistance, making the aluminium alloy more robust and appropriate for harsh environment applications. Friction stir processing can improve aluminium 5086 fatigue performance by minimising the presence of flaws and enhancing the distribution of strengthening precipitates within the microstructure. FSP may also be used as a pre-welding treatment for aluminium 5086, making it simpler to weld and lowering the possibility of weld zone flaws.The particular improvements and advantages obtained by friction stir processing may differ based on process parameters, tool design, and other considerations. As a result, it is critical to properly optimise the FSP settings for the individual application and intended result.

RESEARCH PROBLEM FORMULATION

The chapter covers the research problem formulation on the basis of research gaps. Moreover, this chapter also describes the research objectives for the chosen technique to form aluminum metal matrix composites.

Friction Stir Processing is a technique that integrates micro and nano-scale reinforcements into aluminium alloys to form metal matrix using various process parameters/additives. These investigations can shed light on the effects of various reinforcement sizes and processing techniques on composite characteristics. There characteristics further are incorporated as per the needs of the application to be provided as a resultant specification of the product. Therefore, when dealing with micro- and nano-scale reinforcements in aluminium composites research is required before the incorporation of material.

Aluminum alloys have high surface-to-volume ratios and potential for enhanced dispersion within the matrix, micro- and nano-scale reinforcements provide unique options for improving material characteristics. The dispersion and homogeneity of these small-sized reinforcements, on the other hand, can be difficult, necessitating careful control of processing parameters and possible surface modification approaches. Micro- and nano-scale reinforcements can be made of a variety of materials, including ceramic particles, carbon nanotubes, graphene, and metallic nanoparticles. The reinforcement should be chosen based on the required composite qualities and compatibility with the aluminium matrix.

Achieving a homogenous distribution of micro-scale and nano-scale reinforcements inside the aluminium matrix is crucial for optimizing the composite's performance. Ultrasonic dispersion, surfactant-assisted dispersion, and chemical functionalization can all help achieve uniform dispersion and strong interfacial interaction between the reinforcement and the matrix.

FSP factors, such as tool design, rotation speed, traverse speed, and dwell time, have to be optimized to fit the unique mix of aluminium 5086 and micro-scale/nano-scale reinforcements. The processing factors, such as uniform reinforcement distribution and grain refining, are critical in attaining the necessary microstructural characteristics. Characterization Techniques:

to assess the microstructure, mechanical characteristics, and performance of the produced surface composite, comprehensive characterization techniques to be selected and deployed.

While there is limited study on the combination of micro-scale and nano-scale reinforcements with aluminium 5086 especially with Friction Stir Processing, it is critical to draw on relevant studies in the area and seeking advice from the specialists to direct research efforts. Informed judgements may be utilized and contribute to the advancement of surface composites with micro-scale and nano-scale reinforcements using FSP with vertical machining centers or other comparable systems while considering the fundamental principles of composite material processing.

Because of the possible synergistic effects and the unique features of both materials, the combination of nano-sized silicon carbide (SiC) with graphene reinforcements in composite materials has piqued the curiosity of many researchers. Although research on this particular combination is limited, it has the potential to improve surface characteristics through microstructural improvement.

Combining nano-sized SiC and graphene reinforcements has the potential to provide synergistic effects in which the combined reinforcements outperform the individual reinforcements. The composite's overall performance may be improved by combining the high strength and stiffness of SiC particles with the remarkable mechanical, electrical, and thermal capabilities of graphene. The addition of nano-sized SiC and graphene reinforcements can improve composite mechanical characteristics. SiC particles have great hardness, strength, and wear resistance, but graphene has strong tensile strength and stiffness. The combination of these reinforcements can increase the composite material's tensile strength, hardness, fracture toughness, and fatigue resistance. The thermal characteristics of nano-sized SiC and graphene are both outstanding. SiC has a strong thermal conductivity, which helps improve the composite's heat management capabilities. Graphene, with its high thermal conductivity, can boost heat dissipation even more. When these reinforcements are combined, composites with improved thermal conductivity and heat dissipation qualities can be produced.

Graphene is a highly conductive material, whereas SiC is normally electrically insulating. The inclusion of graphene to the SiC-reinforced composite has the potential to increase electrical conductivity, making it ideal for electrical conductivity or electromagnetic shielding applications.

Achieving uniform dispersion and strong interfacial interaction between the nano-sized SiC, graphene, and matrix material (such as aluminium) is crucial for the composite's effective development. Surface functionalization and dispersion procedures are used to achieve optimal reinforcement distribution and bonding inside the matrix. Processing Techniques such as Powder metallurgy, mechanical alloying, and liquid-phase processes may all be used to create aluminium composites with nano-sized SiC and graphene reinforcements. Furthermore, friction stir processing (FSP) may be used to include these reinforcements into the aluminium matrix, allowing for a solid-state approach to composite production. Optimizing processing factors such as reinforcement content, dispersion methods, FSP parameters (e.g., tool design, rotation speed, traverse speed), and post-processing treatments is critical for attaining the required composite microstructure and attributes. While there is minimal study on the specific combination of nano-sized SiC and graphene reinforcements in aluminium composites.. These investigations can provide light on the individual reinforcement effects and help to guide the creation of the combined reinforcement system.

3.1 RESEARCH GAPS

Following research gaps have been identified:

1. However, limited research is available on micro-scale and nano-scale sized reinforcement combination.
2. Very limited research is available on nano-SiC and graphene reinforcement combination.

RESEARCH OBJECTIVE

Following objectives have been chosen to cover the research gaps for the current study endeavor after an extensive literature review:

1) To synthesis and develop Al-Graphene-SiC surface nano-composite by friction Stir Processing technique.

2) To study the effect of various process parameters such as nano-particles, rotational speed, transverse speed, tool geometry, no of passes (constant parameter) on the microstructure, morphology of Al-Graphene-SiC surface nano-composite using scanning electron microscope (FE-SEM), EDS, TEM, and X- ray diffraction (XRD).

3) To determine the mechanical properties hardness and elastic modulus, and toughness of as-developed Al-Graphene-SiC surface nano-composite.

4) To study the wear resistance of as-developed Al-Graphene-SiC surface nano-composite.

MATERIALS, METHODOLOGY, AND EXPERIMENTATION

The materials and experimental apparatus utilized for the study are described in depth in this chapter. The research includes the employment of an experimental test rig, a friction stir processing machine, a workpiece, a stirring tool and powder additives.

4.1. Selection of Workpiece Material and its Characterization

In the era of modernization, the manufacturing sectors have always been in the search and development of new multiscale and multifunctional materials with superior quality for higher productivity and efficiency. Aluminum alloys and its composites have been the ultimate choice because to their lightweight, outstanding mechanical, and tribological qualities. Aluminum matrix composites (AMCs) are becoming more popular in the automotive and aerospace industries due to their high strength-to-weight ratio and low carbon emissions. The desired properties of AMCs have been tailored by processing the matrix material and a suitable reinforcement. Friction stir processing (FSP) has drawn the most interest from researchers among various plastic deformation and microstructural modification techniques, owing to its outstanding qualities such as solid state and eco-friendly processing. The FSP has been proved an innovative manufacturing method based on the principle of friction stir welding and has been used extensively for a wide range of practical applications, including grain refinement of metal surfaces and the development of functionally graded composites. In the present research work, Al5086 plate dimensions of 110 x 50 x 5 mm were chosen for friction stir processing. Figure 4.1 shows the SEM-micrograph of Un-processed Al5086 alloys. Tables 4.1 and 4.2 show the chemical composition and mechanical properties of the parent metals.
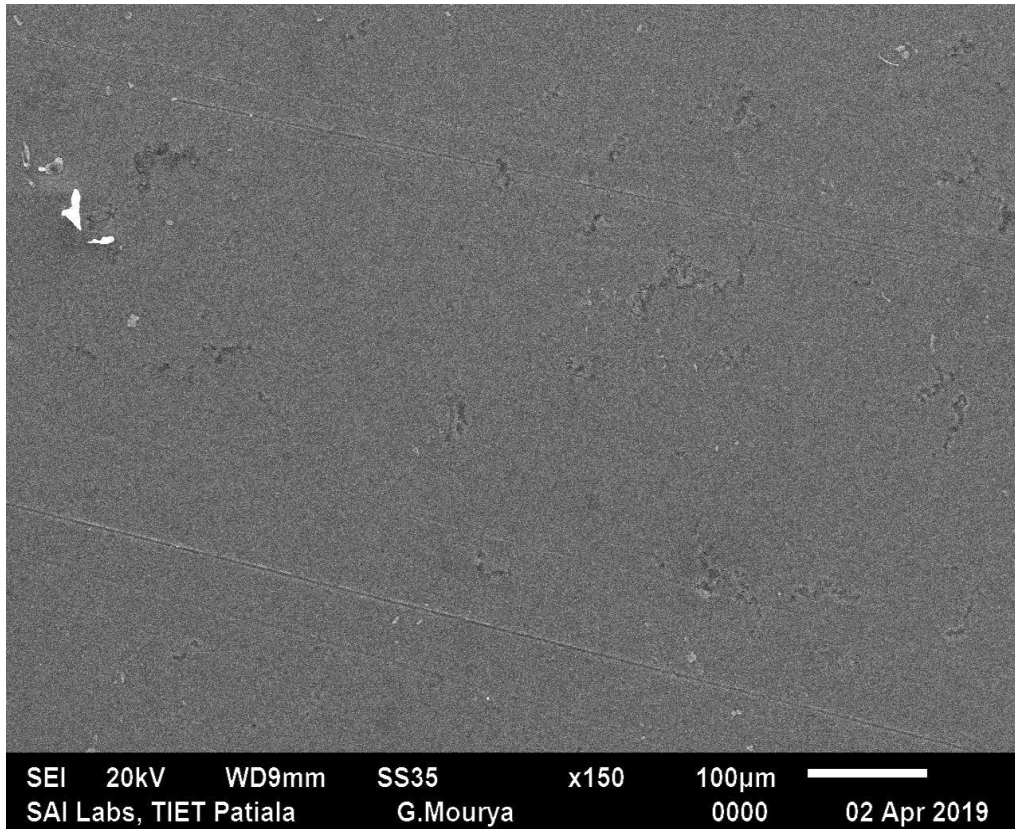
Figure 4.1: SEM-micrograph of Un-processed Al5086 alloys (SAI Labs, TIET Patiala)

Table 4.1. Chemical composition of base material, Al5086 alloys in weight %. (Central Tool Room-Indo German, Ludhiana)

Material	Cu	Si	Mn	Mg	Fe	Cr	Ti	Zn	Al
AA5086	0.001	0.21	0.65	4.25	0.29	0.065	0.007	0.05	94.49

Table 4.2: Mechanical properties of base material (Al5086 alloy). (Central Tool Room-Indo German, Ludhiana)

Ultimate tensile strength (MPa)	Yield strength (MPa)	Elongation (%)	Hardness modulus (Hv)	Elastic Modulus (GPa)
245	117	13	84	75

Figure 4.2 (a-b) shows the SEM micrograph of graphite (GRP) and micro-size silicon carbide (SiC). In order to develop surface composite GRP and SiC was used as reinforcement. The

GRP and SiC powders of were mixed together in the ratio of 1:1 using a high energy planetary ball mill (Make: Retsch, Cryomill) to obtain a homogenized blend. The GRP and SiC powder in 99.99% pure and purity levels can be seen via EDS spectrum and Raman spectrum.
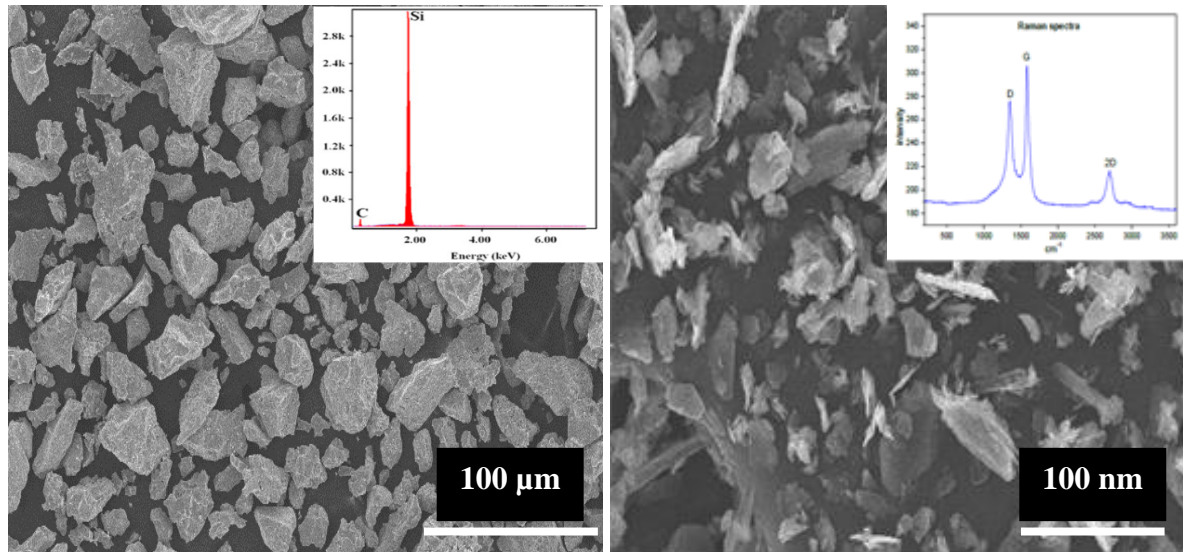
Figure 4.2: SEM image, EDS spectrum and Raman spectrum of powders: (a) SiC and (b) Graphite

4.2. Friction Stir Processing

In the present research work, Al-based surface composite has been developed using micro-size and nano-scale reinforcements. In the first phase nano-scale graphite and micro-size silicon carbide reinforcement was used to develop surface composite using friction stir processing. The detailed characterization and mechanical properties of as-developed Al5086-GRN-SIC surface composite has been studied. In the second phase nano-scale graphene and silicon carbide reinforcement was used to develop surface composite. The detailed characterization and mechanical properties of as-developed Al5086-GRN-ηSIC surface composite has been studied.

4.2.1. Experimental Setup of Friction Stir Processing

Figure 4.3 shows the friction stir processing (FSP) setup designed and developed using vertical milling machine with a maximum motor capacity of 3.7 kW. The dimensions of backing-plates and fixtures were chosen as per length and width of milling machine table. Vertical clamping pressures were used with pressure bars to prevent plates from lifting and provide uniform temperature distribution across the plates. To avoid the discretion of two plates and provide side pressure on the workpieces during welding, two L-shaped mild steel plates are utilized,

with two end-screwed bolts on each plate. Before FSP, the holes (1.5mm depth × 2 mm dia.) were drilled on the Al5086 plate substrate at an interval of 5 mm along the line of processing and the configuration of the holes are shown in Fig. 4.3. The powder particles were filled into these holes. After filling powder in the holes, to prevent sputtering of the filler reinforcements and its ejection from holes during the process, the holes were covered by a straight cylindrical friction stir tool (SD 20 mm) without pin, as can be seen in Fig. 4.4(a). After that, friction stir processing was carried out on the covered surface plate specimens using tool with shoulder diameter of 20 mm.
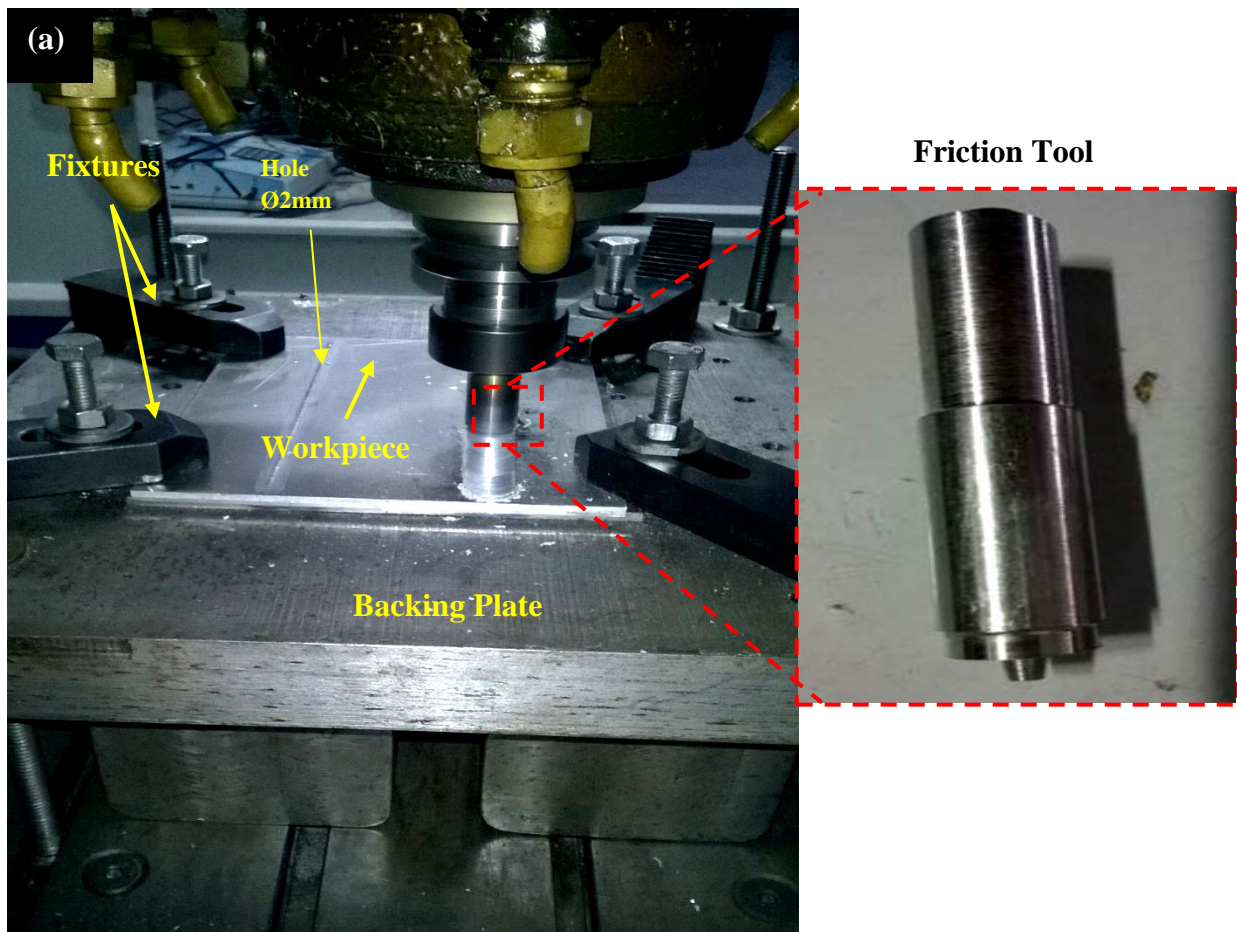
Figure 4.3: Experimental set-up of Friction stir processing and stirring tool

The blended mixture of GRN and SiC powder particles was filled into these holes as shown in figure 4.4(a) and the holes were covered by a straight cylindrical friction stir tool (SD 20 mm) without pin, the friction stir process is initiated by covering the holes so that a layer is formed on the top, then after that the pinned tool is used to form the metal matrix in the stir zone.

 The FSP experiment was carried out by varying the traversal speed (rotation speed & traverse speed) and tool placement(plunge depth) while maintaining the other parameters constant. The

process parameters were chosen based on trial tests that took into account parameters from the literature [64-70] as well as the machine's spindle and transverse speeds. The length of the pin is 2.8 mm and 16 mm shoulder diameter having 2º concave angle which tapered from 3 to 5 mm. The experiment was carried out by varying the transverse speed, rotational speed, and plunge depth, as can be seen in Table 4.3.

Table 4.3: Process parameters and their levels selected for the experimentation (as per literature review minimum intermediate and maximum values are chosen)

S^N	Parameters	Level 1	Level 2	Level 3
1	Rotation speed (rpm)	1200	1500	1800
2	Traverse speed (mm/ min)	30	35	40
3	Plunge Depth (mm)	0.1	0.2	0.3
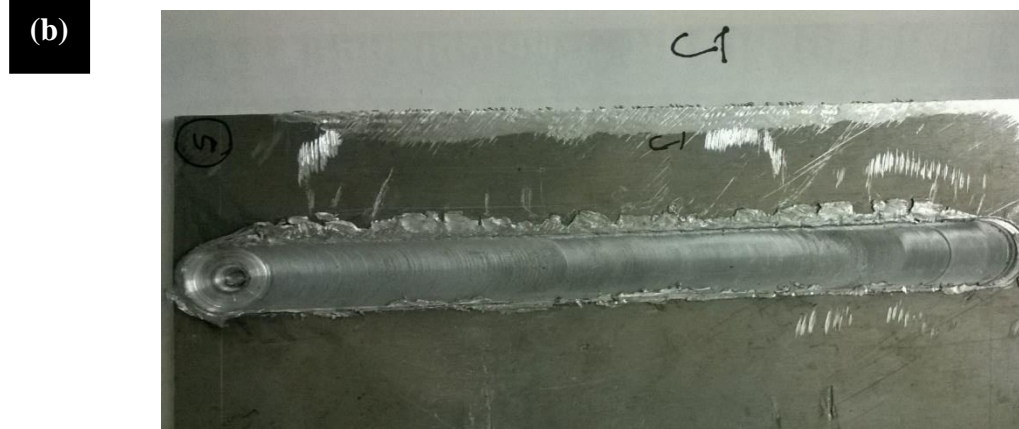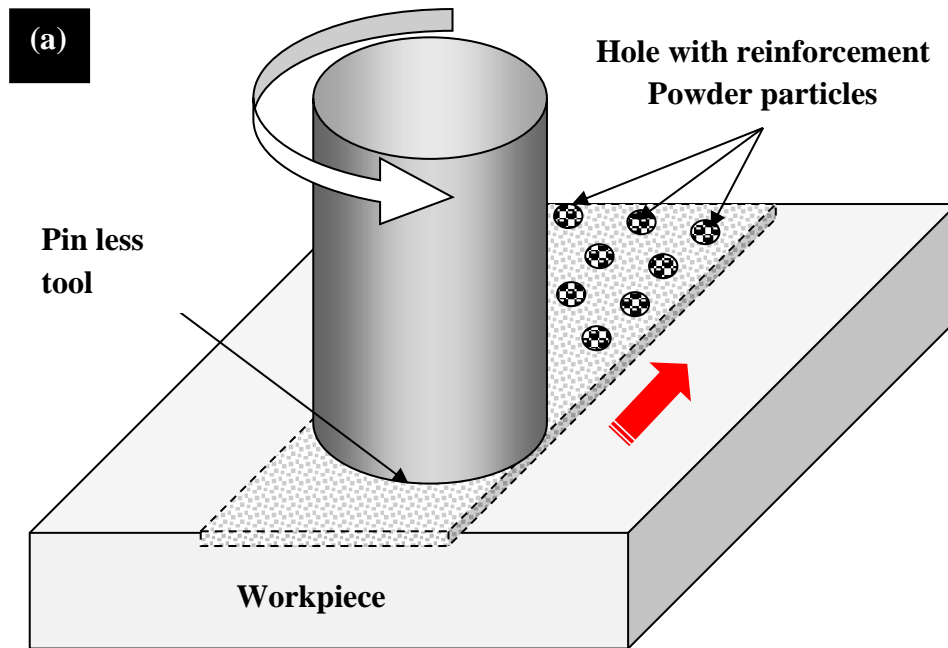
Fig. 4.4: (a) Schematic representation for the development of Al5086-GRN-SiC surface composite using FSP process and (b) workpiece after processing

4.2.1.1.   Taguchi Design of Experiment

Taguchi's methodology has been chosen to design of experimentation. According to table 4.4, L-27 or L-9 orthogonal array can be chosen for experimentation. Table 4.4 and 4.5. shows the design of experimentation for the research work.

Table 4.4: L-27 (3^3) orthogonal array (parameters assigned) with response

Sr. No.	Run order	Responses						
		1	2	3		Raw Data		S/N Ratio
		A	B	C	R_1	R_2	R_3	
1	3	1	1	1	Y_{11}	Y_{12}	Y_{13}	S/N_1
2	11	1	1	1	Y_{21}	Y_{22}	Y_{23}	S/N_2
3	21	1	1	1	-	-	-	-
4	15	1	2	2	-	-	-	-
5	23	1	2	2	-	-	-	-
6	5	1	2	2	-	-	-	-
7	18	1	3	3	-	-	-	-
8	8	1	3	3	-	-	-	-
9	17	1	3	3	-	-	-	-
10	20	2	1	2	-	-	-	-
11	2	2	1	2	-	-	-	-
12	10	2	1	2	-	-	-	-
13	4	2	2	3	-	-	-	-
14	13	2	2	3	-	-	-	-
15	24	2	2	3	-	-	-	-
16	16	2	3	1	-	-	-	-
17	25	2	3	1	-	-	-	-
18	9	2	3	1	-	-	-	-
19	12	3	1	3	-	-	-	-
20	19	3	1	3	-	-	-	-
21	1	3	1	3	-	-	-	-
22	22	3	2	1	-	-	-	-
23	6	3	2	1	-	-	-	-
24	26	3	2	1				
25	7	3	3	2				
26	14	3	3	2	-	-	-	-
27	27	3	3	2	Y_{27}	Y_{27}	Y_{27}	S/N_{27}

Table 4.5: Control log of experimentation as per Taguchi L27 orthogonal array.

Sr. No	Rotational Speed (rpm)	Transverse Speed (mm/min)	Plunge depth (mm)	Taper Angle (Degree)	Tensile strength (MPa)	Micro-hardness (MPa)
1	1200	30	0.1	2	162.7	159.5
2	1200	30	0.2	3	178.1	155.7
3	1200	30	0.3	4	199.4	182.3
4	1200	35	0.1	3	206.6	199.3
5	1200	35	0.2	4	205.8	190.9
6	1200	35	0.3	2	206.9	191.4
7	1200	40	0.1	4	205.1	194.5
8	1200	40	0.2	2	206.3	190.8
9	1200	40	0.3	3	204.5	196.7
10	1500	30	0.1	2	205.6	198.4
11	1500	30	0.2	3	206.7	197.6
12	1500	30	0.3	4	206.8	191.5
13	1500	35	0.1	3	205.1	192.4
14	1500	35	0.2	4	204.8	193.8
15	1500	35	0.3	2	204.3	194.9
16	1500	40	0.1	4	206.9	198.9
17	1500	40	0.2	2	208.4	193.7
18	1500	40	0.3	3	207.4	192.9
19	1800	30	0.1	2	206.3	198.5
20	1800	30	0.2	3	208.7	192.5
21	1800	30	0.3	4	207.1	196.1
22	1800	35	0.1	3	208.8	196.7
23	1800	35	0.2	4	209.6	193.8
24	1800	35	0.3	2	208.1	196.8
25	1800	40	0.1	4	209.8	191.9
26	1800	40	0.2	2	207.8	199.2
27	1800	40	0.3	3	208.2	195.5

4.2.2. Additive Powder Fed Friction Stir Processing (APF-FSP)

In the current research work, the additive powder fed friction stir processing (APF-FSP) as an innovative surface engineering technique has been proposed for the synthesis of graphene (GRN) and nano-silicon carbide (ηSiC) reinforced Al-alloy based hybrid surface composite. Figure 4.5(b) shows the experimental set-up of powder fed friction stir processing (APF-FSP) using vertical milling machine with a maximum motor capacity of 3.7 kW. The APF-FSP comprised two system including screw extruder and tool, refer Fig. 4.5(a). The screw extruder rotates at the same speed of tool and exerts hydrostatic pressure that feeds the colloidal nanoparticle paste of graphite and ηSiC in the Al5086 alloy matrix, refer Fig. 4.5(b). For friction processing a special design tool was fabricated from tungsten-carbide materials, which comprised threads that increased the materials flow due to plastic deformation during processing and micro-sized drilled hole (0.8 mm) for injecting colloidal nano-particle paste. The length of the pin is 3 mm and 16 mm shoulder diameter having 2º concave angle.
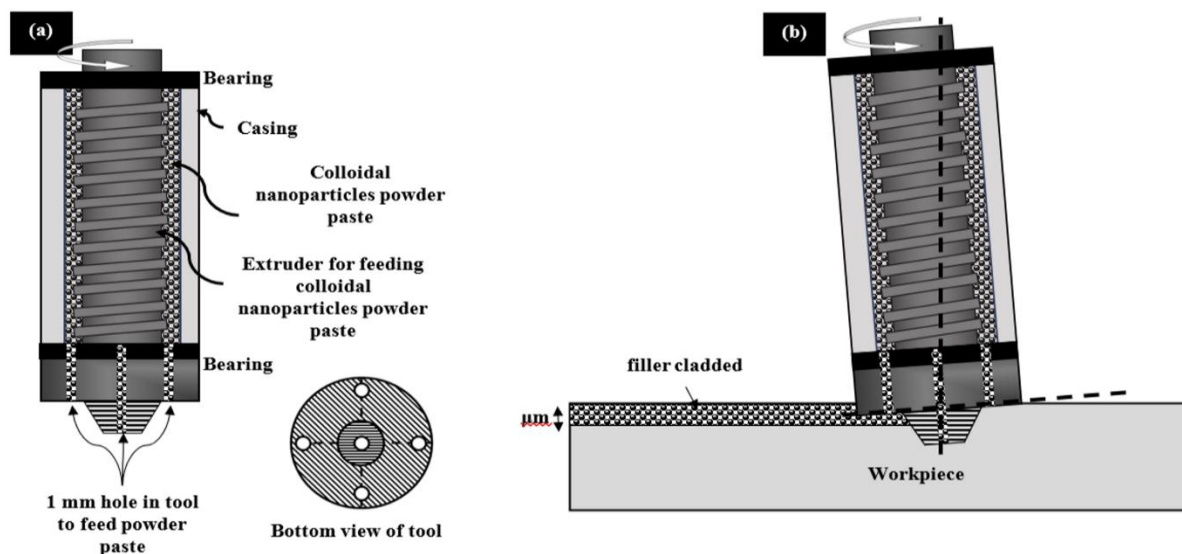
Figure 4.5: (a) Tool geometry, (b) Additive powder fed friction stir processing (APF-FSP)

The colloidal paste was prepared by mixing nanoparticles of GRN (10-50 nm) and ηSiC (~25 nm) in 1:1 ratio by dispersing in water/ethanol. The dimensions of backing-plates and fixtures were chosen as per length and width of milling machine table. Vertical clamping pressures were used with pressure bars to prevent plates from lifting and provide uniform temperature distribution across the plates. To avoid the discretion of two plates and provide side pressure on the workpieces during welding, two L-shaped mild steel plates are utilized, with two end-screwed bolts on each plate. The width of the backing plate was made somewhat smaller than

the entire width of the two plates to be processed for direct lateral pressure on specimens. The FSP experiment was carried out by varying the traversal speed and plunge depth while maintaining the other parameters constant. The process parameters were chosen based on trial tests that considered parameters from the literature as well as the machine's spindle and transverse speeds. The experiment was carried out by varying the traversal speed and material placement while maintaining the other parameters constant. The process parameters were chosen based on trial tests that considered, parameters from the literature, as well as the machine's spindle range and traverse speeds. The APF-FSP experiments were carried out by varying the traversal speed (30-40 mm/min) and rotational speed (1200 -1800 RPM) at plunge depth (0.1-0.3 mm) as shown in figure 4.5.1.
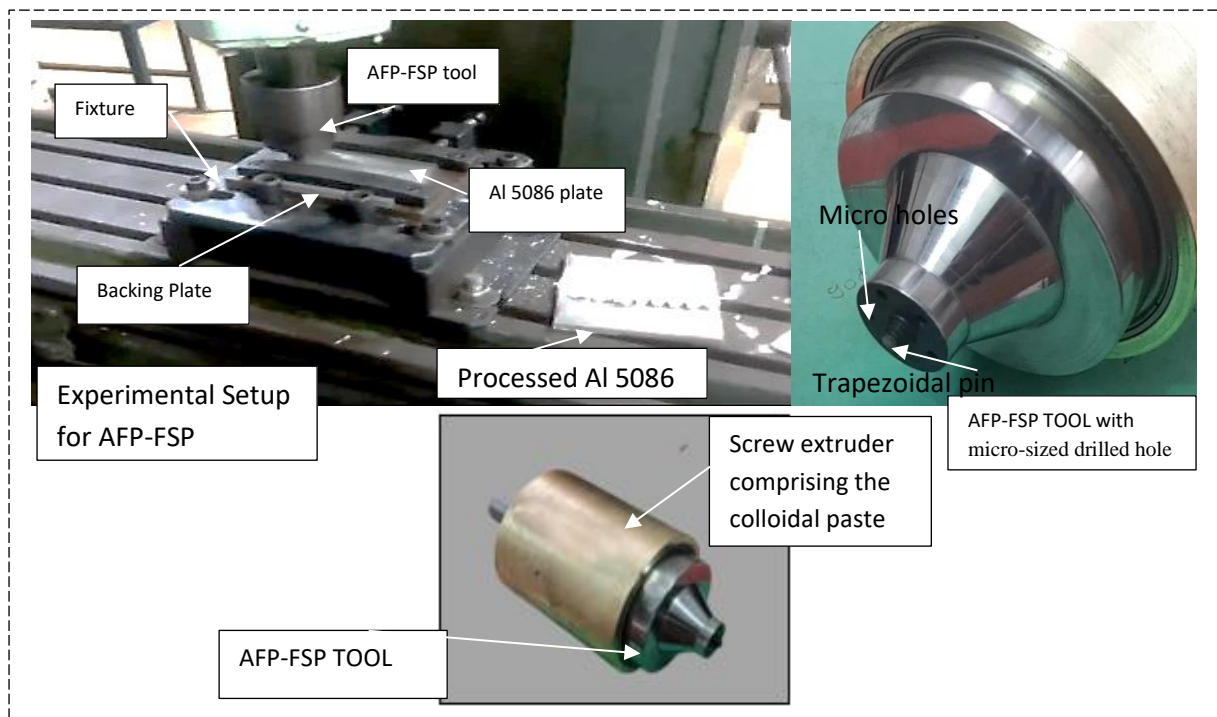
Figure 4.5.1. Experimental Set-up of APF-FSP
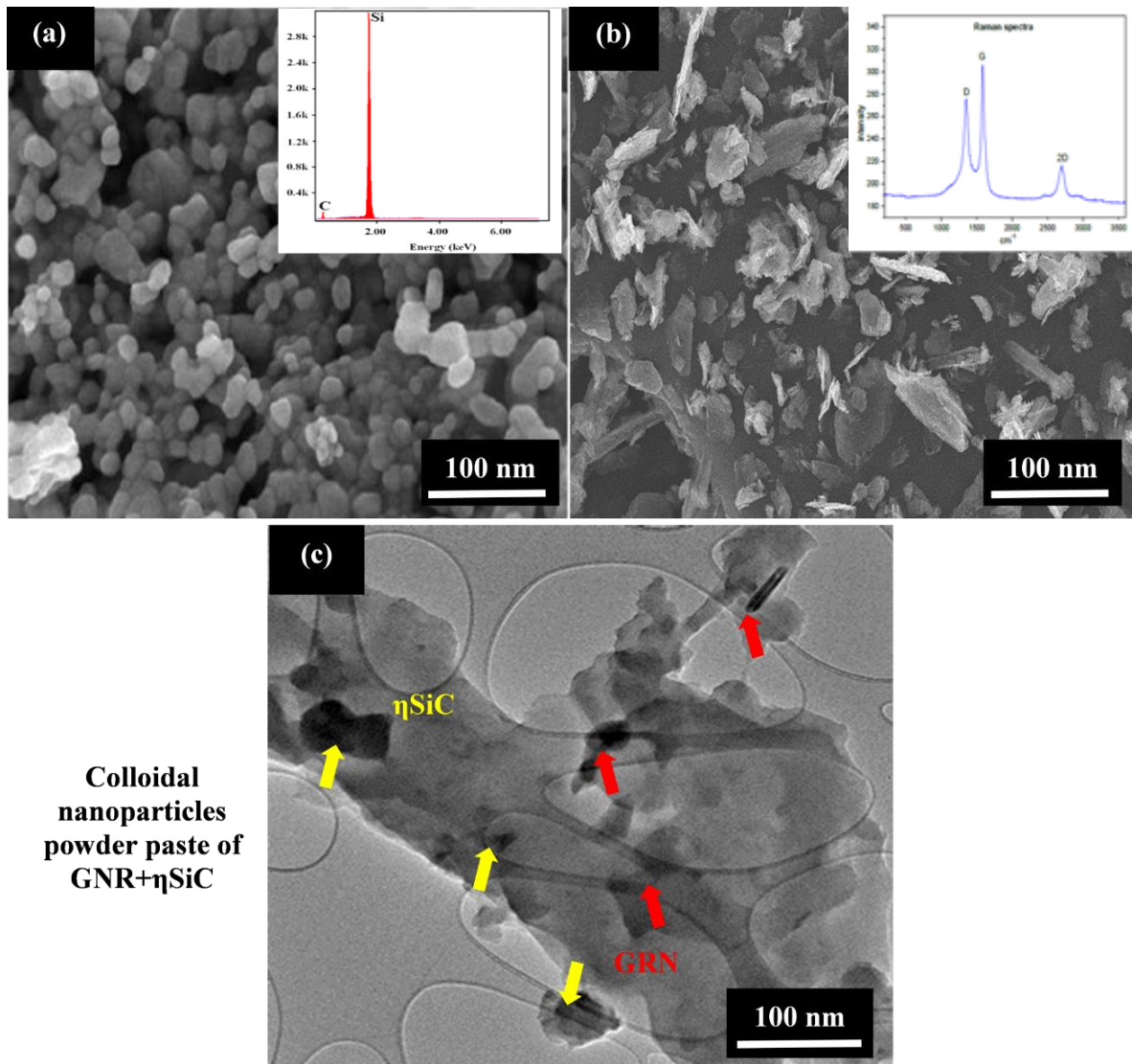
Figure 4.6: SEM and TEM image of powders: (a) Nano-SiC, (b) Nano-graphene, and (c) colloidal nanoparticle paste of ηgraphene and ηSiC. EDS spectrum and Raman spectrum of nanosized SiC powder and graphene particles

4.3. Macro-graph, Microstructure, and Surface Morphology Analysis

Samples for metallographic analysis were cut into required size $20 \times 10 \times 3$ mm and cleaned with acetone to remove impurities. Then samples were manually mounted with epoxy resin and hardener. The optimum mixing ratio is the key to get best cured properties. The resin and hardener were measured to 2:1 mixing ratio with measuring device and subsequently mixed thoroughly until the mixture appears homogenous. Then poured the mixture over the mounting cup and allow it to cure for 24 hours in room temperature. The mounted samples were polished

to mirror-like surface with emery paper ranging from 600-2000 grit followed by cloth polishing using alumina paste on disk polishing machine. Then samples were etched for 15 seconds in the solution prepared from nitric acid 40 ml, hydrochloric acid 30 ml, hydrofluoric acid 2.5 ml and distilled water 42.5 ml. Microstructures of the transverse section of butt joints were examined via X-ray diffraction (XRD), optical microscopy (OM), and field emission scanning electron microscopy (FE-SEM), as mentioned in Appendix-A.

4.4. Micro-mechanical behavior

Micro-mechanical behavior of FSP-developed Al5086-GRN-ηSiC hybrid composite was investigated in terms of surface hardness, elastic modulus, and compressive strength. The surface hardness was measured by micro-hardness tester and Hyistron TI-950 system. The cross-section of friction-processed surface was chosen surface hardness measurement. The cross-section surface of cladded layer was prepared using an adequate polishing process using ASME standard. Micro - hardness tests were carried on the cross-sectional surface of the samples using a Vickers hardness tester (Mitutoyo HM-125). With a holding time of 10 seconds, a 2.45 N indentation load was applied. To confirm the results, the surface hardness was measured using the nano-indentation technique by Hyistron TI-950 system at indentation load of 1000μN for 3s dwell time using Berkovich tip. An optical 3D surface profiler was used to determine the roughness of the surface. Figure 4.8 (a) and (b) shows the microhardness equipment and well-polished cross section surface of the sample for microhardness measurements, respectively.

Using a nano-indentation device, the tensile properties and compressive strength of an Al5086-GRN-SiC hybrid composite produced by FSP were examined. The indenter was a diamond Berkovich tip and the nanoindentation was done using a PI-88 nano-inventor (Hysitron Inc., USA).
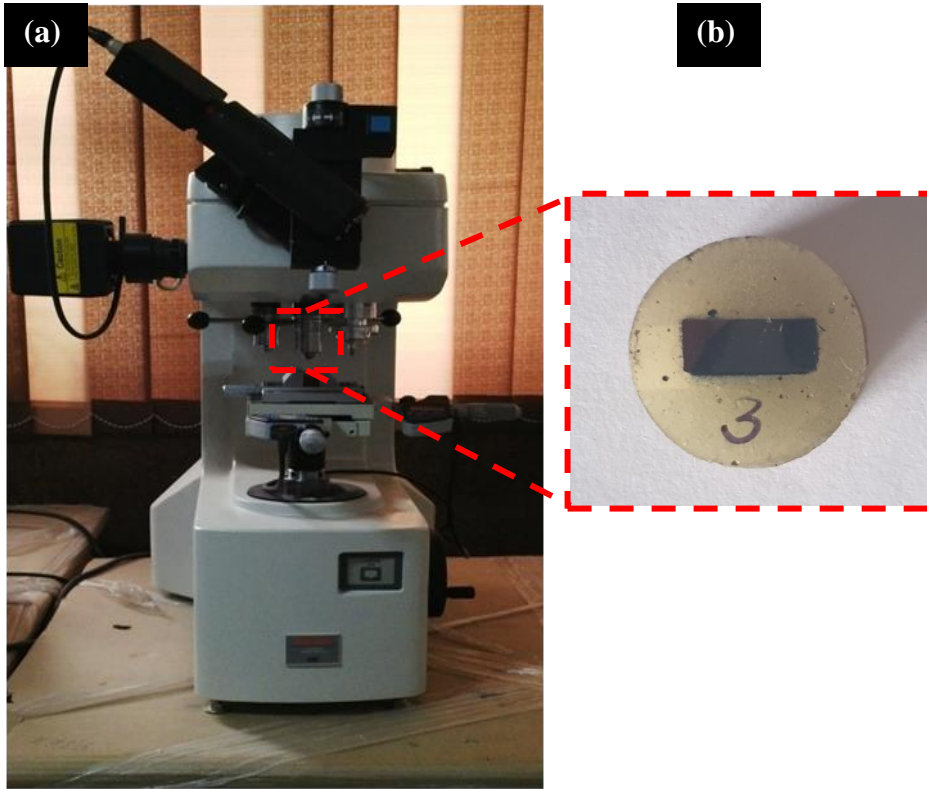
Figure 4.7: (a) Mitutoyo micro hardness tester and (b) well-polished cross section surface of the sample for microhardness measurements
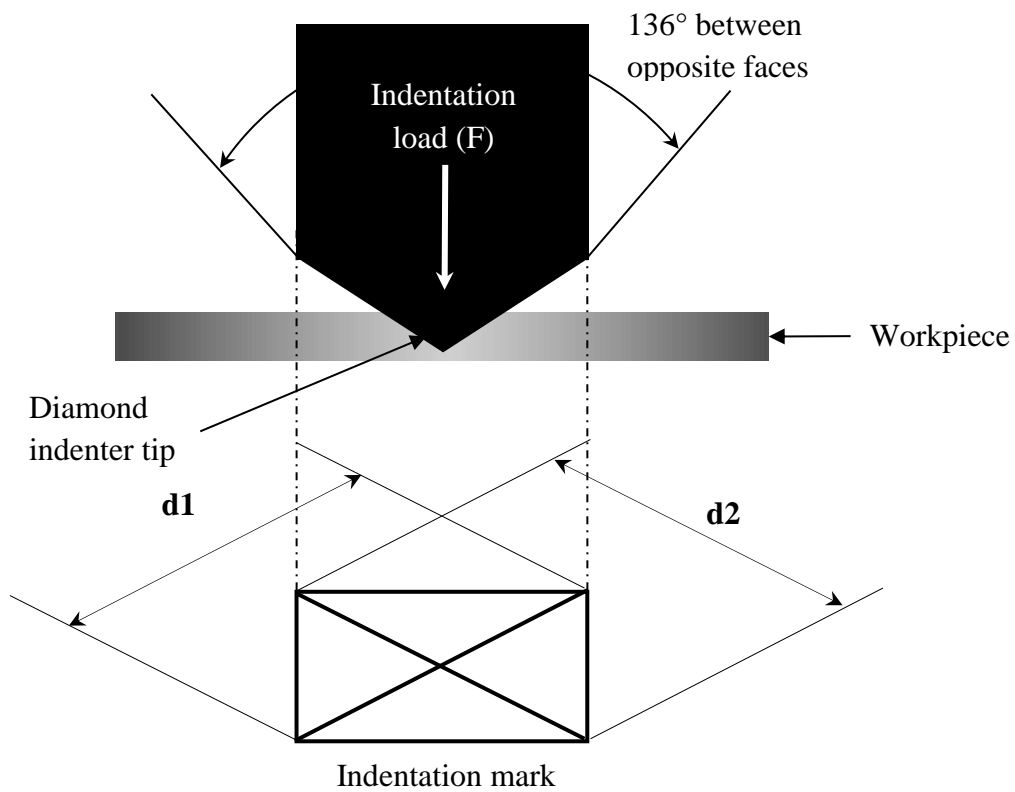
Figure 4.8: Schematic representation of indentation mark of diamond-indenter.

According to Basak et al., the tip is a three-sided pyramid with an inclination angle of 142.3°, a half angle (Ø) of 65.35°, and a tip radius of roughly 150 nm (2018). The maximum indentation force (Fmax) was 1 mN, with loading and unloading speeds of 0.5 mN/s. There was a 5-second hold interval at peak load to allow for stability before emptying. At least 10 separate indentation were performed in each sub-surface layer to verify repeatability, and average values were supplied for result analysis and discussion [88,89].

Figure 4.9: Hyistron TI-950 indentation system available at IIT, Ropar

A SEM with Ga+ focused beam (FIB-SEM) was used to produce the micro-pillars. To ensure that the indenter does not touch the sample surface during compression, a suitable space (30 m) was maintained between the micro-pillar and surrounding materials. The milling pattern was first performed at a higher current (6.5 nA at 30 kV), followed by final polishing at 0.46 nA at 30 kV. On the same nanoindentation device, the indenter tip was replaced with a 5 m diameter flat diamond for in-situ compression testing. The loading and unloading rates during in-situ compression were 3 and 50 nm/s, respectively, with the loading rate comparable to 10-3 s-1 strain rate. The load-displacement graphs were recorded alongside a video of the compression process. According to Basak et al. the load-displacement curves were transformed to stress-strain curves [88].
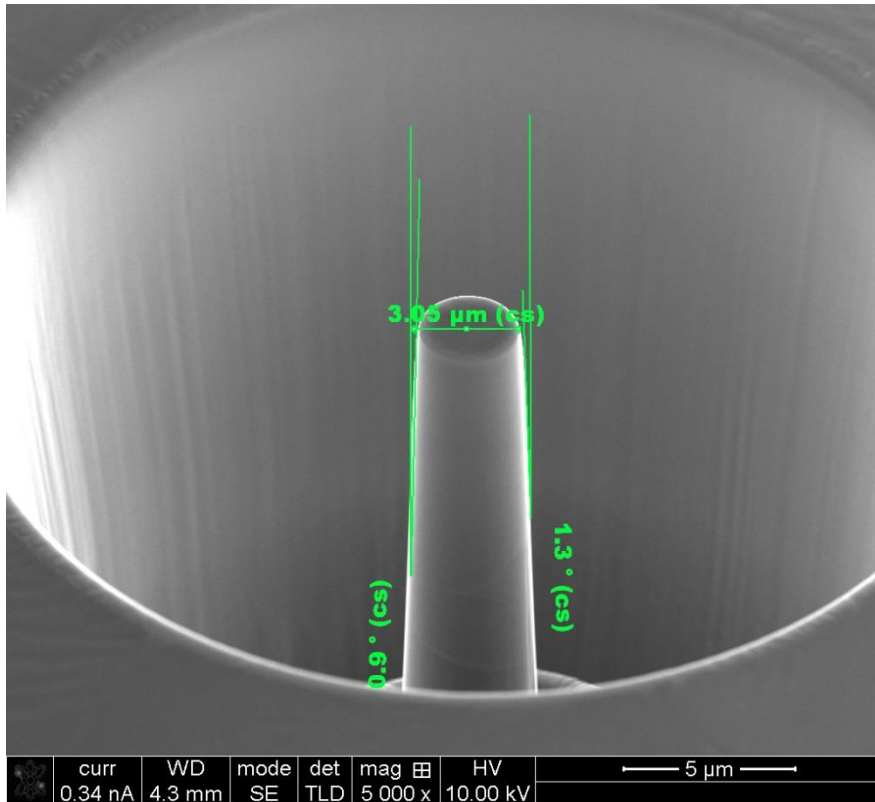
Figure 4.10: Micro-pillar on un-treated Al5086 alloy
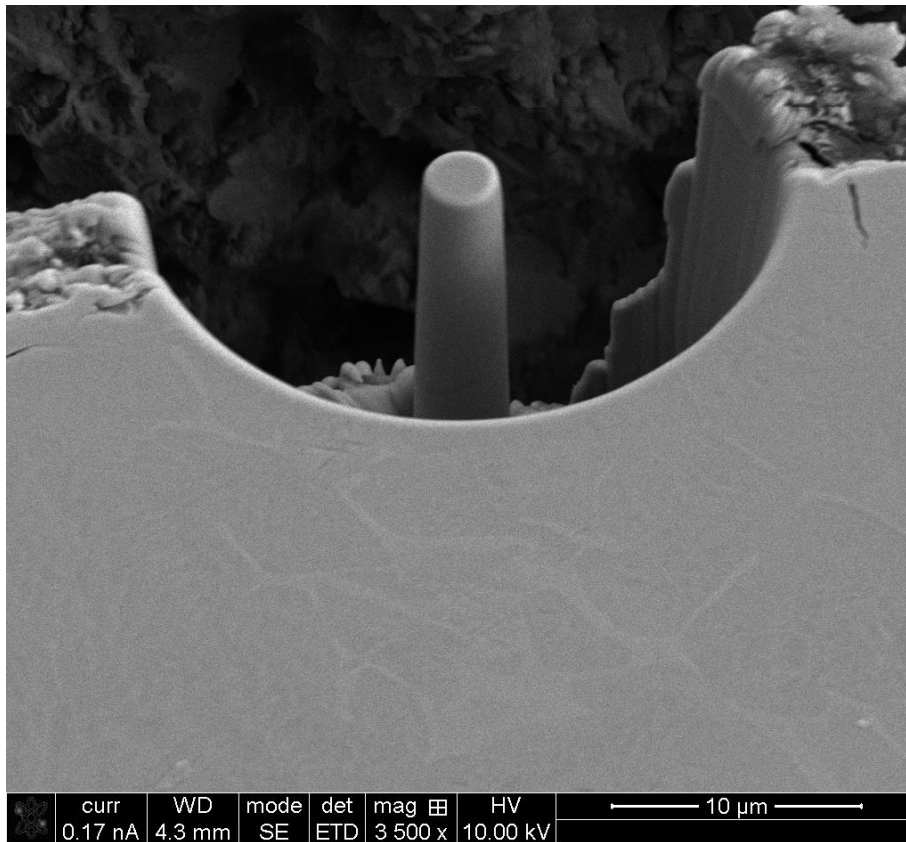
Figure 4.11. Micro-pillar on FSP-developed Al5086-GRN-SiC surface composite
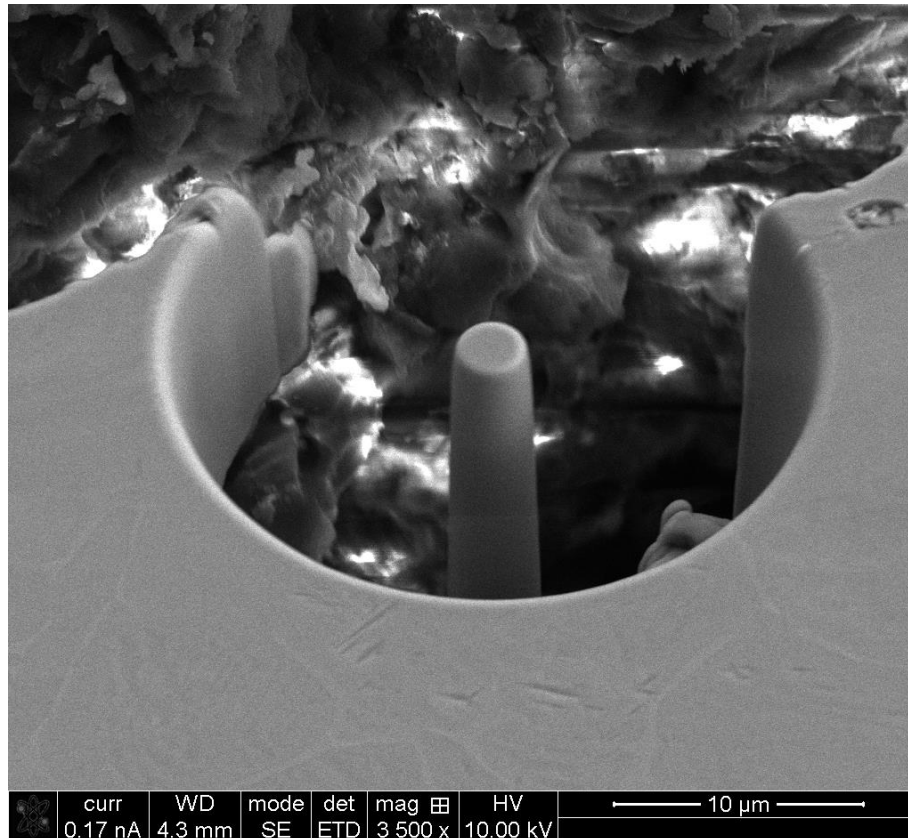
Figure 4.12. Micro-pillar on FSP-developed Al5086-GRN-ηSiC surface composite

4.5. Wear Testing

The tribological performance of untreated Al5086 alloy, Al5086-GRN-SiC and Al5086-GRN-ηSiC specimens was measured by frictional wear test. The test was carried out with a load of 10 N in air at room temperature using a pin-on-disc frictional wear-testing system (DUCOM, Instruments Pvt. Ltd, Banglore, India), as can be seen in Figure 4.13

The tribological performance of untreated Al5086 alloy, Al5086-GRN-SiC and Al5086-GRN-ηSiC specimens was measured by frictional wear test. Sliding wear test were conducted via pin on disc tribometer. Cylindrical pins with diameter 5mm and height 10mm were extracted from the base and composite material using wire cut electric discharge machine. Wear tests were carried out at 19.6N load. All of the aluminum composite samples were put through the test against an EN32 steel disc with a hardness of 65HRC. During the experiments, the relative humidity ranged between 45 and 50 percent. Wear rate was determined by considering average of the three values. The track was thoroughly cleaned with acetone before each test. a constant sliding velocity of 1.75 m per sec was maintained for sliding distance of 3000 meters. The wear

rate was estimated by utilizing a linear variable displacement transducer to measure the change in specimen height (LVDT).
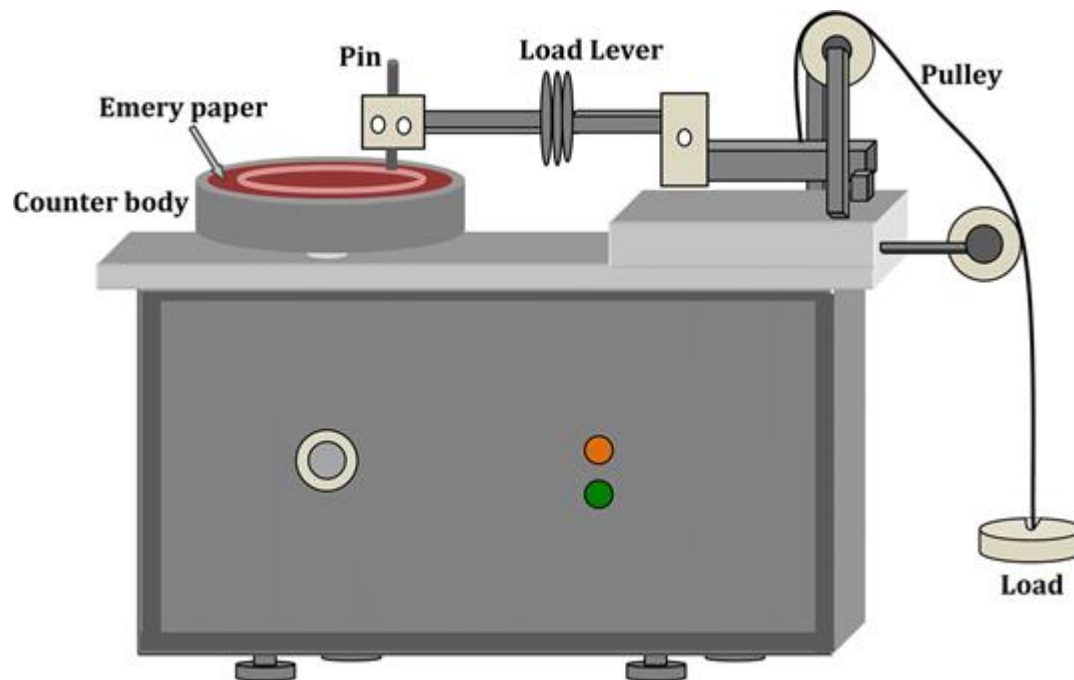
Figure 4.13: Photograph of wear test rig

RESULTS AND DISCUSSIONS
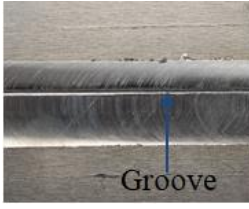
This chapter covers the discussions of results and analysis in two phases. The first phase covers the discussion of the results and analysis of surface composite developed by friction stir processing (FSP) technique using micro-size silicon carbide and nano-scale graphite as a reinforcement. A comprehensive and critical investigation of the microstructure, surface morphology, surface chemistry, surface microhardness, tensile strength has been studied. In second phase, the discussion of the results and analysis of surface composite developed by additive powder fed friction stir processing (APF-FSP) technique using nano-scale silicon carbide and graphite as a reinforcement.

5.1. Effect of process parameters on Defect formation

The influence of plunge depth, tool rotational speed and travel speed on joint conditions is evaluated in the current work through defect analysis to determine the optimum parameters for achieving defect-free and higher strength welds. It has noticed that the higher RS of 1800 rev/min, average WS of 40 mm/min and the highest PD of 0.3 mm produced a joint with the maximal strength in the second phase of experimentation. The defect-free joints were created with 0.2 mm and 0.3 mm PD except welds B1 and C1 given in Table 5.1. FSP process tends to produce defects like surface galling, tunnel, void, surface groove, crack, and kissing bond. These defects arise due to inappropriate selection of process parameters which leads to inadequate heat development and improper material intermixing [90, 91]. But this process is completely free from defects such as solidification cracks, slag inclusion, porosity etc., that occurs in other fusion welding processes [89,90].

Table 5.1: Friction stir welding joints and macrostructures produced with different parameters.

Data set no.	Weld joint	Macrograph	Observation
A1			Defective
A2			Defective
A3			Defective
A4			Defective
B1		Defect occurred due to excess heat input	-

B2		Defect-free
B3		Defect-free
B4		Defect-free
C1	Groove	Defect occurred due to excess heat input	-
C2		Defect-free
C3		Defect-free
C4		Defect-free

A1-A4 data set represents 1200 rpm, B1-B4 data set represents 1500 rpm, C1-C4 data set represents 1800 rpm.

The weld joints obtained with different parameters and their macrographs are presented in Table 5.1. Surface galling is observed on the weld joint A4. Appearance of galling can be attributed to an inadequate applied load and low rotational and high traverse speeds. In addition to that it is often caused by an amalgamation of both the friction and adhesion during FSP process. Surface groove has appeared in weld sequence B1 and C1. They are formed due to excessive welding temperature owing to high spindle speed and low transverse speed. These two parameters are primarily responsible for heat generation, heat transfer and material flow in FSP process. The joints that possessed surface groove could not be processed for further analysis because of its deep and shallow indentations. The joint produced with 0.2 mm plunge depth, 1500 rpm tool rotation and 40 mm/min tool traverse speed (or feed rate), has less groove size when compared with joint produced with 0.3 mm at 1800 rev/min and 40 mm/min.

Flash generally forms because of excessive heat produced owing to high rotating speed and low transverse speed [36]. FSP process tends to produce surface flash, since the tool shoulder is obliged to penetrate below the workpiece surface and the joining is associated with heat generation and mechanical mixing. Generally excess materials occurred during the welding process flashing out but some materials somehow tend to stuck on the welded surface. These flashes could be eliminated by machining the top and bottom surfaces of welded plate, as evidenced in Rodriquez et al. [92]. In the present work, it has been observed that, surface flash dissociates with the joint quality as weld C3(1800 rpm) showing the highest UTS, but possessed the maximum flash.

The tensile strength, often known as the ultimate tensile strength, is defined as the load at failure divided by the original cross-sectional area, where $max = P_{max}/A_0$, where $P_{max} = $ maximum load and $A_0 = $ original cross sectional area.

The internal defects of the welded joints have been observed through macrostructure analysis. It is noticed that all the joints fabricated with 0.1 mm plunge depth yielded different types of defects such as crack, line defect, tunnel, void and kissing bond. The main cause of tunnel defect is identified as insufficient plunge depth while line defect is due to less plunging force and improper material mixing. The longitudinal cracks have occurred due to high shrinkage stresses while inappropriate material mixing and deficient plunge depth are the reason for void formation [90, 91]. Friction stir welded joint often present a defect like kissing

bond, this defect arises due to inappropriate coalescence between the materials owing to poor heat input.

The MINITAB-16 tool was used to analyse the experimental data based on orthogonal array (OA) L-27 runs after they were collected. The signal-to-noise ratio (S/N ratio) was tabulated during the analysis, and main effect plots were created to demonstrate the effect of various input parameters on surface properties. The analysis of variance (ANOVA) was used to identify the significant parameters and their percentage contributions to producing the output response.

5.1.1. Analysis of Surface Hardness

Table 5.2 shows the measured mean of values and S/N ratios for surface micro-hardness (SH) following experimentation. The mean and S/N ratio plots were used to investigate the effect of rotating speed (RPM), transverse speed (Ts), plunge depth (Pd), and taper angle (Ta) on surface hardness. For analysing the effect of input parameters on SH, the larger-the-better criterion was chosen. Tables 5.3 and 5.4 show the average value of mean (raw data) and the S/N ratio for SH at various values of input parameters.

Table 5.2: Results of SN ratios and mean for Surface hardness

Sr. No.	Surface Hardness (SH)				
	Raw Data			**Average Value**	**S/N Ratio**
	R1	R2	R3		
1	145	166	167.5	159.5	44.06
2	168	142	157.1	155.7	43.85
3	175	187	184.9	182.3	45.22
4	190	205	202.9	199.3	45.99
5	206	176	190.7	190.9	45.62
6	188	198	188.2	191.4	45.64
7	197	188	198.5	194.5	45.78
8	193	190	189.4	190.8	45.61
9	195	195	200.1	196.7	45.88
10	192	199	204.2	198.4	45.95
11	199	205	188.8	197.6	45.92
12	187	198	189.5	191.5	45.64

13	179	195	203.2	192.4	45.68
14	194	189	198.4	193.8	45.75
15	189	194	201.7	194.9	45.80
16	205	189	202.7	198.9	45.97
17	185	200	196.1	193.7	45.74
18	200	189	189.7	192.9	45.71
19	194	201	200.5	198.5	45.96
20	193	195	189.5	192.5	45.69
21	197	189	202.3	196.1	45.85
22	198	188	204.1	196.7	45.88
23	203	192	186.4	193.8	45.75
24	190	198	202.4	196.8	45.88
25	195	191	189.7	191.9	45.66
26	189	202	206.6	199.2	45.99
27	205	191	190.5	195.5	45.82

Table 5.3: Response table for S/N Ratio of SH

Level	Rotational Speed (rpm)	Transverse Speed (mm/min)	Plunge depth (mm)	Taper Angle (Degree)
1	45.29	45.35	45.66	45.62
2	45.8	45.78	45.54	45.6
3	45.83	45.8	45.71	45.69
Delta	0.54	0.45	0.17	0.09
Rank	1	2	3	4

Table 5.4: Response table for Mean of SH

Level	Rotational Speed (rpm)	Transverse Speed (mm/min)	Plunge depth (mm)	Taper Angle (Degree)
1	184.6	185.8	192.2	191.5
2	194.9	194.4	189.8	191
3	195.7	194.9	193.1	192.6
Delta	11.1	9.1	3.3	1.6
Rank	1	2	3	4

The surface hardness depends upon the microstructure change undergone by the workpiece during the FSP process. In the FSP process, the materials flow induced by the plastic deformation produced by tool pin geometry and stirring action, as a result the grains of matrix were re-arranged and recrystallized; thus, fine grain growth occurred that improve the mechanical properties. Based on the observations recorded, Fig. 5.1 shows the mean and S/N ratio response, at larger the better option, of the input process parameters on the surface hardness of the as-developed Al-based surface composite. It can be seen that with an increase in the rotational speed, from 1200 to 1800rpm, the surface hardness of the developed composite specimens increased.
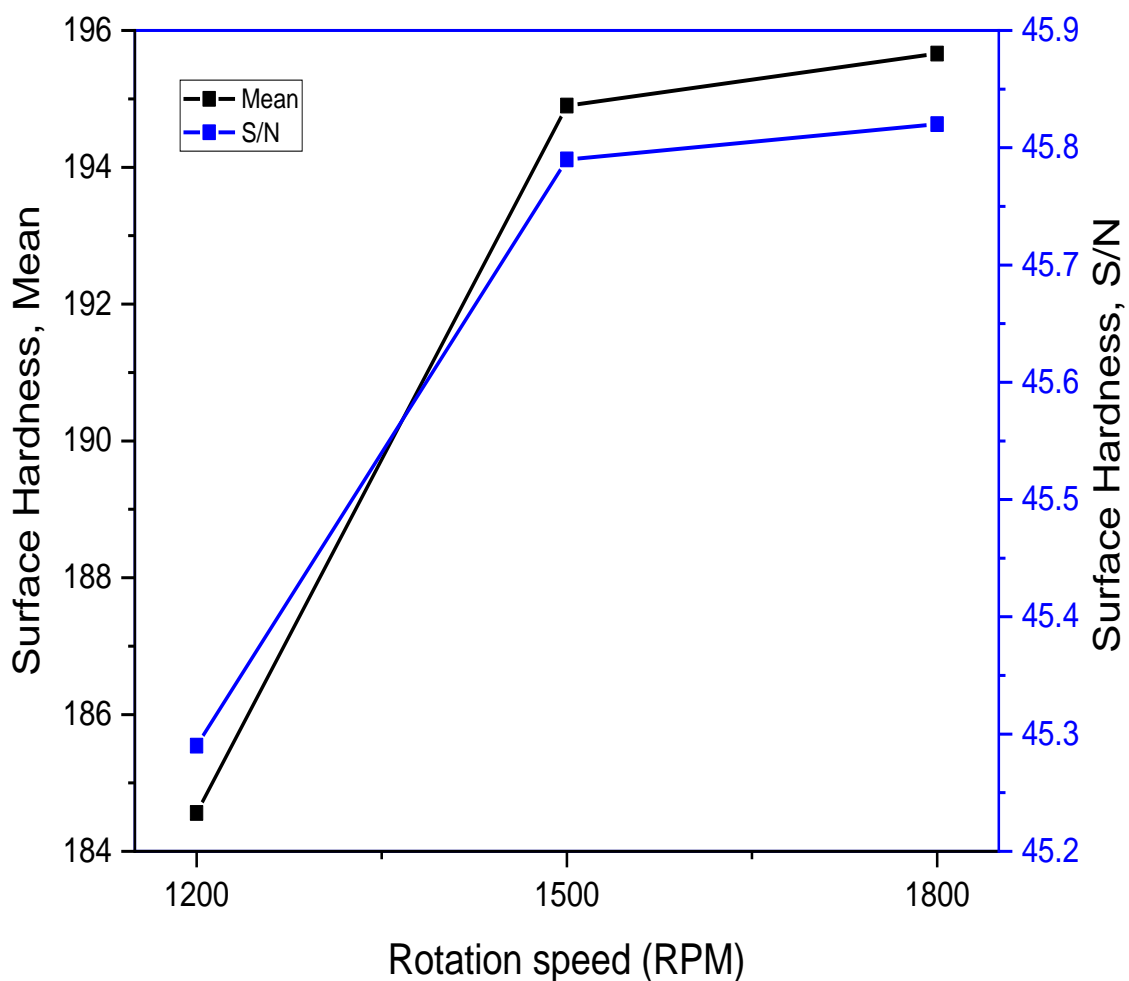
Figure 5.1. Effect of rotational speed on surface hardness

The SH and RS have a nearly linear relationship. When the RS is increased from 1200 to 1800 RPM, the mean of SH jumps from 188 Hv to 195 Hv, indicating that the RS is the most influential parameter. The prime reason behind this trend is because of the fact that by increasing the rotation speed of the tool developed higher frictional force, thereby heat energy.

The higher amount of the heat resulted in: (i) refinement of the surface and (ii) fine dispersion of Gr and SiC particles. As the rotating speed increased to 1800rpm, the material flow was improved and regions with clustered small particles were observed beneath the stir zone. It can be clearly seen that when the rotational speed is 1200rpm, the improper heating of matrix resulted in the repulsion of the reinforcements from the set locations and, therefore, resulted in the reduction of micro-hardness of the developed AMCs. However, in case of 1500rpm of rotational speed, it has been found that the processed zone had some structural defects that impacted the structural integrity of the composites. A sound, with visibly embedded reinforcements (indicated by yellow circles) can be seen in case of 1800rpm.

Figure 5.2 shows the effect of transverse peed (Ts) on the surface hardness. It has been found that with an increase in the speed from 30 to 40 mm/min, the surface hardness of the developed surface composites also increased. The *TS* is the 2nd most influencing parameter showing a sharp increase in the mean of SH from 185.78 Hv to 194.9 Hv, when *TS* increases from 30 to 40 RPM. With the increase in transverse speed, the plasticized metal flow increased as a result finer grain growth occurred in the Al-matrix and more uniform distribution of reinforcement particles occurred. It has been found that the regions namely stir; transition and heat affected zone (HAZ) are greatly affected by the different levels of transverse speeds. Further, as reported in the literature, width of the processed zone increases with decreasing tool transverse speeds, however, the depth of the processed zone reduced by reducing the transverse speed.
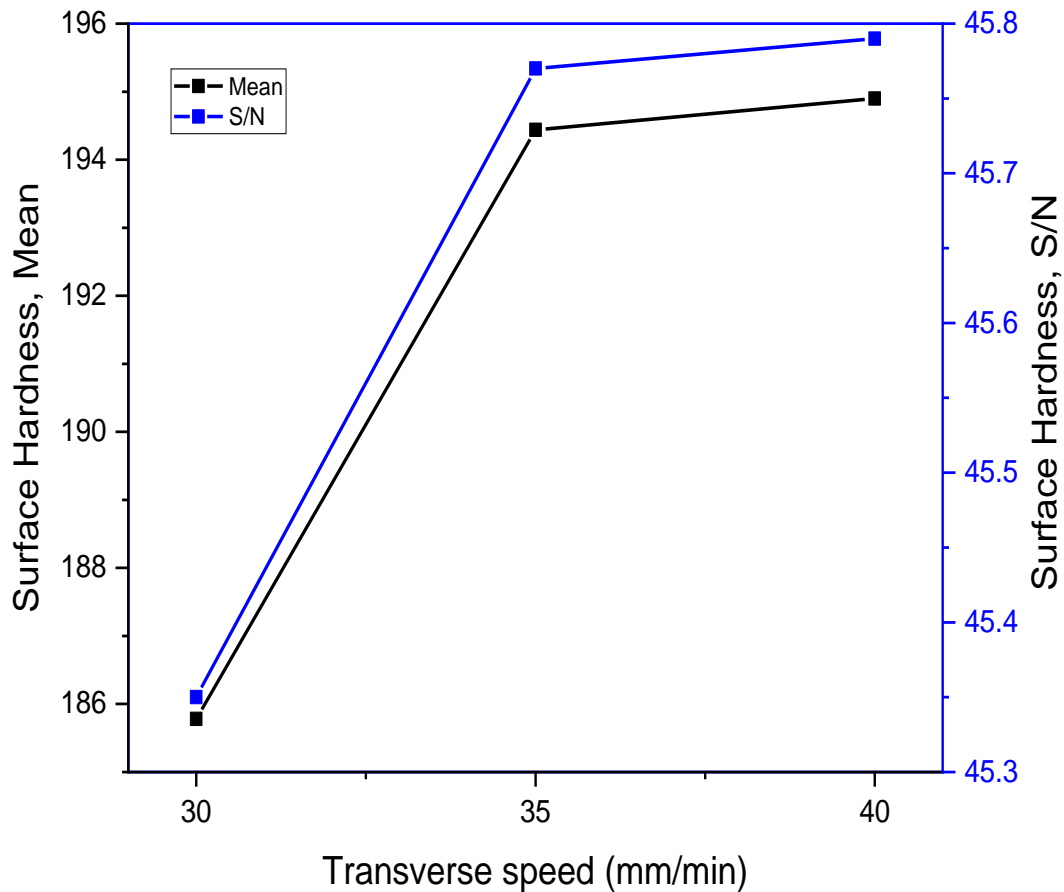
Figure 5.2. Effect of transverse speed on surface hardness

The influence of plunge depth (PD) on the surface hardness (SH) of an as-developed surface composite is shown in Figure 5.3. SH has a nonlinear relationship with PD, as can be observed. It has been discovered that when PD increases, the SH reduces dramatically up to 0.2 mm, then progressively increases as PD climbs more. Among all criteria, the PD is the third most influential. When PD goes from 0.1 mm to 0.2 mm, the mean of SH drops sharply from 192 Hv to 189 Hv, then rises sharply from 189 Hv to 193 Hv when PD grows from 0.2 mm to 0.3 mm. The greatest level (C3) of PD (0.3 mm) has the highest SH, whereas the lowest level (C2) of PD has the lowest SH (0.2 mm). The change in SH of SN ratio as a function of PD levels matched the variation in SH of mean.
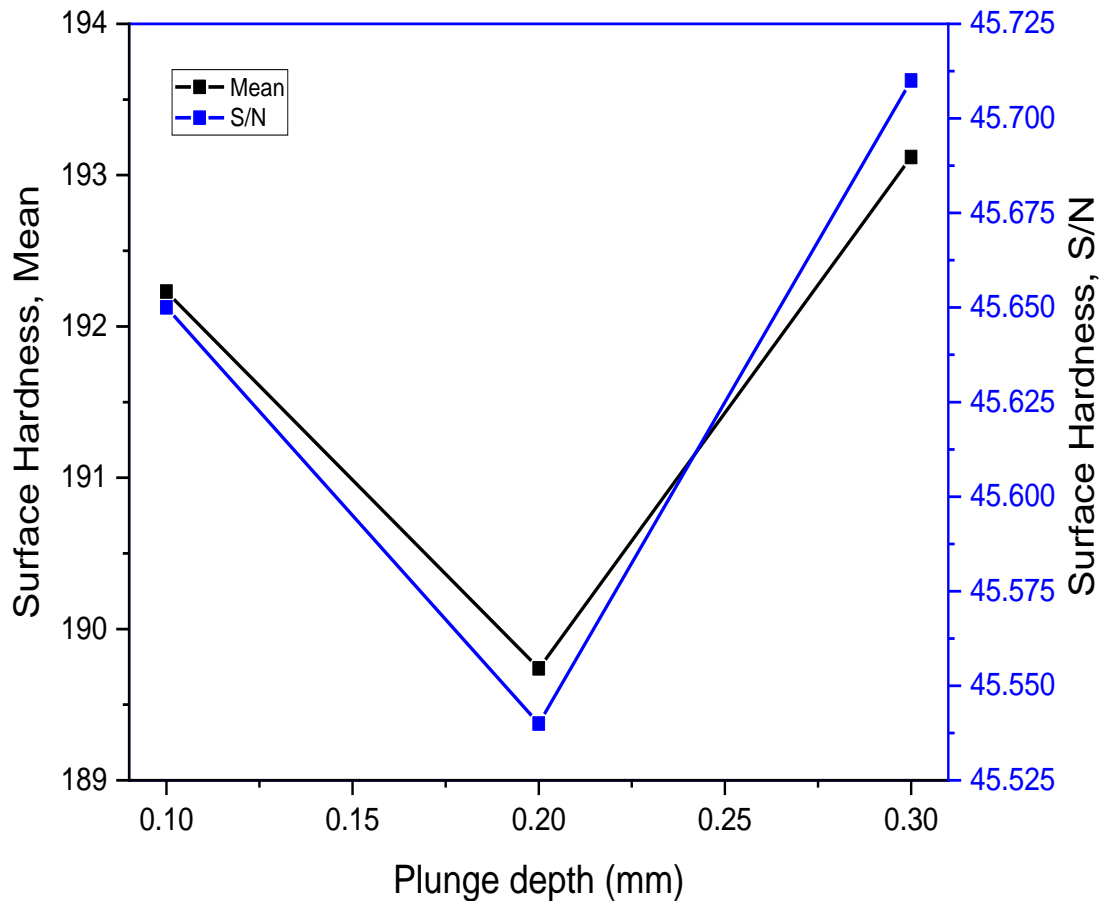
Figure 5.3. Effect of plunge depth on surface hardness

Indeed, the tilt angle affected the dispersion of reinforcement particles into the matrix as it is a critical process parameter which influences the material flow, and particle breakup and distribution in the processed zone. Figure 5.4 shows the effect of tilt angle on the surface hardness. It can be seen that when the tool tilt angle increased from 2 to 3 degree, the defect formation in the processed zone has eliminated. As the tool inclined, the tool front end was lifted upward and the tool rear end was lowered downward, and the front end acted as the reservoir to accommodate the material flow and decreases the wastage of material. However, the macrostructure examination showed that when the tilt angle was increased to 4 degrees, the processed zone formed surface crack, particle agglomeration, and tunneling defect because of the attainment of insufficient state of heat and material flow.
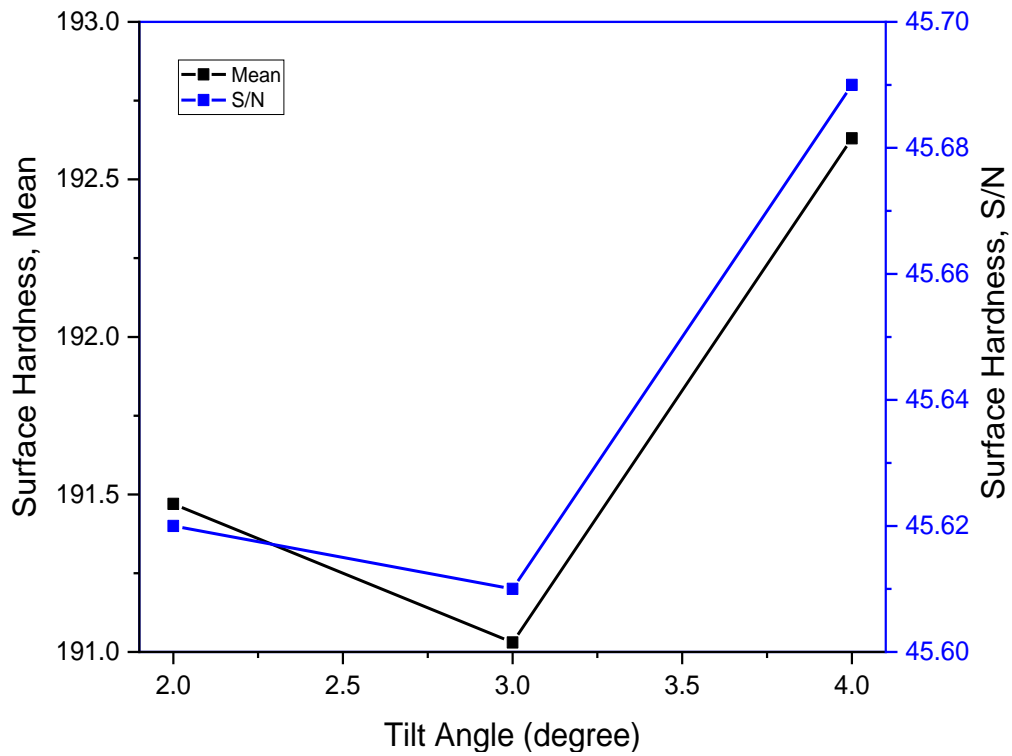
Figure 5.4. Effect of tilt angle on surface hardness
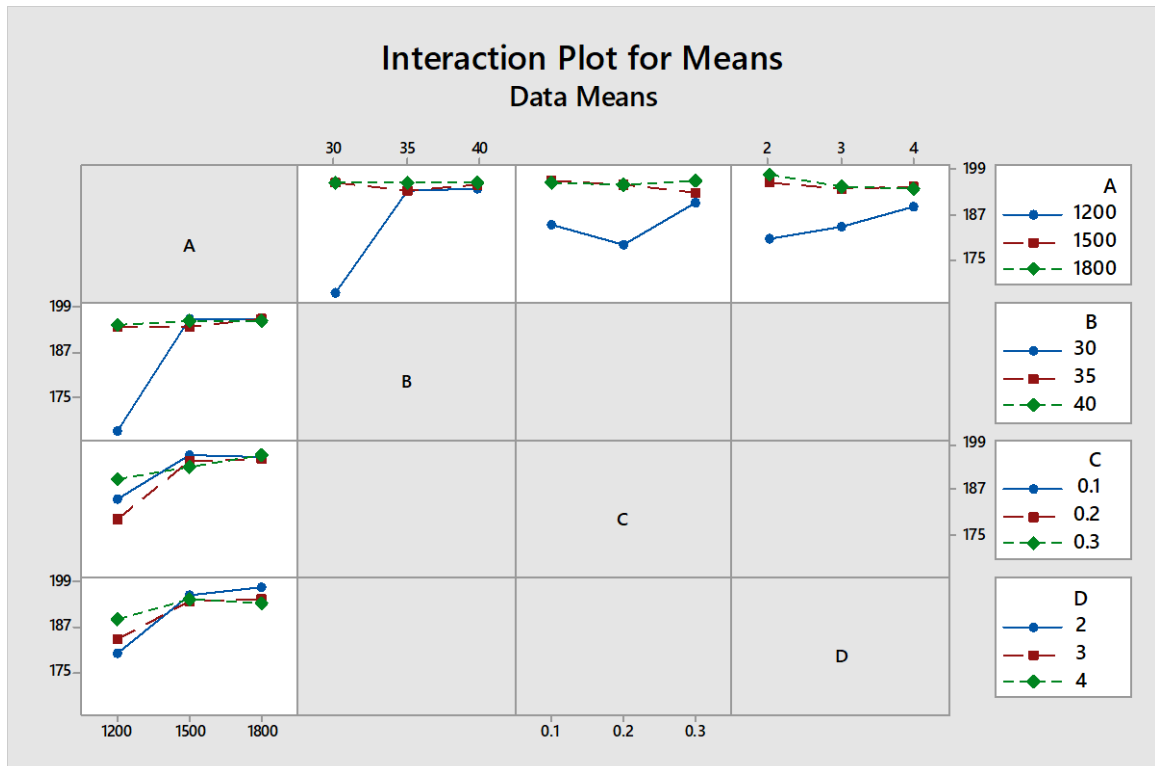
Figure 5.5. Graphical summarisation of results obtained for Surface Hardness

(Plot for Means)

According to the results of the foregoing research, the optimal combination of FSP parameters for optimising SH is a greater rotation seed (RS=1800 RPM), a higher transverse speed (TS=40 mm/min), a higher lever of plunge depth (PD=0.3 mm), and a larger tilt angle (TA=4°). ANOVA has also been used to assess the relevance of each input parameter. The analysis of variance for surface hardness is shown in Table 5.5. The variables, degree of freedom (DOF), sequential sum square error (Seq SS), adjusted sum square error (Adj SS), adjusted mean square error (Adj MS), F statistic, p-values, and cumulative percentage (percent) are all represented in columns in the table. For important parameters, the p-value of lack of fit should be less than 0.05, indicating statistically insignificant lack of fit at the 95 percent confidence level. The p-value of the regression model and all of its terms, on the other hand, is less than 0.05, indicating that they are statistically significant at 95 percent confidence. As a result, the model accurately depicts the experimental data. The ANOVA analysis shows that RS and TS both contribute significantly to the SH. With a contribution of 38.91 percent, the combination between rotational and transverse speed is quite significant. Individual contributions to rotational and transverse speeds are 24.20 percent and 16.60 percent, respectively. Plunge depth and tilt angle both contribute 1.89 and 0.43 percent respectively. The mistake contribution percentage is only 8.10 percent.
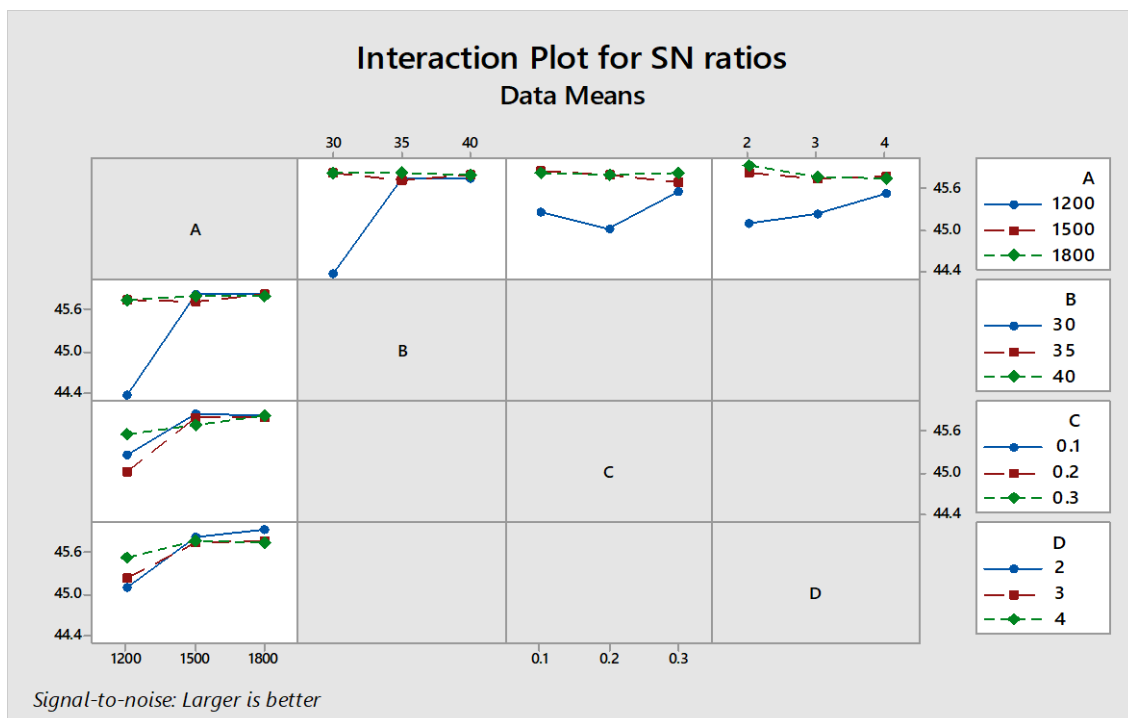
Figure 5.6. Graphical summarisation of results obtained for Surface Hardness (Plot for SN Ratios)

Table 5.5: Analysis of variance of surface hardness

Factors	DOF	Seq SS	Adj MS	F	P	%
Rotation Speed (RS)	2	691.73	345.863	8.97	0.016	24.20*
Transverse Speed (TS)	2	474.42	237.208	6.15	0.035	16.60*
Plunge Depth (PD)	2	54.02	27.008	0.7	0.533	1.89
Tilt Angle (TA)	2	12.33	6.163	0.16	0.856	0.43
Rotation Speed (RS)× Transverse Speed (TS)	4	1112.06	278.016	7.21	0.018	38.91*
Rotation Speed (RS)× Plunge Depth (PD)	4	147.08	36.769	0.95	0.495	5.15
Rotation Speed (RS)× Tilt Angle (TA)	4	134.79	33.698	0.87	0.531	4.72
Residual Error	6	231.47	38.578			8.10
Total	26	2857.89				
*Significant Terms						

5.1.1. Analysis of Tensile strength

A material's tensile strength is a measurement of its capacity to sustain pulling or stretching forces without breaking or deforming. There are various ways for determining a material's tensile strength, but one typical approach is the tensile test, often known as a tension test.

Table 5.6 shows the observed average of means and S/N ratios for surface tensile strength of surface composites following experimentation. The mean and S/N ratio graphs were used to investigate the effect of rotating speed (RPM), transverse speed (Ts), plunge depth (Pd), and taper angle (Ta) on tensile strength. For examining the effect of input parameters on tensile strength, the larger-the-better criterion was chosen. Tables 5.7 and 5.8 show the average value of mean (raw data) and S/N ratio for tensile strength at different levels of input parameters.

Table 5.6: Results of SN ratios and mean for Tensile Strength

Sr. No.	Tensile Strength				
	Raw Data			Average Value	S/N Ratio
	R1	R2	R3		
1	165	167	156.1	162.70	44.23
2	173	179	182.3	178.10	45.01
3	200	194	204.2	199.40	45.99
4	205	199	215.8	206.60	46.30
5	215	190	212.4	205.80	46.27
6	210	215	195.7	206.90	46.32
7	185	200	230.3	205.10	46.24
8	190	210	218.9	206.30	46.29
9	212	200	201.5	204.50	46.21
10	198	218	200.8	205.60	46.26
11	220	195	205.1	206.70	46.31
12	225	200	195.4	206.80	46.31
13	192	219	204.3	205.10	46.24
14	202	213	199.4	204.80	46.23
15	209	201	202.9	204.30	46.21
16	207	203	210.7	206.90	46.32

17	214	212	199.2	208.40	46.38
18	211	215	196.2	207.40	46.34
19	188	208	222.9	206.30	46.29
20	221	201	204.1	208.70	46.39
21	224	202	195.3	207.10	46.32
22	227	198	201.4	208.80	46.39
23	217	206	205.8	209.60	46.43
24	226	206	192.3	208.10	46.37
25	208	214	207.4	209.80	46.44
26	215	207	201.4	207.80	46.35
27	222	204	198.6	208.20	46.37

Table 5.7: Response table for S/N Ratio of tensile Strength

Level	Rotational Speed (rpm)	Transverse Speed (mm/min)	Plunge depth (mm)	Taper Angle (Degree)
1	45.87	45.9	46.08	46.08
2	46.29	46.31	46.18	46.17
3	46.37	46.33	46.27	46.28
Delta	0.5	0.42	0.19	0.21
Rank	1	2	4	3

Table 5.8: Response table for Mean of tensile strength

Level	Rotational Speed (rpm)	Transverse Speed (mm/min)	Plunge depth (mm)	Taper Angle (Degree)
1	197.3	197.9	201.9	201.8
2	206.2	206.7	204	203.8
3	208.3	207.2	205.9	206.1
Delta	11	9.2	4	4.3
Rank	1	2	4	3

The tensile strength depends upon the microstructure change undergone by the workpiece during the FSP process. In the FSP process, the materials flow induced by the plastic deformation produced by tool pin geometry and stirring action, as a result the grains of matrix were re-arranged and recrystallized; thus, fine grain growth occurred that improve the mechanical properties.

Based on the observations recorded, Fig. 5.5 shows the mean and S/N ratio response, at larger the better option, of the input process parameters on the tensile strength of the as-developed Al-based surface composite. It can be seen that with an increase in the rotational speed, from 1200 to 1800rpm, the tensile strength of the developed composite specimens increased. The tensile strength has almost a linear relation with *RS*. The *RS* is the 1st most influencing parameter showing a sharp increase in the mean of tensile strength from 197 MPa to 208 MPa when *RS* increases from 1200 to 1800 RPM. The reason for possessing excellent tensile properties is an effective stirring action owing to appropriate temperature distribution. This trend is because of the fact that by increasing the rotation speed of the tool developed higher frictional force, thereby heat energy.
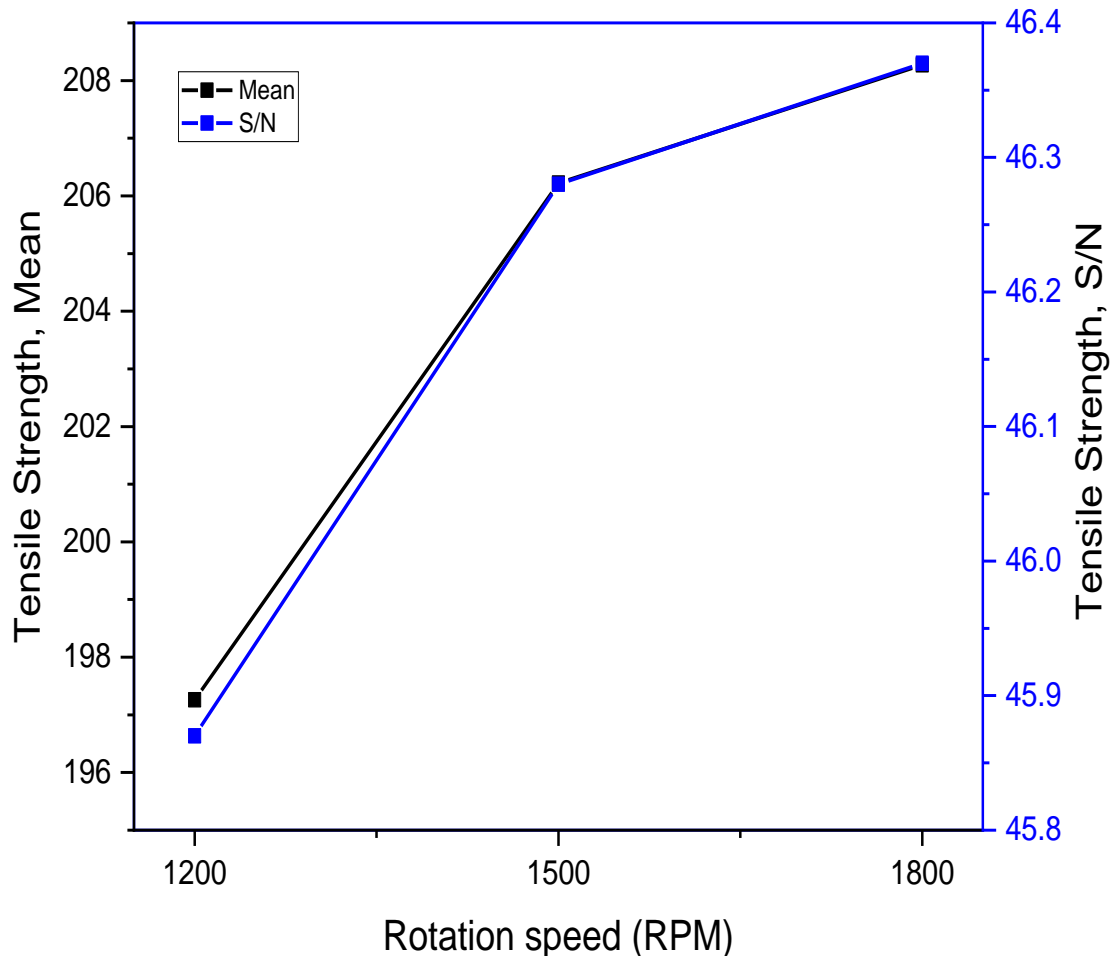
Figure 5.7. Effect of rotational speed on tensile strength

The higher amount of the heat resulted in: (i) refinement of the surface and (ii) fine dispersion of Gr and SiC particles. As the rotating speed increased to 1800rpm, the material flow was improved and regions with clustered small particles were observed beneath the stir zone. At low speed the material flow is low as a result tensile strength obtained is low. It can be clearly seen that when the rotational speed is 1200rpm, the improper heating of matrix resulted in the repulsion of the reinforcements from the set locations and, therefore, resulted in the low tensile strength of the developed AMCs. A sound, with visibly embedded reinforcements (indicated by yellow circles) can be seen in case of 1800rpm. As a result, the tensile strength is very high. Figure 5.7 shows the mean and S/N ratio response of tensile strength according to transverse speed (Ts). It has been found that with an increase in the speed from 30 to 40 mm/min, the tensile strength of the developed surface composites increased.
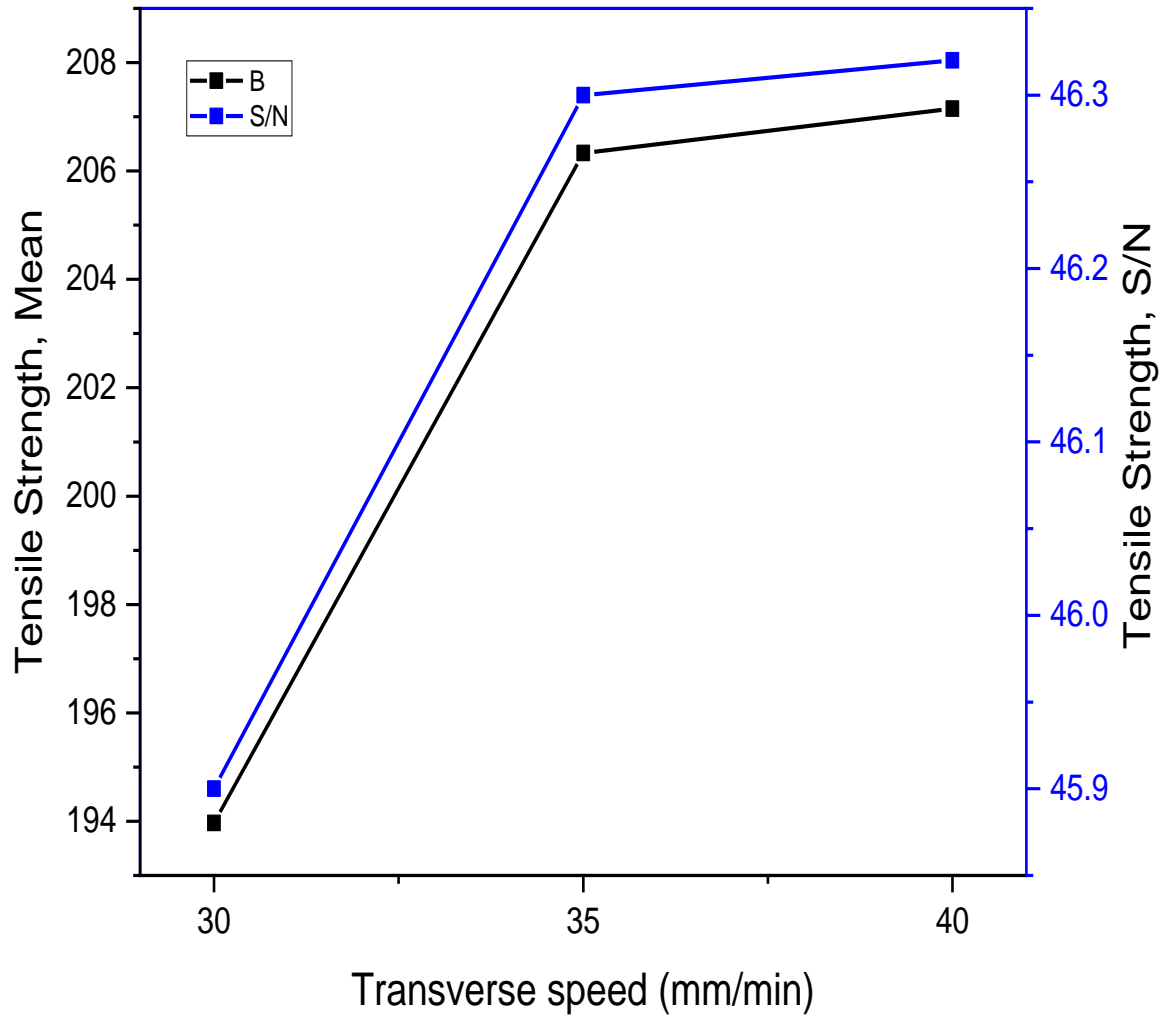
Figure 5.8. Effect of traverse speed on surface hardness

The *TS* is the 2nd most influencing parameter showing a sharp increase in the mean of tensile strength from 197 MPa to 207 MPa, when *TS* increases from 30 to 40 RPM. With the increase in transverse speed, the plasticized metal flow increased as a result finer grain growth occurred in the Al-matrix and more uniform distribution of reinforcement particles occurred. Moreover, in the processing zone ultrafine microstructure were developed, which further increased the tensile properties of as-developed composite. It has been found that the regions namely stir; transition and heat affected zone (HAZ) are greatly affected by the different levels of transverse speeds. Figure 5.8. shows the mean and S/N ratio response of tensile strength according to plunge depth (PD) of as-developed surface composite. It can be seen that tensile strength has linear relation with *PD.*
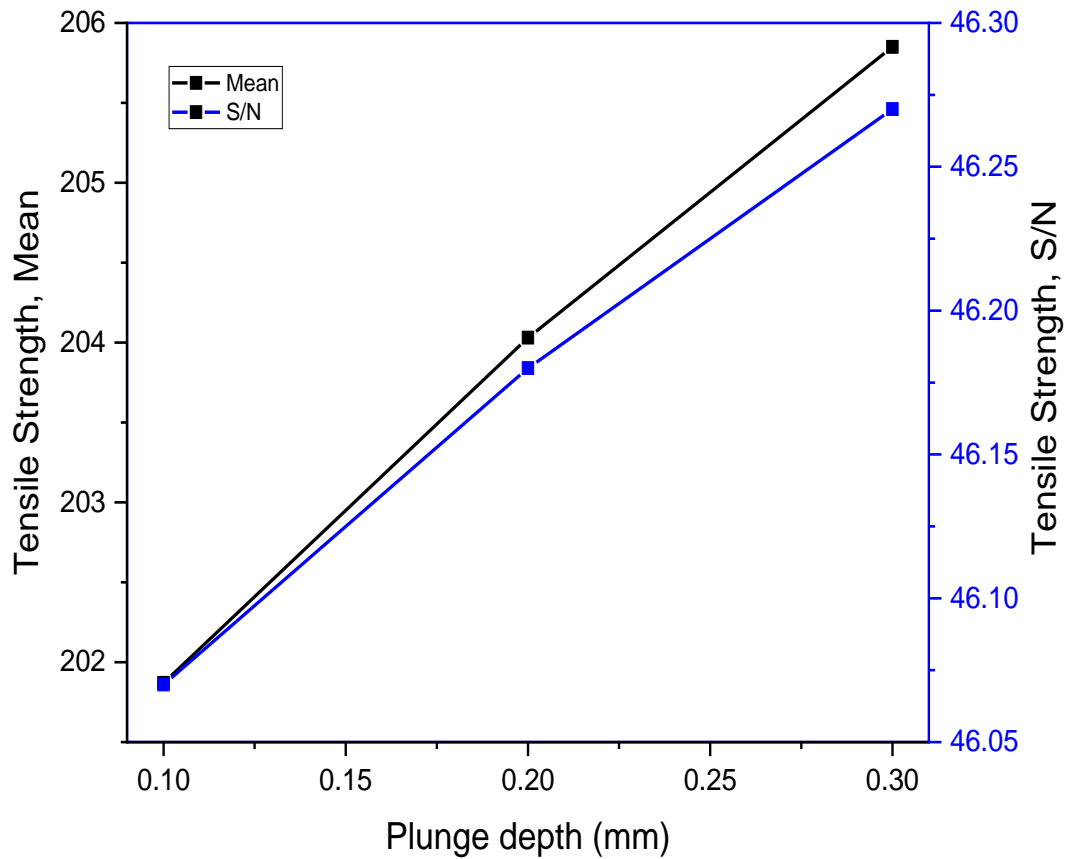
Figure 5.9. Effect of plunge depth on tensile strength

Tensile strength increases as PD grows, according to research. Among all criteria, the PD is the third most influential. When PD is increased from 0.1 mm to 0.3 mm, the mean of SH drops sharply from 201 MPa to 205 MPa. At the highest level (C3) of PD, the maximum tensile strength is obtained (0.3 mm). The change in tensile strength of the SN ratio as a function of PD levels matched the fluctuation in mean tensile strength. The plunge depth has no significant effect on the tensile properties of as developed surface composite. Indeed, the tilt angle affected the dispersion of reinforcement particles into the matrix as it is a critical process parameter which influences the material flow, and particle breakup and distribution in the processed zone. Figure 5.9 shows the mean and S/N ratio response of tensile strength according to tilt angle (TA) of as-developed surface composite. It can be seen that tensile strength has linear relation with *TA*.
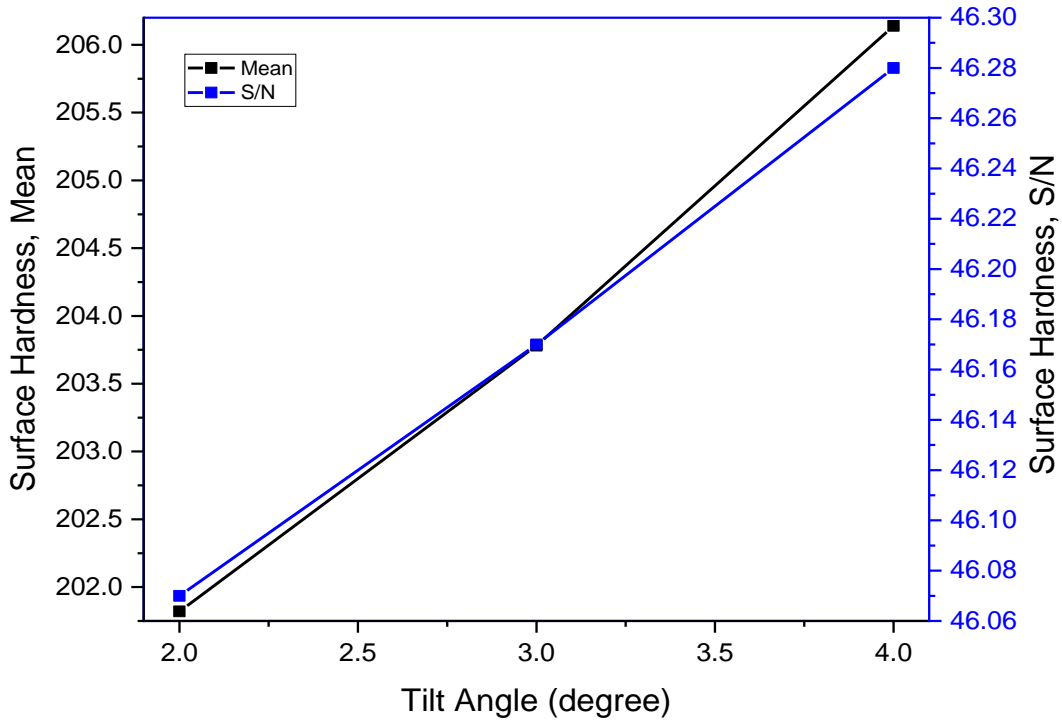
Figure 5.10. Effect of tilt angle on surface hardness
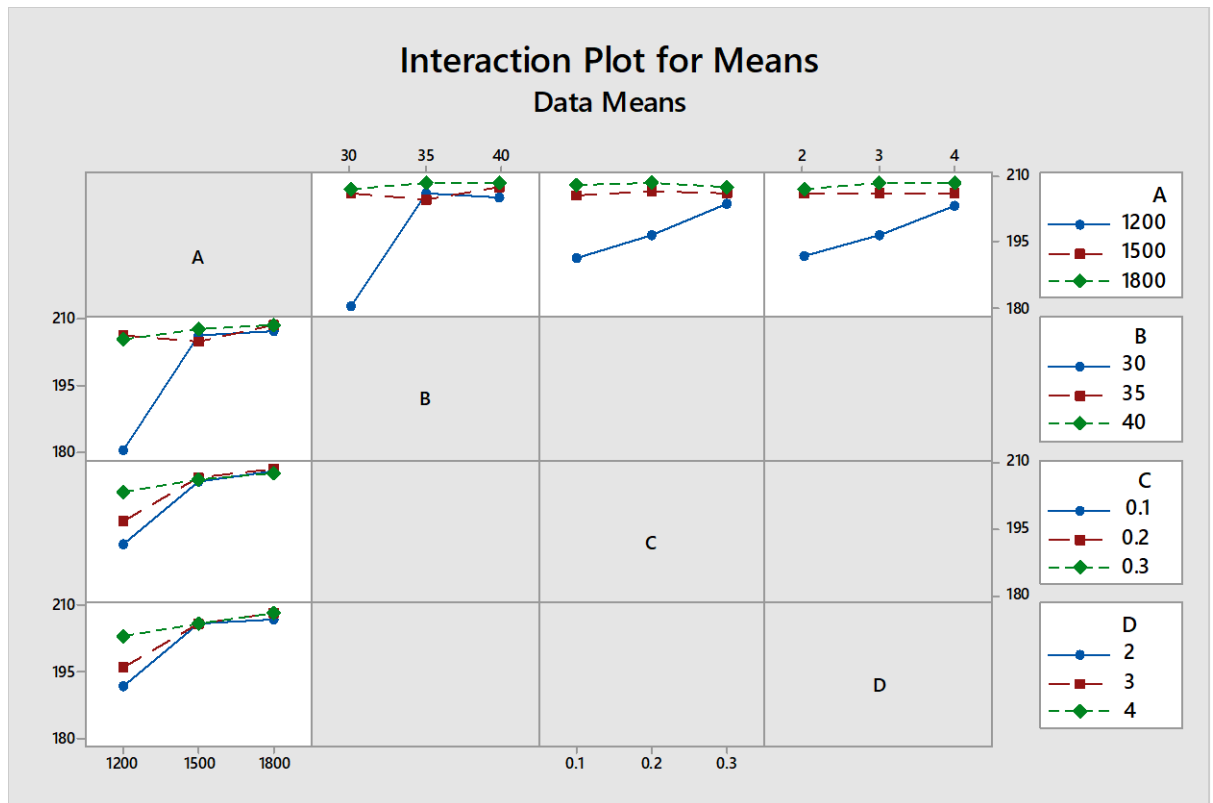
Figure 5.11. Graphical summarisation of results obtained for Tensile Strength (Plot for Means)

85

It can be seen from Figure 5.10 that when the tool tilt angle increased from 2 to 3 degree, the defect formation in the processed zone has eliminated. As the tool inclined, the tool front end was lifted upward and the tool rear end was lowered downward, and the front end acted as the reservoir to accommodate the material flow and decreases the wastage of material. However, the macrostructure examination showed that when the tilt angle was increased to 4 degrees, the processed zone formed surface crack, particle agglomeration, and tunneling defect because of the attainment of insufficient state of heat and material flow.

The ideal combination of FSP parameters for increasing tensile strength is higher rotation seed (RS=1800 RPM), higher transverse speed (TS=40 mm/min), higher lever of plunge depth (PD=0.3 mm), and higher tilt angle (TA=40), according to the above research. ANOVA has also been used to assess the relevance of each input parameter. The analysis of variance for tensile strength is shown in Table 5.9. The variables, degree of freedom (DOF), sequential sum square error (Seq SS), adjusted sum square error (Adj SS), adjusted mean square error (Adj MS), F statistic, p-values, and percentage contribution (percent) are all represented in columns in the table. For important parameters, the p-value of lack of fit should be less than 0.05, indicating statistically insignificant lack of fit at the 95 percent confidence level. The p-value of the regression model and all of its terms, on the other hand, is less than 0.05, indicating that they are statistically significant at 95 percent confidence. As a result, the model accurately depicts the experimental data. The ANOVA analysis shows that RS and TS have a considerable impact on tensile strength. With a contribution of 32.5 percent, the interaction between rotational and transverse speeds is quite significant. Individual contributions to rotational and transverse speeds are 23.20 percent and 18.25 percent, respectively. Plunge depth and tilt angle both contribute 2.69 and 3.17 percent respectively. The mistake contribution percentage is merely 9.86 percent.
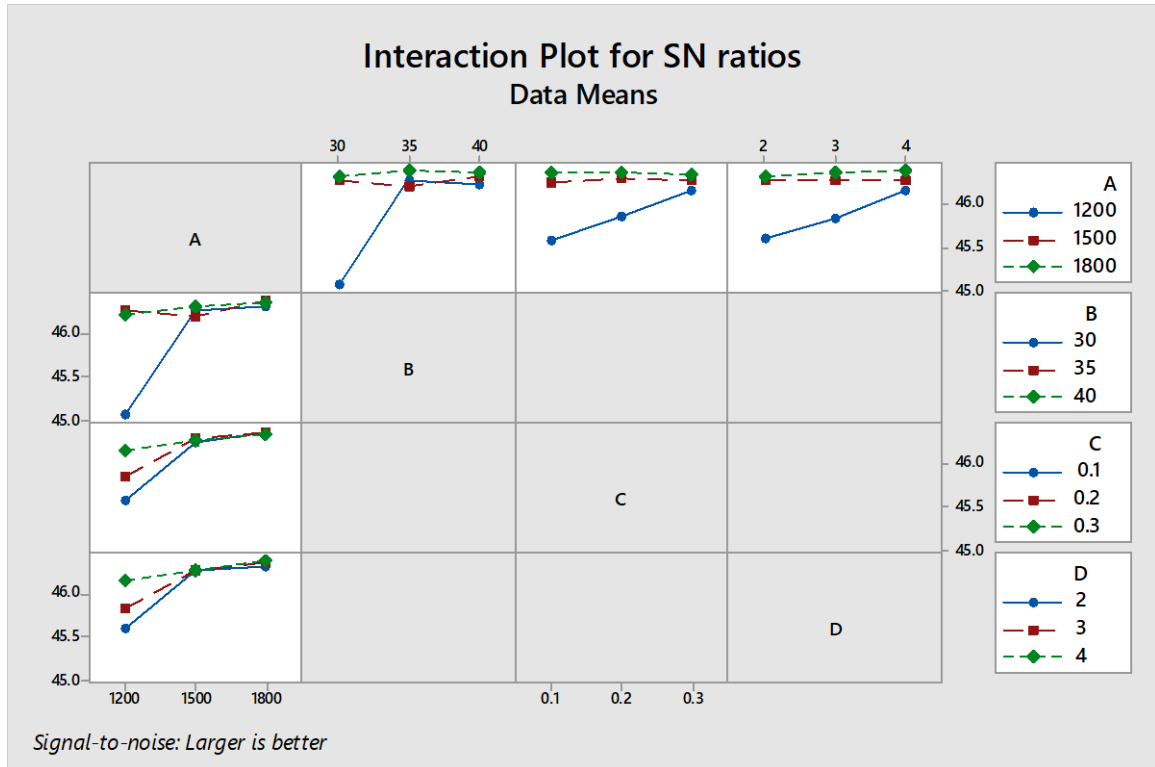
Figure 5.12. Graphical summarisation of results obtained for Tensile Strength (Plot for SN Ratios)

Table 5.9: Analysis of variance of tensile strength

Factors	DOF	Seq SS	Adj MS	F	P	%
Rotation Speed (RS)	2	616.15	308.07	7.06	0.027	23.20
Transverse Speed (TS)	2	484.68	242.34	5.55	0.043	18.25
Plunge Depth (PD)	2	71.35	35.67	0.82	0.485	2.69
Tilt Angle (TA)	2	84.29	42.15	0.97	0.433	3.17
Rotation Speed (RS)× Transverse Speed (TS)	4	864.39	216.1	4.95	0.042	32.55
Rotation Speed (RS)× Plunge Depth (PD)	4	152.87	38.22	0.88	0.53	5.76

Rotation Speed (RS)$\times$ Tilt Angle (TA)	4	119.95	29.99	0.69	0.627	4.52
Residual Error	6	261.84	43.64			9.86
Total	26	2655.52				
*Significant Terms						

5.1.2.1 Confirmation of Experiments

A confirmation test was done for a few optimal solutions produced using Taguchi's methodology in order to verify them. Table 5.10 shows the optimal condition predicted by Taguchi's methodology for surface hardness and tensile strength responses, as well as the confidence interval for both responses within which the optimal value should reside. The confirmation trials for a different factor combination are shown in Table 5.11. The tests were done three times, and the average values were compared to Taguchi's methodology's expected solutions. Surface hardness and tensile strength improvements have been measured. The creation of fine microstructure and strain hardening mechanisms improve surface hardness with the FSP process. Tensile strength improved as a result.

Table 5.10. Confidential interval of the response values

Response	Optimal Levels	Predicted Value of Response using Taguchi's Method	Confidential Interval (CI$_{CE}$)
Surface hardness	A$_3$ B$_3$ C$_3$ D$_4$	198	155.9 to 227.
Tensile strength	A$_3$ B$_3$ C$_3$ D$_4$	209 MPa	168.1 to 239.8

Table 5.11: Confirmation test

Sr. no	A	B	C	D	Predicted		Confirmation		% Error	
					SH	TS	SH	TS	SH	TS
1	1200	30	0.2	2	156	174	160	179	2.5	2.79
2	1500	40	0.3	3	193	205	195	210	1.025	2.38
3	1800	40	0.3	4	198	209	200	210	1	0.47

5.1.2.2 Fractured surfaces

Figure 5.13 shows the scanning electron microscopy (SEM) images of the fractured surface and its magnified view. The SEM micrographs of the fractured surface of as-developed composite at experiment number 1 (C1) and 3 (C3) as per conformation test of experiment are presented in Figures 5.13(A) and (B), which reveal the surface information. Figures 5.13(C) and (D), exhibited the magnified SEM images of deformation dimples. The fractured surface of the joint produced under condition C1 corresponding to Table 5.1 exhibits shallower impressions when compared with data set C2. The reason for shallower dimples is plausibly due to extreme precipitate coarsening occurred during FSP. From the fractographic images it has evinced the presence of large, fine and equiaxed dimples, voids and micro voids of different shapes and sizes in fractured surfaces, however, they were unable to identify through metallographic analysis. This confirmed that these voids and micro voids are the root cause of failure in TMAZ, furthermore, in such dimple rupture mode, overloads act as the main cause of fracture.
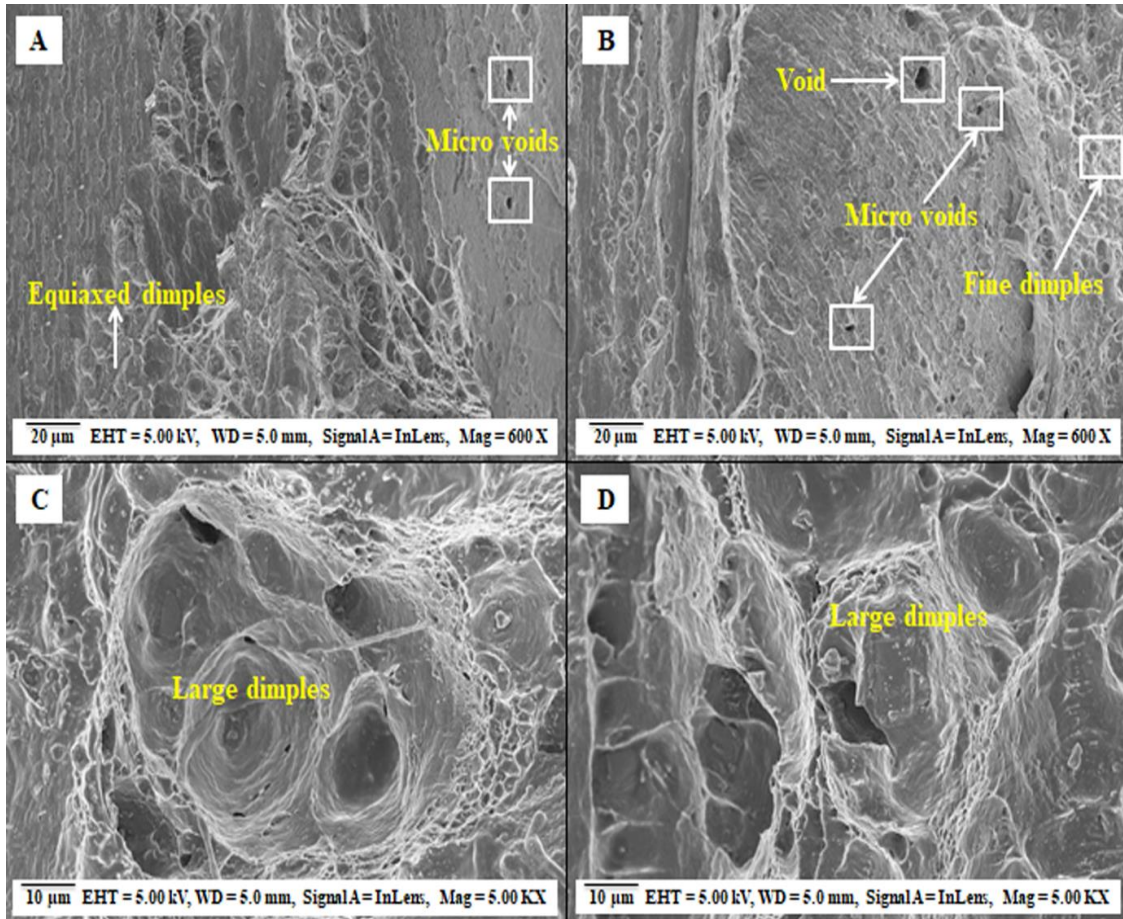
Figure 5.13. Fractured surface of the tensile tested specimens under SEM for welds B2 and C3 given in Table 5.1.

5.2 Effect of FSP process parameters on Microstructure

Figure 5.13 shows the cross-section macrograph of FSP processed zone with different transverse speed and the material location at a constant rotational speed. Friction stir processing zone (FSPZ), thermomechanical affected zone (TMAZ), and heat-affected zone (HAZ) were clearly identified in the macrograph. From the macrograph, it can be seen that the Al5086-GRN-SiC hybrid composite was defect free and sound. Numerous onion rings appear in the stir zone, which comprises different lamellar structures generated due to dynamic stirring of tool pin, and it occurs excess in processing. In the literature, similar results were reported that the emergence of onion rings in FSPZ due to the combined effect of geometric nature of pin driven plastic flow and vertical movement of the material owing to shoulder interaction [93]. Flash generally forms because of excessive heat produced owing to high rotating speed and low rotational speed [94]. FSP process has a tendency to produce surface flash, since the tool shoulder is obliged to penetrate below the workpiece surface and the processing is associated

90

with heat generation and mechanical mixing. Generally excess materials occurred during the process flashing out but some materials somehow tend to stuck on the processed surface. These flashes could be eliminated by machining the top and bottom surfaces of processed plate, as evidenced in Rodriquez et al. [92].
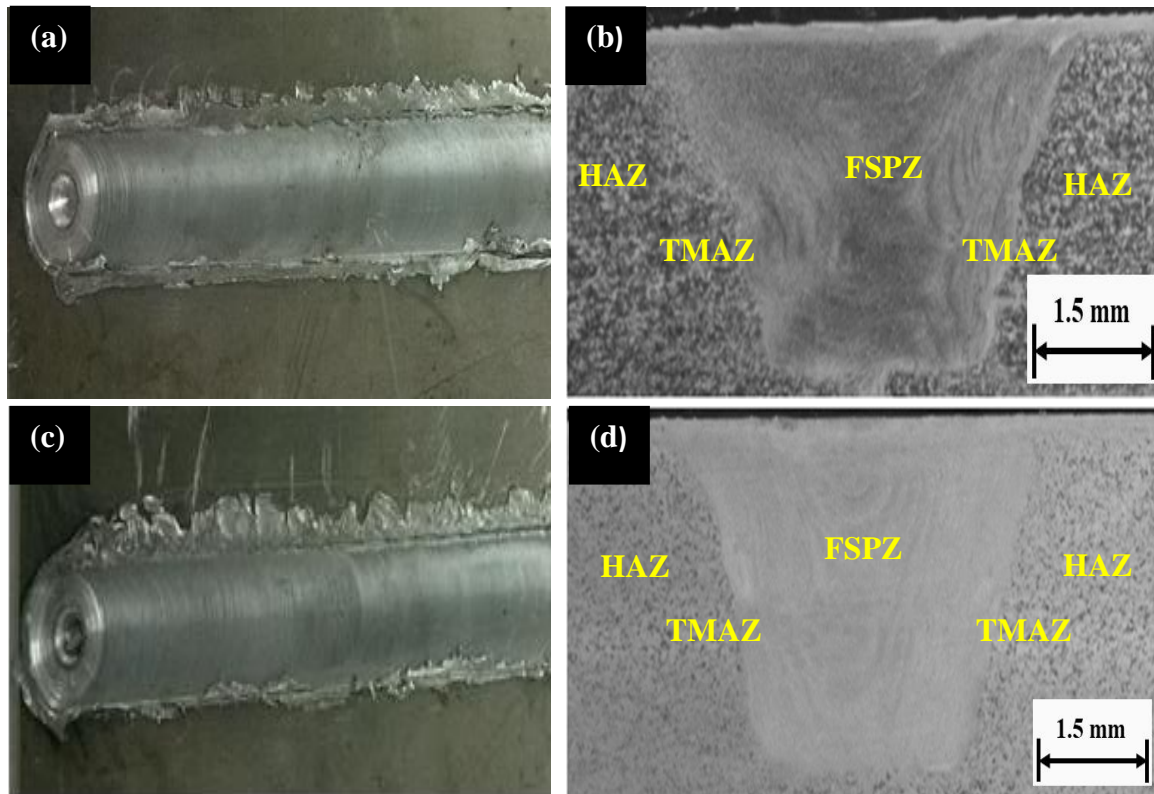
Fig. 5.14. Macrograph of FSP processed zone under different speed: (a-b) 1200 RPM and (b) 1800 RPM

Microstructure of materials determines the mechanical properties. Figure 5.14 shows the microstructure of heat affected zone (HAZ) and friction stir processed zone (FSPZ) at 1200rpm speed with 30mm/min and 40 mm/min transverse speed. At 30 mm/min feed, it can be seen that HAZ has coarse grain size in the range of 20-25 µm (refer Fig. 5.14a), whereas FSPZ comprised grain size grain size in the range of 13-15 µm (refer Fig. 5.14b). This is attributed due to that fact that in FSPZ region, the grains of Al-matrix were re-arranged and recrystallized due to plastic deformation induced by tool.

Fig. 5.15: Microstructure of heat affected zone (HAZ) and friction stir processed zone (FSPZ) at 1200rpm speed with (a) 30mm/min and (b) 45 mm/min feed

From micrograph, non-homogenous distribution of SiC can be clearly seen in the Al-matrix, owing to limited amount of metal flow and low plasticity at low speed (1200 RPM). However, the GRN layer was homogenously and uniformly distributed and entered up to certain micrometers in Al-matrix. The uniform graphene film was developed due to shearing of particles developed by friction tool near the subsurface regions where subsurface strains are extremely high. With the increase in feed (transverse speed), the significant change in the microstructure were observed. At 80 mm/min feed, it can be seen that HAZ has coarse grain size in the range of 18-22 µm (refer Fig. 5.15c), whereas FSPZ comprised grain size grain size in the range of 10-12 µm (refer Fig. 5.15d). With the increase in transverse speed, the

plasticized metal flow increased as a result finer grain growth occurred in the Al-matrix and more uniform distribution of reinforcement particles occurred.

Figure 5.16 shows the microstructure of heat affected zone (HAZ) and friction stir processed zone (FSPZ) at 1800 rpm speed with 30mm/min and 40 feed. Similarly, the HAZ region comprised coarse gain and FSPZ comprised fine grain structure, however, the gain size in HAZ and FSPZ is smaller as compared to the microstructure obtained at 1200 RPM. At 30 mm/min feed, it can be seen that HAZ has coarse grain size in the range of 20-22 µm (refer Fig. 5.16a), whereas FSPZ comprised grain size grain size in the range of 8-10 µm (refer Fig. 5.16b). It can be seen that SiC and GRN were homogeneously and uniformly distributed. The dark grey patches correspond to GRN layer and SiC reinforced and deposited in the Al-matrix. This is attributed due to high materials flow and plastic deformation owing to heat generated during high rotation speed. With the increase in feed (transverse speed), the grain structure further recrystallized and finer grain growth was obtained. At 40 mm/min feed, it can be seen that HAZ has coarse grain size in the range of 12-15 µm (refer Fig. 5.16c), whereas FSPZ comprised grain size grain size in the range of 6-8 µm (refer Fig. 5.16d). Yellow arrow and yellow circles correspond to distribution of SiC and GRN particles, respectively, owing to low density, the GRN particles floats on the surface. Due to high speed, large amount of heat generated, which causes more plastic low of material. As a result, strain increased in the region where GRP present and film squeezed out form there and floats on the top surface. This results in the improvement in mechanical properties.
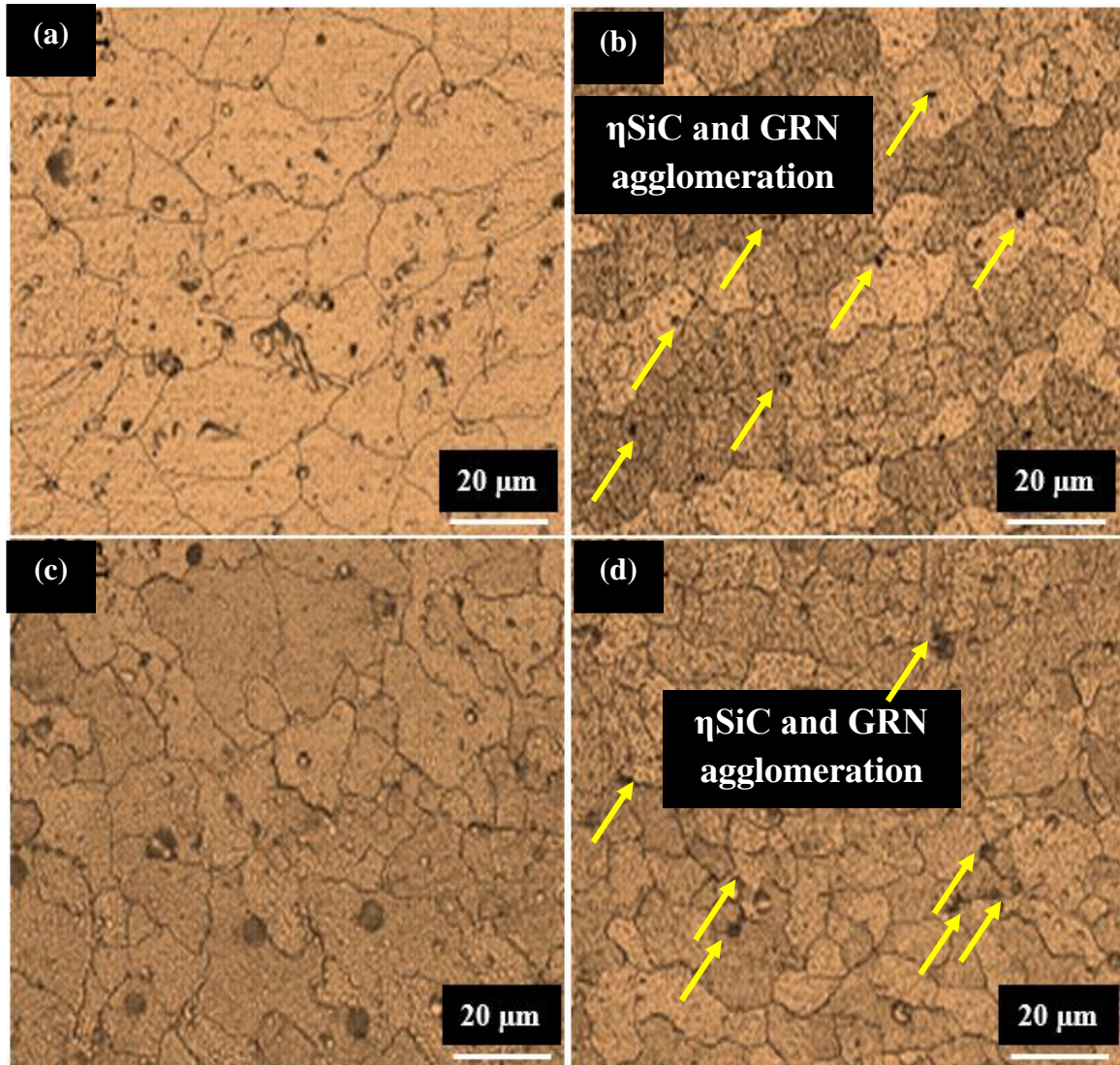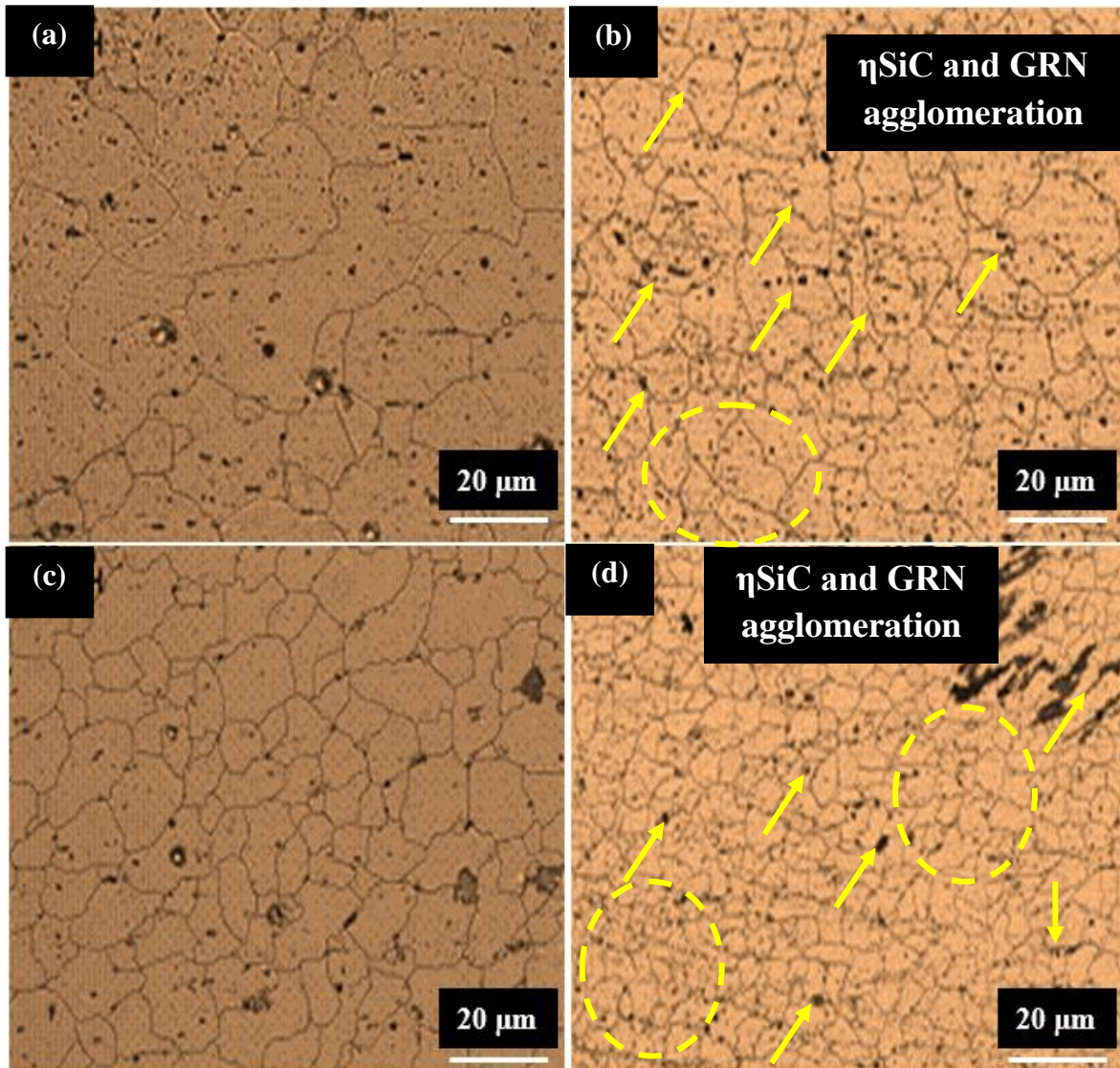
Figure 5.16. Microstructure of heat affected zone (HAZ) and friction stir processed zone (FSPZ) at 1800rpm speed with (a) 30mm/min and (b) 45 mm/min feed

Figure 5.17 shows the EDS spectrum and FE-SEM micrograph of base Al5086 alloy and as developed Al5086-GRN-ηSiC hybrid composite. Figures 5.17(a) and (b) shows the FE-SEM micrograph and EDS spectrum of unprocessed base Al5086 alloy. From the FE-SEM micrograph, it can be seen that unprocessed base Al5086 alloy compromised plan surface morphology and EDS spectrum confirmed the presence of Al, Mg, C, and O elements, which further conferred the elemental composition of base alloy. Figures 5.17(c) and (d) shows the FE-SEM micrograph and EDS spectrum of FSP-developed Al5086-GRN-ηSiC hybrid composite. From the FE-SEM micrograph, the agglomeration GRN and ηSiC can be clearly observed (refer Fig. 5.17c). The presence of Si and C peak along with Al peaks confirmed the uniform and homogeneous distribution of GRN and ηSiC.
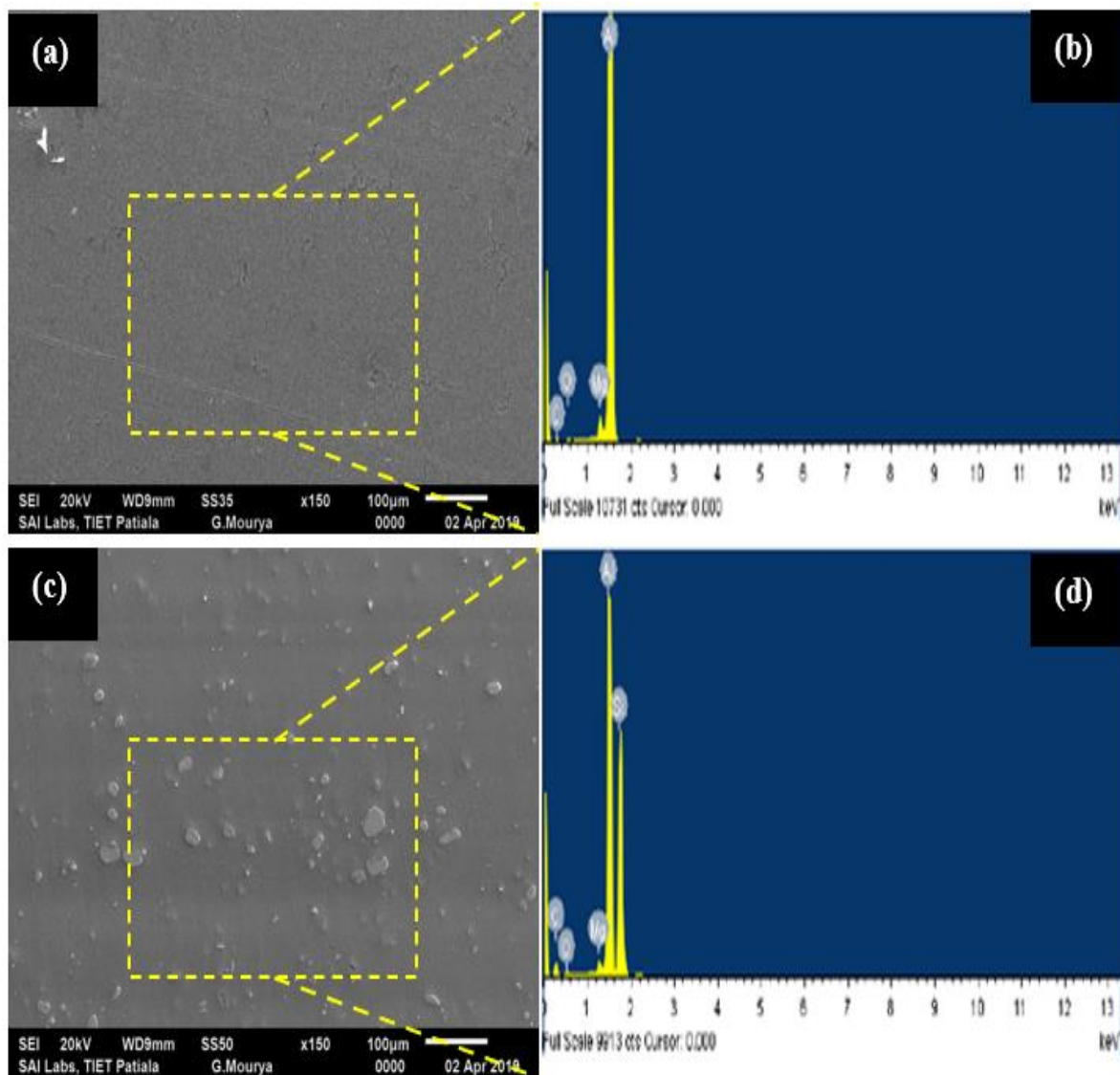
Figure 5.17. EDS and SEM-micrograph of (a-b) Al5086 alloy and (c-d) Al5086-GRN-ηSiC hybrid composite

Figure 5.18 shows the XRD pattern of un-processed Al5086 alloy and FSP-developed Al5086-GRN-ηSiC hybrid composite at RS; 1800 and F:120 mm/min. It can be seen that the un-processed Al5086 alloy comprised only Al, Mg, and Cu-peaks. Different intensities of the peak were noticed at diffraction angles (2θ) and in the same manner, an intensity of these peaks was observed to be low in the un-processed Al5086 alloy whereas higher in the FSP-developed Al5086-GRN-SiC hybrid composite developed at RS: 1800 rev/min and F:160 mm/min. Graphene, Al, SiC peaks can be clearly seen in the FSP-developed Al5086-GRN-SiC hybrid composite. The intensity of (200) peak for FSP-developed Al5086-GRN-SiC hybrid composite corresponding to aluminum which has FCC crystal structure was observed significantly higher that is an indication of texture effect caused due to stirring action in the thermo-mechanically

affected zone. The close packed planes (111) in HCP metals and (200) in FCC metals are the highest density planes that serve an important role in material properties. The FSP-developed Al5086-GRN-ηSiC hybrid composite consist a higher fraction of FCC metal that excellently enhance the mechanical properties of a joint and mechanical properties.

Figure 5.18. XRD patterns for un-processed (B) Al-5086 and (A) FSP-developed Al5086-GRN-ηSiC hybrid composite

Figure 5.19 shows the microhardness profile of Al5086-GRN-ηSiC hybrid composite processed at different rotational speed and feed. The hardness measurements were recorded across the center of the joint cross-section, using Vickers microhardness testing machine. The hardness values of all the processed zone revealed asymmetry along the weld length due to high temperature generated in the SZ and improper heat dissipated into the adjoining material during the processing zone.
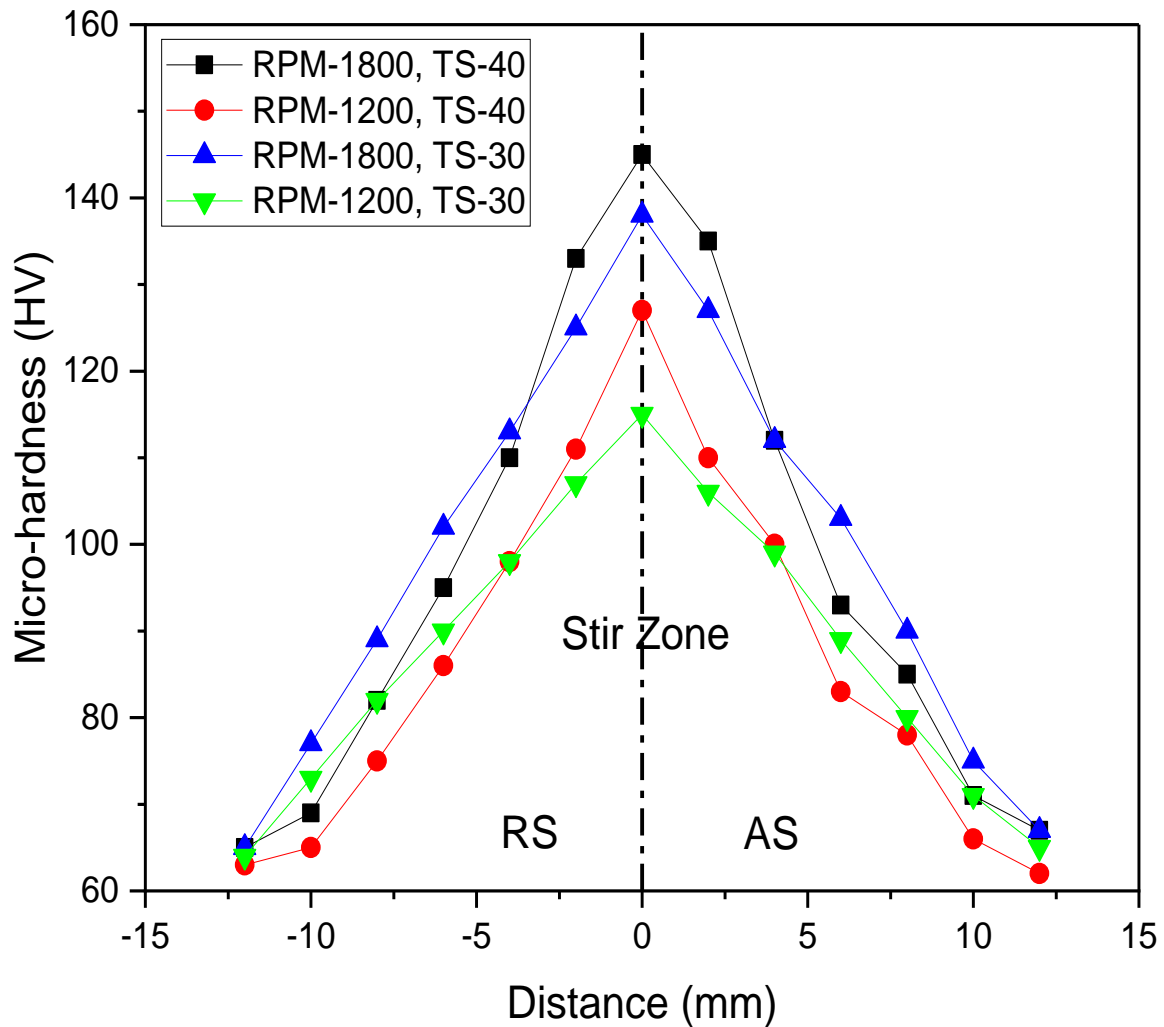
Figure 5.19: Vickers microhardness profile across the Al5086-GRN-SiC hybrid composite

The low hardness values are noticed in Stir zone (TMAZ) on advancing side where the fracture occurred and the lowest value of 62 HV is observed for a zone obtained with 80 mm/min travel speed and 1200 rpm spindle speed. The Al5086-GRN-SiC hybrid composite developed with RS: 1800 rpm and WS: 112 mm/min produced highest hardness value of 145 HV in SZ adjacent to thermo-mechanically affected zone on retreating side. This could be the consequential

reason for the higher ultimate tensile strength of the joint fabricated with these parameters. The small particles of intermetallic compound and fine grains in the stir zone are the key reason for improved hardness values in the SZ because grain size refinement has a significant role in material robustness.

5.3   Microstructure of Al5086-GRN-ηSiC hybrid composite by APF-FSP

Figure 5.20 presents the SEM-micrograph, EDS-spectrum, and TEM-mage of base Al5086 alloy and APF-FSP developed Al5086-GRN-ηSiC hybrid composite. The unprocessed base Al5086 alloy compromised plan surface morphology and EDS spectrum confirmed the presence of Al, Mg, C, and O elements, which further conferred the elemental composition of base alloy (refer Fig. 5.20a). The agglomeration GRN and ηSiC can be clearly observed in the APF-FSP developed Al5086-GRN-ηSiC hybrid composite (at 1800 RPM and 40 mm/min) and associated EDS-spectrum confirm the Si and C peak along with Al peaks refer Fig. 5.20(b). The agglomeration GRN and ηSiC can be clearly seen in the Al-matrix in the form of large clusters. During APF-FSP processing, the graphite powder was exposed to high material flow owing to plastic deformation induced by stirring action, which results in a large amount of graphene exfoliated in the form of thin films form graphene (refer Fig. 5.20c). The dark/bright-field diphasic nano-mixture cluster of ηSiC and GRN in the range (100-200 nm) can be seen in SEM and TEM-micrograph, refer Fig. 5.20(d). The GRN co-exist in multi-layer of atoms in Al-matrix owing to mechanical exfoliation of graphite. There were no visible defects, cracks, and impurities formed at the carbon-to-aluminum interface.
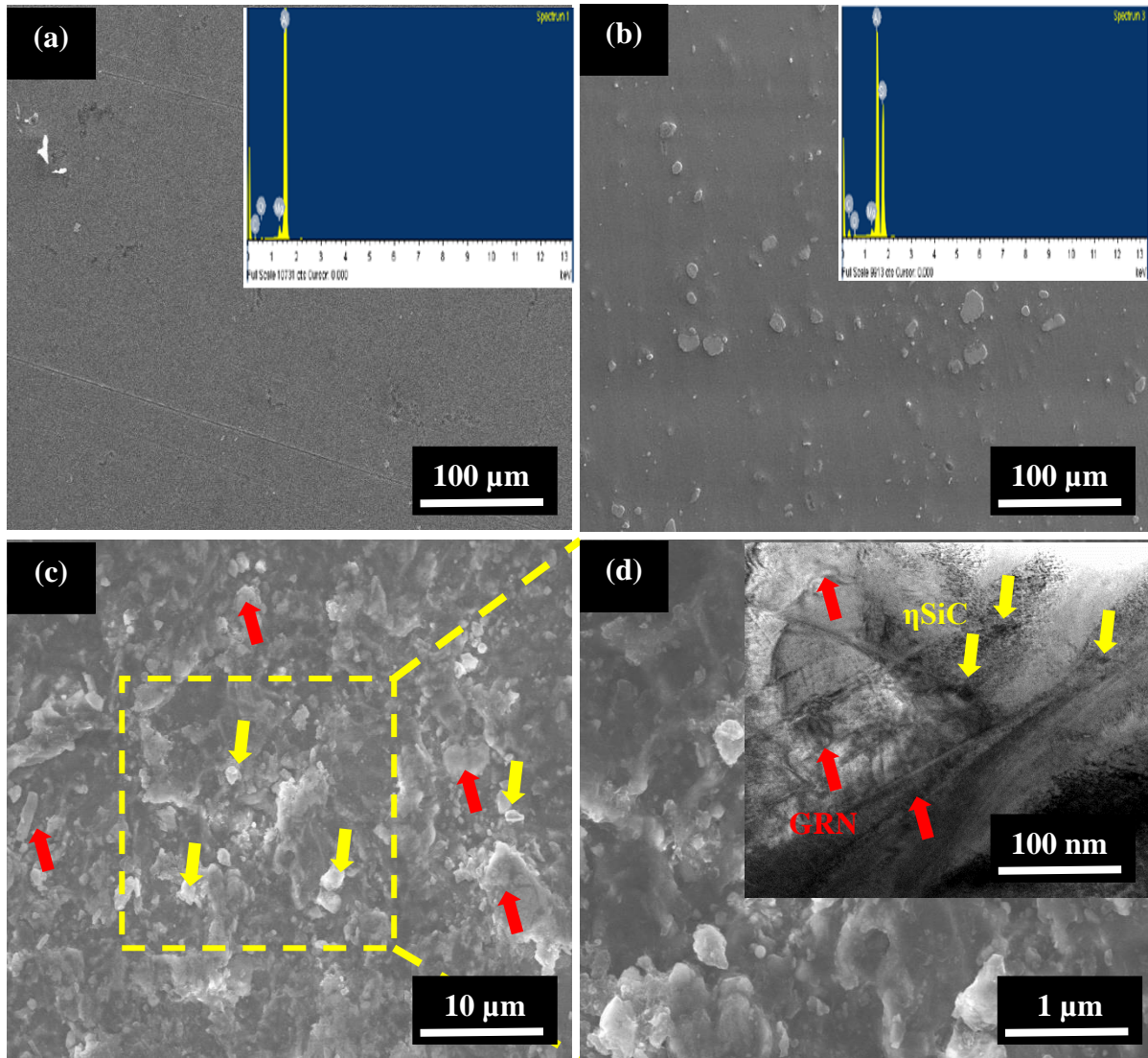
Figure 5.20. EDS and SEM-micrograph of (a) Al5086 alloy, (b) Al5086-GRN-ηSiC hybrid composite, (c) SEM-micrograph (2500 ×), (d) SEM micrograph (10000 ×) and TEM micrograph

Figure 5.20 shows the XRD pattern of un-processed Al5086 alloy and FSP-developed Al5086-GRN-ηSiC hybrid composite at RS; 1800 and F:40 mm/min. It can be seen that the un-processed Al5086 alloy comprised only Al, Mg, and Cu-peaks. Different intensities of the peak were noticed at diffraction angles (2θ) and in the same manner, an intensity of these peaks was observed to be low in the un-processed Al5086 alloy higher in the FSP-developed Al5086-GRN-ηSiC hybrid composite developed. Graphene, Al, SiC peaks can be clearly seen in the FSP-developed Al5086-GRN-ηSiC hybrid composite.
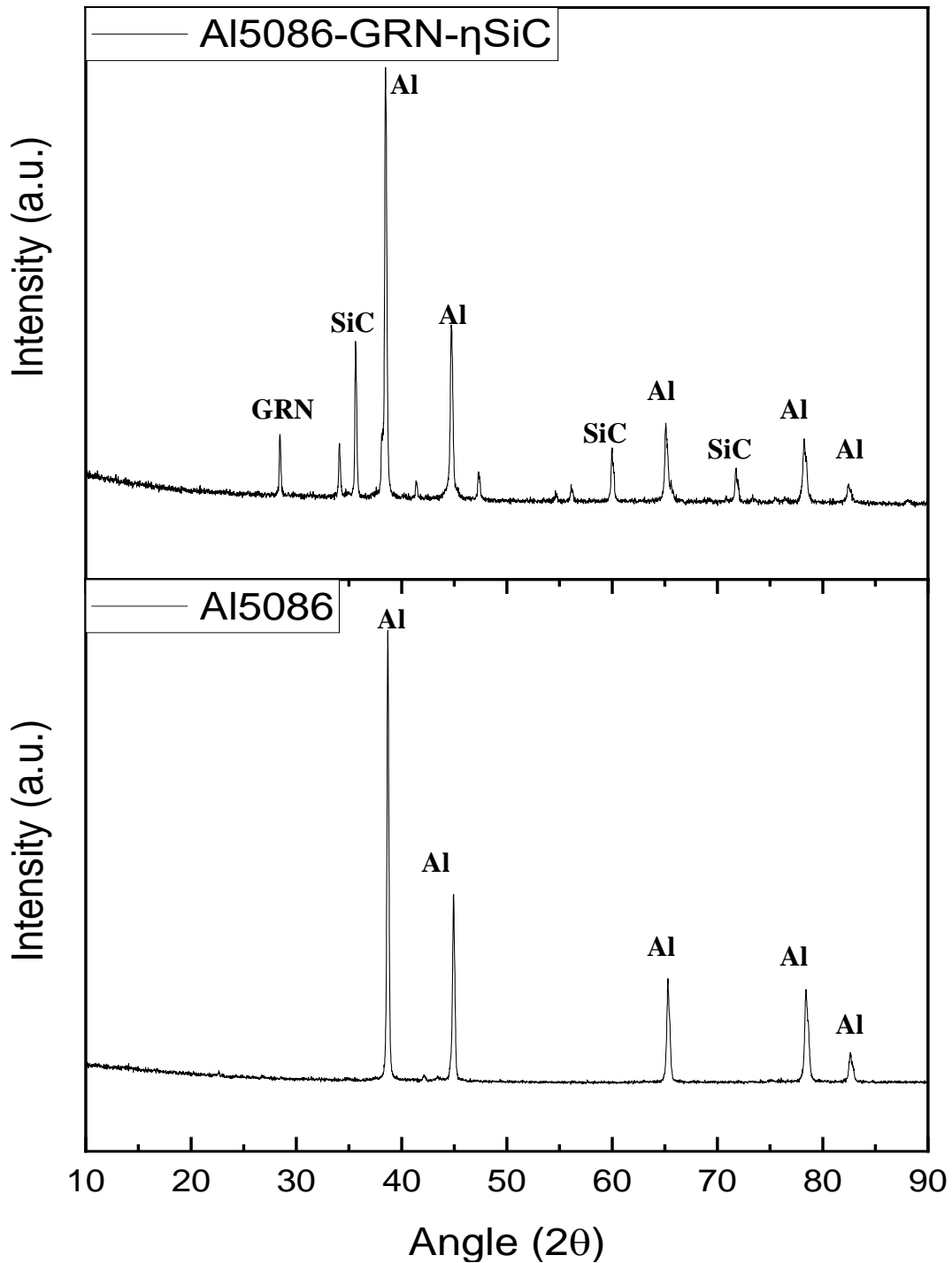
Figure 5.21: XRD patterns for un-processed Al-5086 and FSP-developed Al5086-GRN-ηSiC hybrid composite

The intensity of (200) peak for FSP-developed Al5086-GRN-ηSiC hybrid composite corresponding to aluminum which has FCC crystal structure was observed significantly higher that is an indication of texture effect caused due to stirring action in the thermo-mechanically affected zone. The close packed planes (111) in HCP metals and (200) in FCC metals are the highest density planes that serve an important role in material properties. The FSP-developed

Al5086-GRN-ηSiC hybrid composite consist a higher fraction of FCC metal that excellently enhance the mechanical properties of a joint and mechanical properties.

The micromechanical behavior of un-treated Al5086 alloy and FSP-developed Al5086-GRN-ηSiC hybrid composite was investigated in terms of elastic modulus and compressive strength using nano-indentation system. Figure 5.22(a) shows the loading/unloading indentation curve, which indicates that the materials showed both elastic and plastic deformation, with some elastic recovery after full unloading. The elastic modulus was determined using Oliver–Pharr method. The slope of FSP-developed Al5086-GRN-ηSiC hybrid composite was less than the slope of un-treated Al5086 alloy. The is attributed because, the top layer of Al5086-GRN-ηSiC hybrid composite comprised fine grain structure which exhibit high hardness. Correspondingly, the Al5086-GRN-ηSiC hybrid composite samples possessed high elastic modulus (172 GPa) as compared to un-treated Al5086 alloy (75 GPa).

Figure 5.22(b) shows the stress-strain curves of the micro-pillars as converted from associated load-displacement curves of un-treated Al5086 alloy and FSP-developed Al5086-GRN-ηSiC hybrid composite. From the graph, it can be seen that the stress-strain behaviour of the Al5086-GRN-ηSiC hybrid composite is distinct from the un-treated Al5086 alloy. The Al5086-GRN-SiC hybrid composite's top surface layer shows to be able to withstand more stress than the untreated Al5086 alloy, but it is unable to assimilate strain. It is not wonder, given that the Al5086-GRN-SiC hybrid composite is hard and brittle in nature when compared to untreated Al5086 alloy, as evidenced by nanoindentation data. The micro-pillars on the top surface layer of the Al5086-GRN-SiC hybrid composite break down (collapse) completely within less than 12 percent of strain, as evidenced by the videos taken during the micro-pillar compression tests. The Al5086-GRN-ηSiC hybrid composite sample offered high ultimate tensile strength of 209.8 MPa (385 MPa as an exception in case of AFP-FSP). In comparison to that, stress-strain curves of un-treated Al5086 alloy appear to sustain considerably more strain (up to 15 %). The un-treated Al5086 alloy sample offered high ultimate strength (245 MPa).
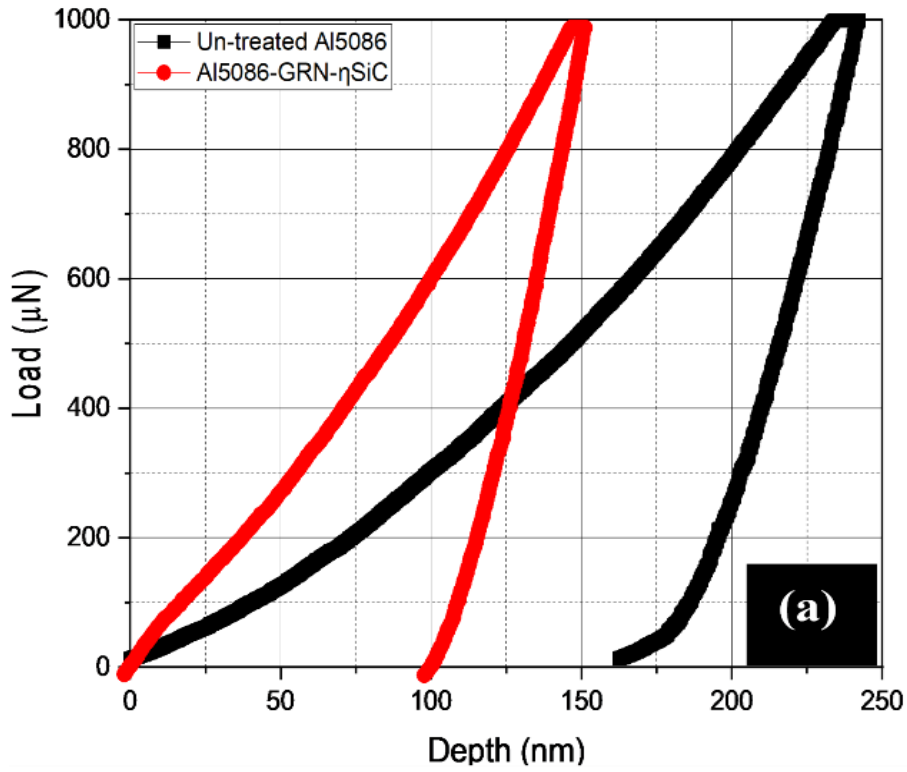
Figure 5.22(a). Micro-mechanical behavior in terms of elastic modulus of un-treated Al-5086 alloy and FSP-developed Al5086-GRN-ηSiC hybrid composite
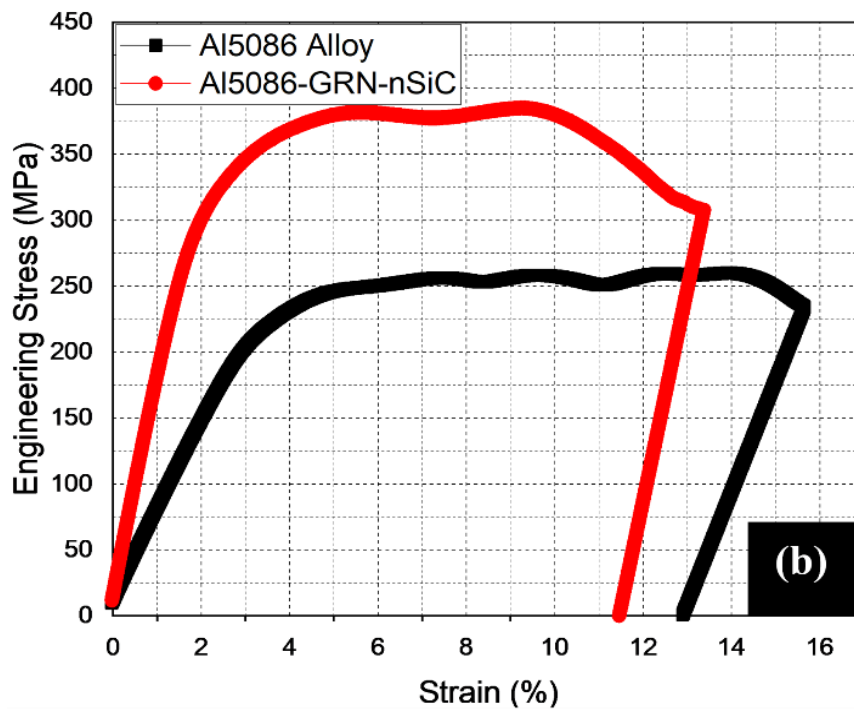
Figure 5.22(b). Micro-mechanical behavior in terms of compressive strength of un-treated Al-5086 alloy and FSP-developed Al5086-GRN-ηSiC hybrid composite

5.4   Wear and tribological properties of Al5086-GRN-ηSiC hybrid composite by APF-FSP

The tribological characteristics for the sample 1 and sample 2 pins developed has been studied. The sample 1 and 2 of Al5086-GRN-ηSiC hybrid composite was developed as per process parameters of experimental sr. no. 1 and 3, respectively, reported in Table 5.12 The influence of operating parameters on the friction and wear behavior was studied. Table 5.12 presents the values for COF and wear obtained from experiments performed as per wear testing parameters.

Table 5.12: Tribological performance of sample 1 and sample 2

Load	Speed	Sliding distance	Sample 1 COF	Sample2 COF	Sample1 Wt. loss	Sample 2 Wt. loss
50	53	500	0.527	0.492	0.0043	0.0067
50	106	1000	0.464	0.470	0.0061	0.0099
50	160	1500	0.526	0.585	0.0065	0.0077
75	53	500	0.573	0.499	0.0038	0.0048
75	106	1000	0.472	0.499	0.0058	0.0095
75	160	1500	0.585	0.552	0.0126	0.0113
100	53	500	0.517	0.594	0.0112	0.0092
100	106	1000	0.476	0.569	0.0125	0.0169
100	160	1500	0.504	0.575	0.0220	0.0156

5.4.1. Contact Friction

The friction plot for a given load and varying speeds is shown in figure 5.23 (a-b). It is observed from the figure that the sample-1 pins resulted in lower friction as compared to the sample-2 pins at given load of 75N. At lower loads the distinction is clearer while with increase in load from 75N to 100 N the coefficient of friction is reducing in the case of sample-2 pins as compared to two-hole pin. The change of sample-1 to sample-2, shows a higher in friction value as increase in speed at the same load. The variation in speed influences the friction in materials. It is observed from the figure 5.23(a) that at a fixed load of 75 N the value of coefficient of friction (COF) observed at 53 RPM in case of sample-1 pins is 0.499. As the speed increase from 53 RPM to 160 RPM at the 75 N load, the COF is increases with approximate 10 % in case of sample-1 pins, but comparing with the sample-2 pins at the same parameters the COF increase by approximate 3%. At the same parameters sample-1 pins shows the approximate 0.516 COF, whereas sample-2 pins show the COF value of 0.543. Approximately 5 % higher value has been recorded. This behavior can be attributed as the sample-2 comprised uniform distribution ηSiC and GRN, which offer hard surface. As a result, owing to friction, materials get released on the surface and the wear increased. But at the higher load of 100N, the values of COF are very close to each other and the distinction can be easliy made between the sample-1 and sample-2 pins. At higher load as shown in figure 5.23(b) the COF decreases with increase in speed in case of sample-1 pins. Similar behavior is observed in case of sample-2 pins as the COF decreases with increase in speed. At 100 N load the average COF has been recorded in case of sample-1 is .579, whereas .499 COF has been recorded in case of sample-2 pin. Approximately 16 % lower COF value has been recorded, when sample-2 was used as pin. This is observed that at the higher load as ηSiC and GRN acted as self-lubricated medium and the value of COF decreases. Also, the overlapping is observed due to approximately closer values of COF which acts when the pin is subjected to 53 RPM to 160 RPM at the 75 N load/100 N load.
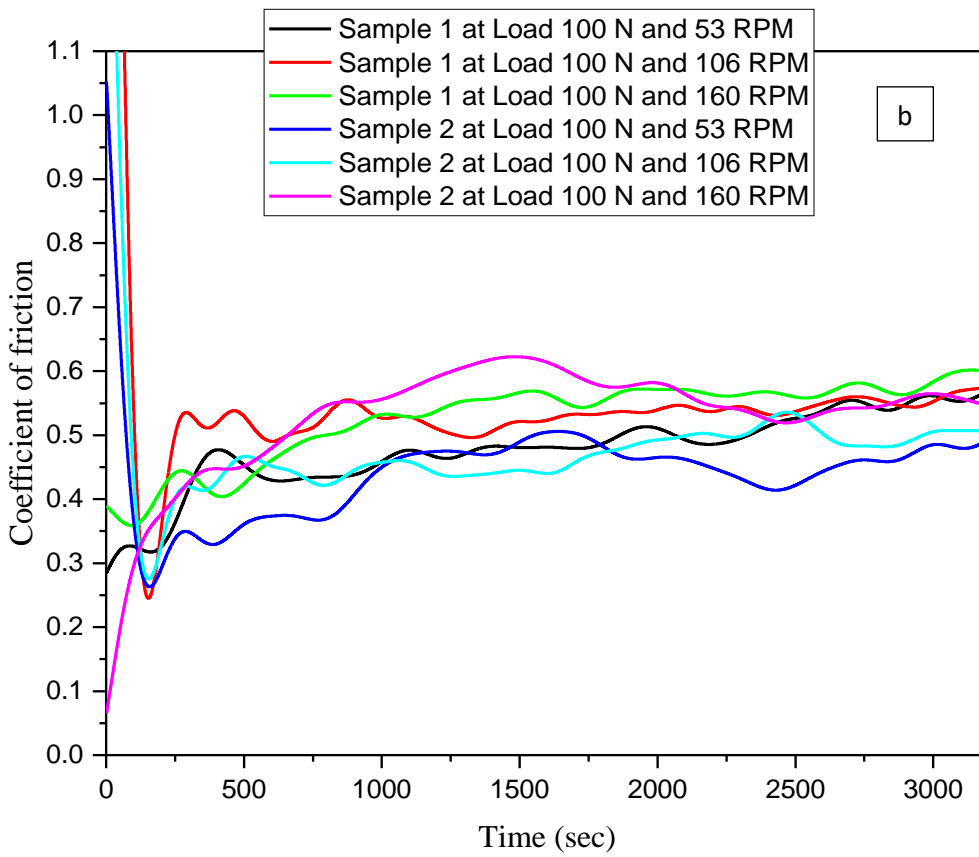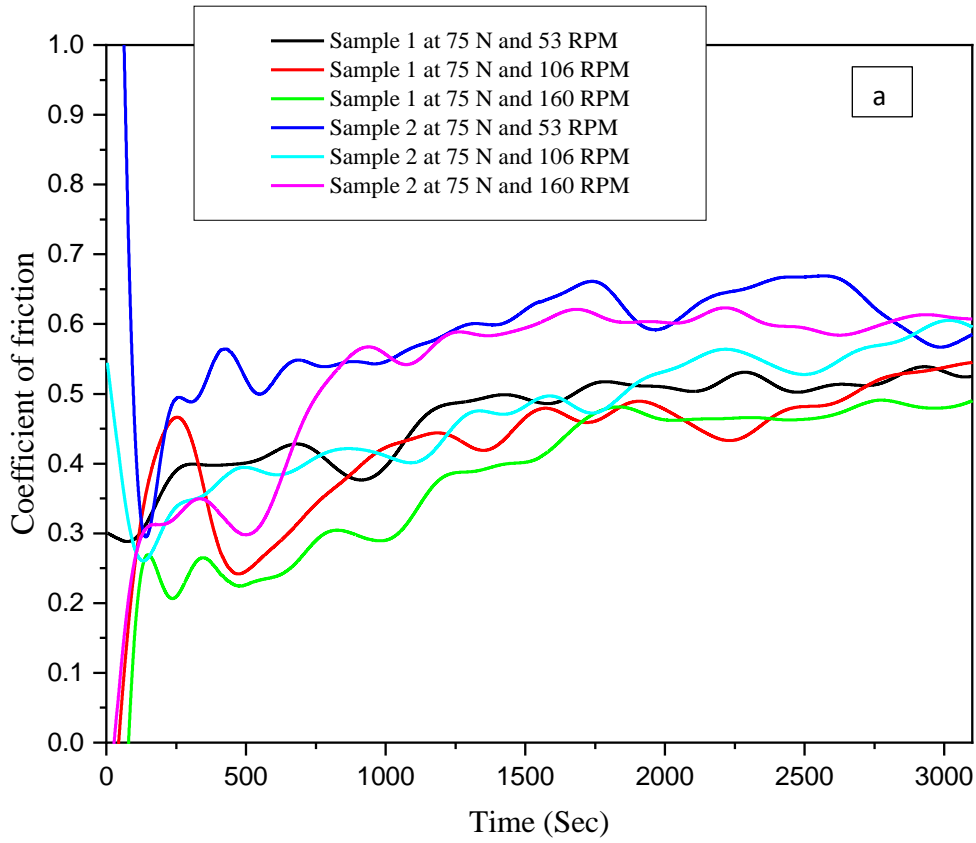
Figure 5.23: Friction behavior with varying speed at (a) 75N and (b) 100N load.

Figure 5.24 (a-c) shows the variation in friction with change in load at given speed. It is observed from the figure that as the load increases from 50 N to 75 N followed by 100 N, the COF increases as 0.470, 0.499, and 0.569 respectively in case of sample-1 pins, whereas in case of sample-2 pin sample the similar pattern has been recorded, as the load increase the COF increase. The value of COF has recorded as 0.464, 0.472, and 0.476 at 50N, 75N, and 100 N respectively. The average value of Coefficient of friction is 0.512 at 106 RPM with varying load from 50 N to 100 N in case of sample-1 pin, whereas at the same parameters for the three holes pin the value of COF has been recorded as 0.470. Approximately 8 % lower COF has observed while change in concentration of the solder materials from sample-1 pins to sample-2 pins.
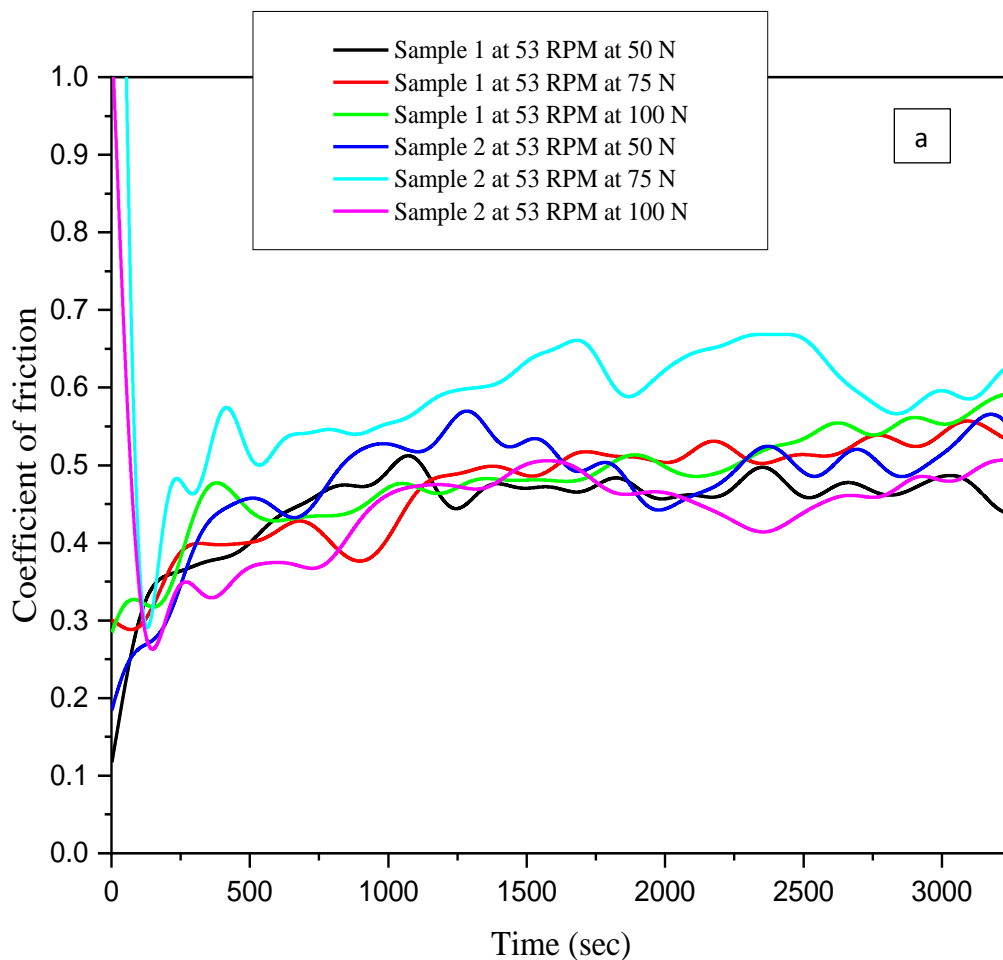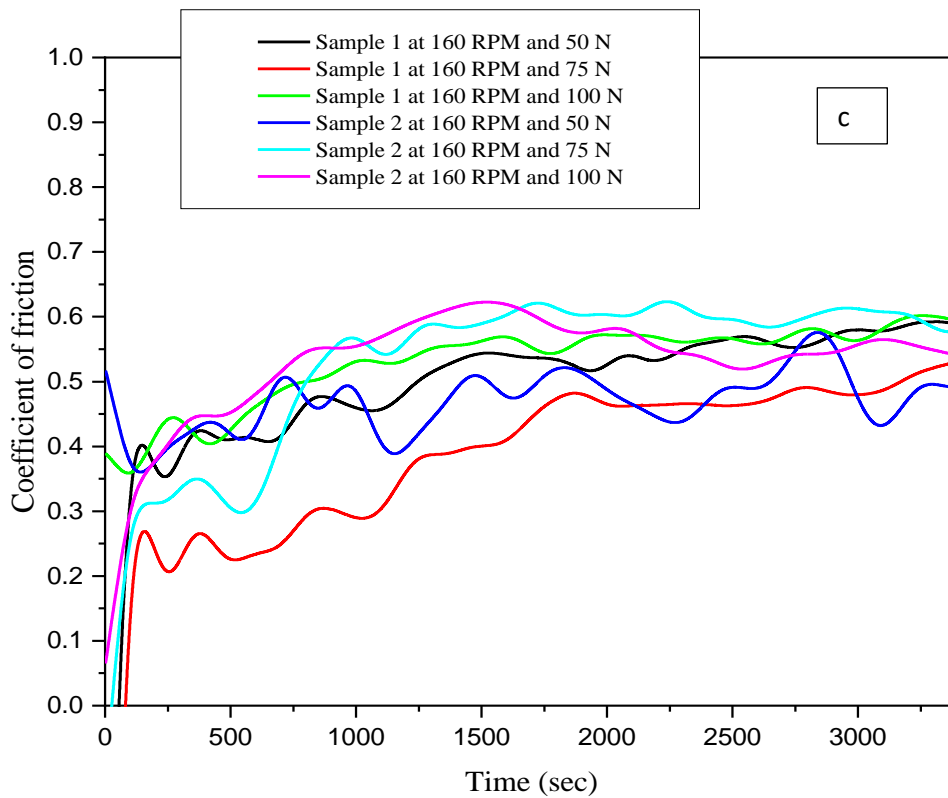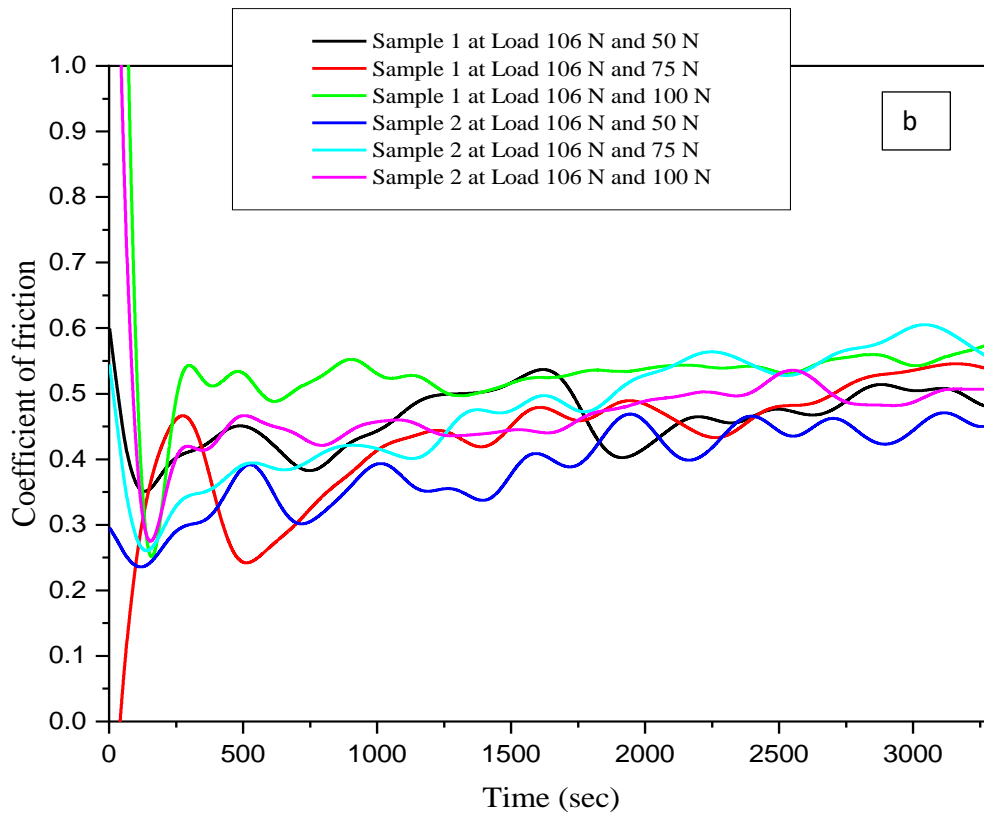
Figure 5.24: Friction behavior with varying load at (a) 53RPM, (b) 106RPM and (c) 160RPM

5.4.2. Influence of sliding distance

The influence of sliding distance on the coefficient of friction observed at the end of the test for two distinct loads is shown in figure 5.25 (a-c). It is observed from the figure 5.25 (c) that the pins with three holes have slightly lower friction values as compared to pins with two holes at 100 N load and longer sliding distance. The reduction in value of COF is observed as 12%, 16% and 12% respectively at 53RPM, 106RPM and 160RPM.
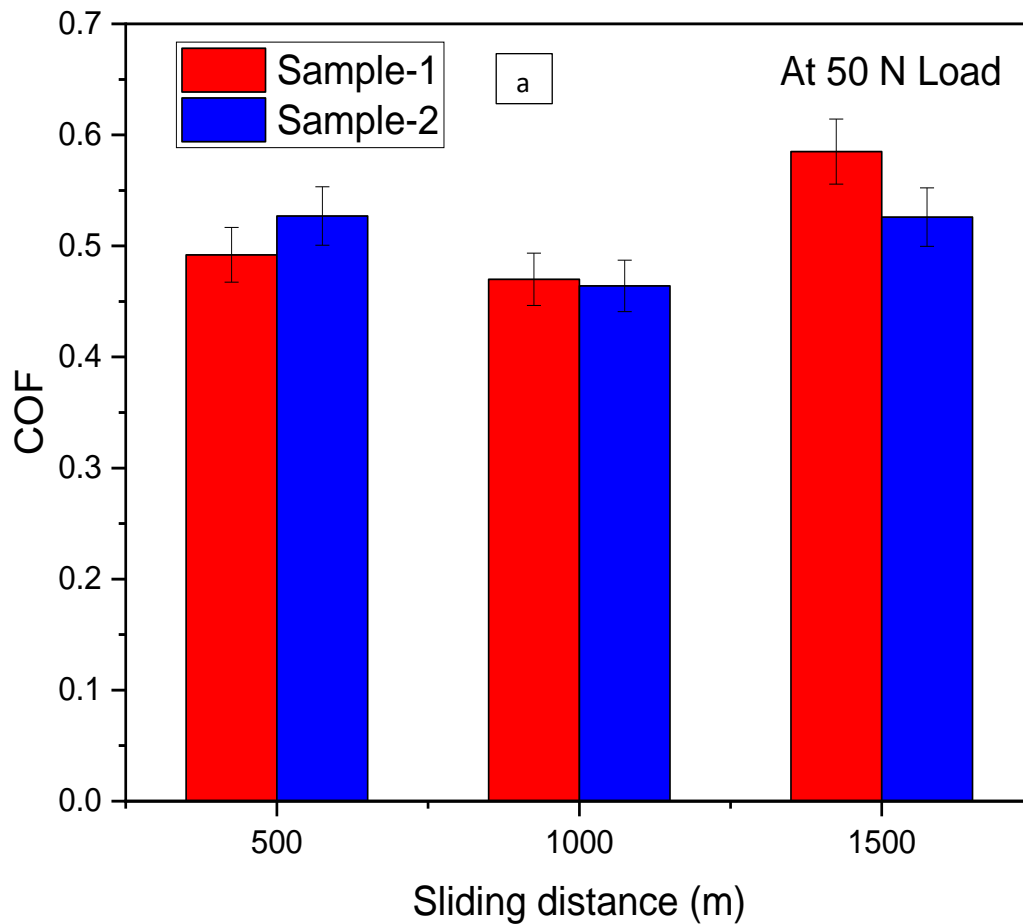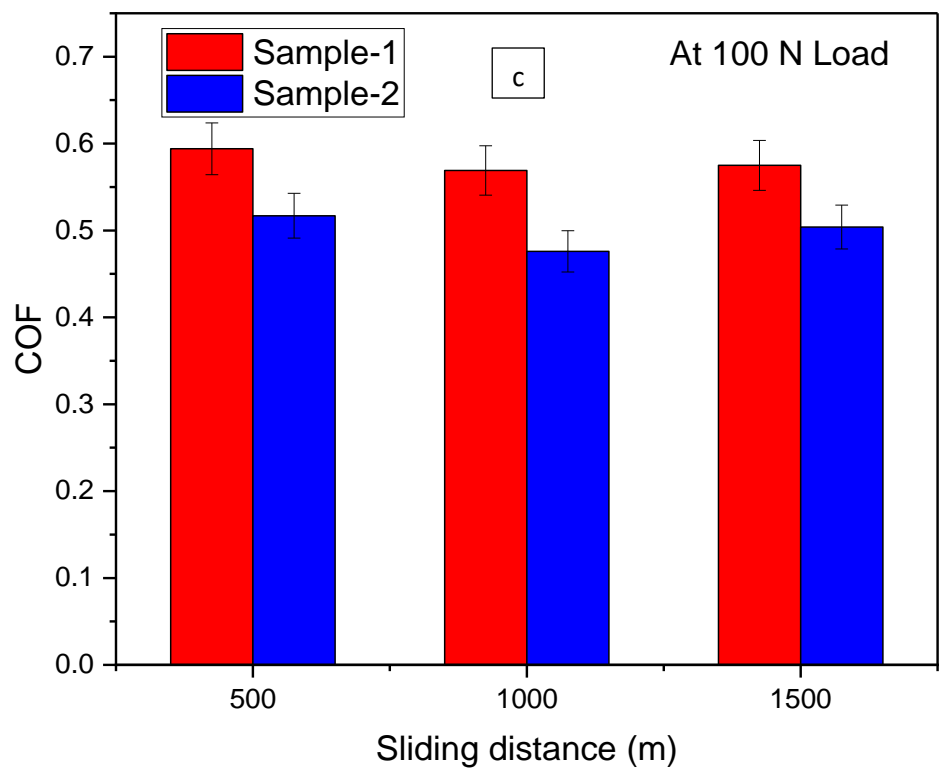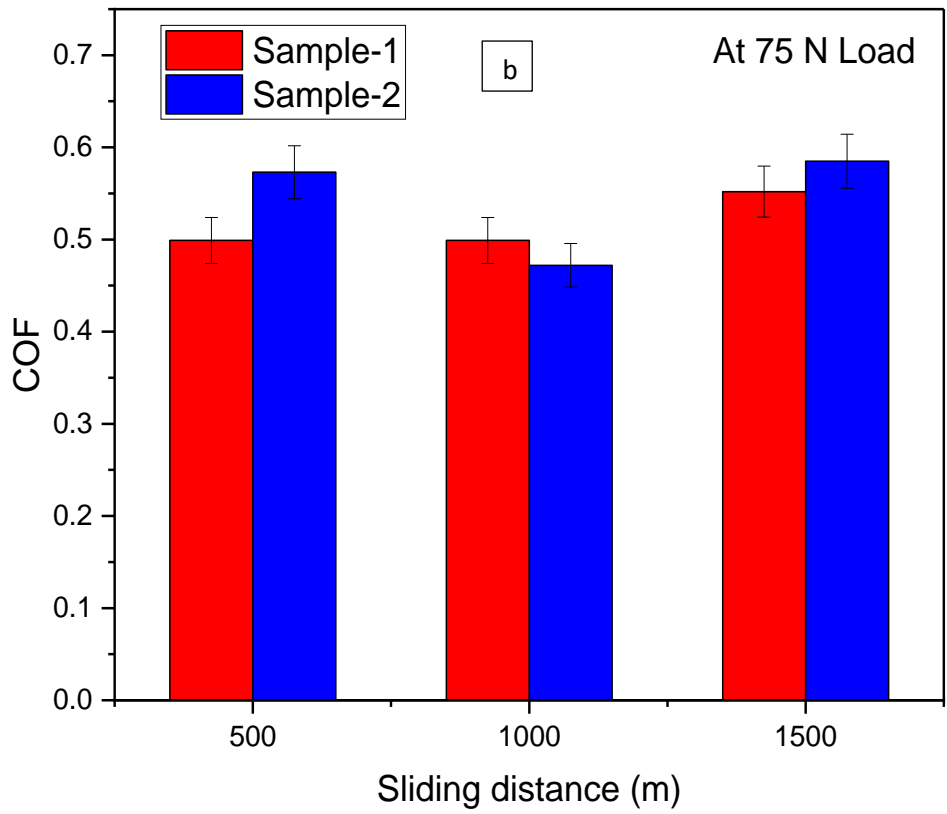
Figure 5.25: Influence of sliding distance on friction with varying speed at applied load of (a) 50N, (b) 75N and (c) 100N

5.4.3. Weight loss

Weight loss has been measured to understand the wear behavior in the developed materials. A comparative assessment in wear behavior has been made between the sample-1 and sample-2 pins. As the rollers were made up of EN-31 steel relatively harder than the pin material, no measurable wear is observed on the rollers. The influence of applied load and the speed on wear behavior of the developed sample-1 and sample-2 test pins has been analyzed. Figure 5.26 (a, b) shows the weight loss of the pins for different speeds at an applied load of 50N and 75N. It is observed from the figure that the weight loss due to wear is consistently higher in case of sample-2 when compared with sample-1 pins irrespective of the applied load.
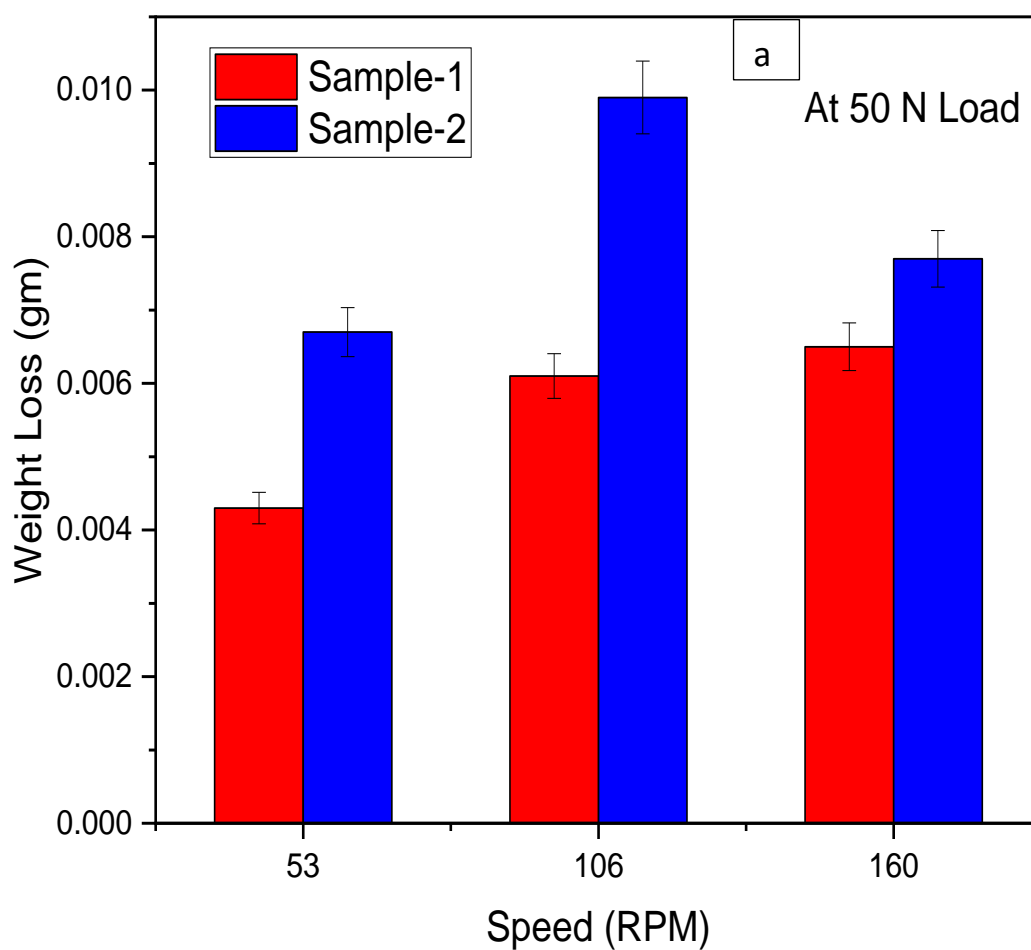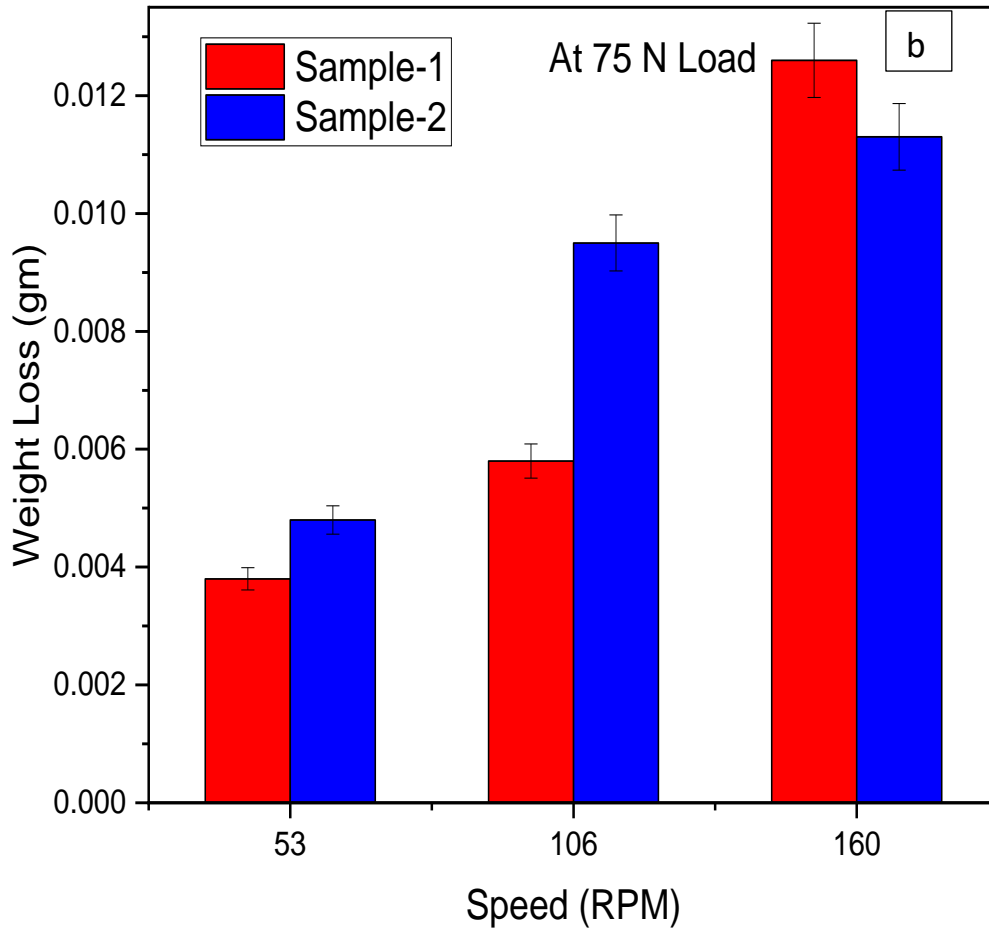
Figure 5.26: Wear behavior of the developed samples at applied load of (a) 50N and (b) 75N.

Further it is observed that the weight loss increases with increase in speed in case of sample-1 pins. However, in case of sample-2 pins the weight loss increases initially but at higher speeds slightly lesser weight loss is observed. Such a behavior can be attributed due formation of self-lubricating film of ηSiC and GRN on the surface of the pins. This ηSiC and GRN layer not only helps in reducing the wear but also reduces the contact friction. The increase in wear in case of sample-2 pins as compared to sample-1 pins is to the order of 55% at lower speeds of 53 rpm and 20% at higher speeds of 160 rpm. The influence of load on the wear of developed pins at the speeds of 106 RPM and 160RPM is shown in figure 5.27 (a, b). It is observed from the figure 5.27 (a) that the value of wear increases with increase in load from 50N to 100N. While comparing wear in both the samples, sample-2 pins show higher wear rate. Approximately 62% higher wear has been observed in sample-2 pins at 50N load and 63% higher wear at 75N load. Similarly, 35% higher wear values have been observed in sample-2 pins. This behavior can be accounted to the increase in contact area between the roller and pins

at higher loads. Figure 5.27(b) shows the wear at 160 rpm, where both the sample shows increase in wear with increase in load. However, at 160 RPM with increase in load the sample-2 specimens show lower wear as compared to sample-1 pins. Approximately 10 % lower wear has been observed at 75N load with 160 RPM, whereas 29 % lower value has been observed at 100 N with 160 RPM. This behavior can be attributed to the increase in contact area between pins and roller.
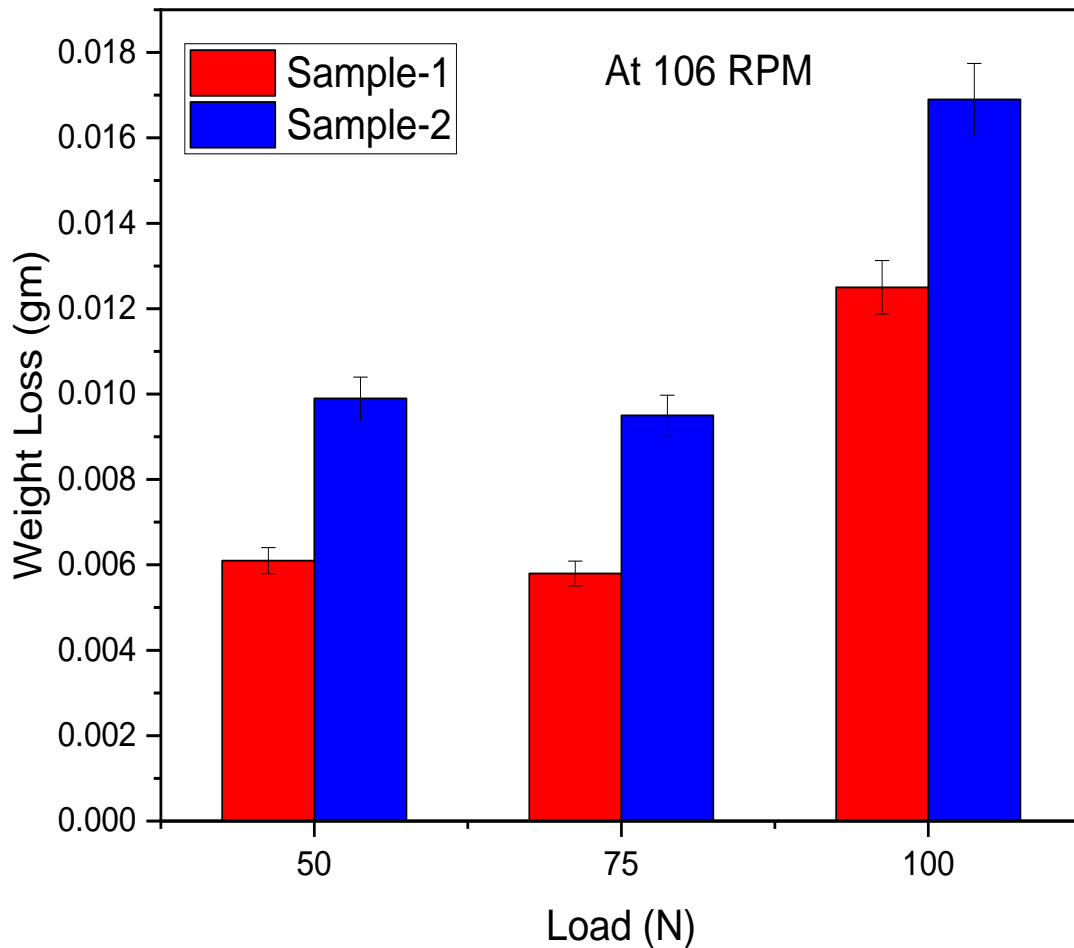
Figure 5.27: Wear behavior of the developed samples at (a) 106 RPM
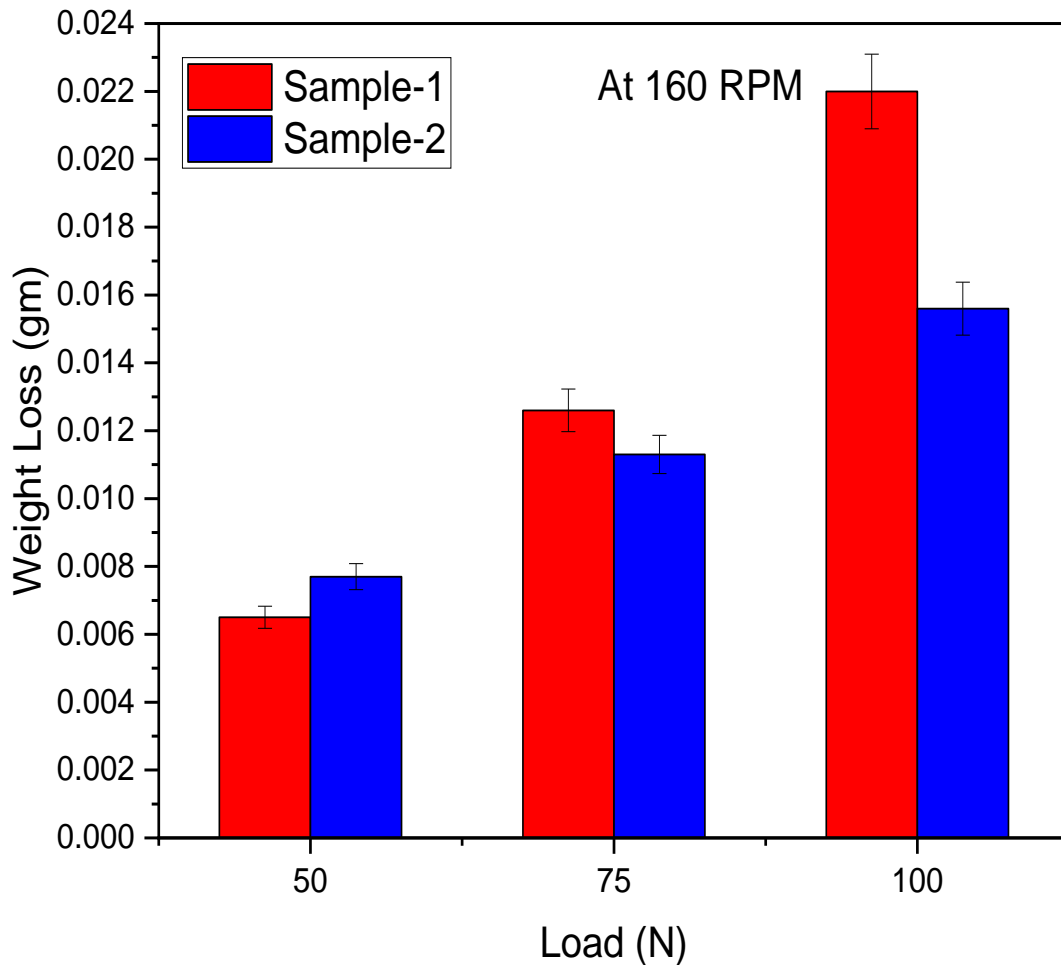
Figure 5.27(b). Wear behavior of the developed samples at (b) 160 RPM

From the figure, the grooves, eroded debris, and delamination can be seen clearly. Due to significant work hardening in the localized region, a large number of dislocations are formed and stacked up during wear testing. This phenomenon starts fissures at the subsurface level, which spread to the surface and cause the surface layer to delaminate. Figure 5.28(a-b) shows the worn-out surface of sample-1 pin. The worn surface show grooves and delamination, this is attributed because, the surface has low hardness and unformed ηSiC has delaminated from the Al-matrix and wear took place. Figure 5.28(c-d) depicts the worn-out surface of sample-2 pin, as well as the morphology of the grooves on the worn surface along the sliding direction. The abrasion component of the wear process is shown by deep grooves. In the case of unreinforced produced Al5086 alloy, both adhesion and abrasion wear mechanisms are present. However, the increased hardness caused by substantial grain refinement precludes surface delamination, as evidenced by the lower size of produced debris (Fig. 5.28d).
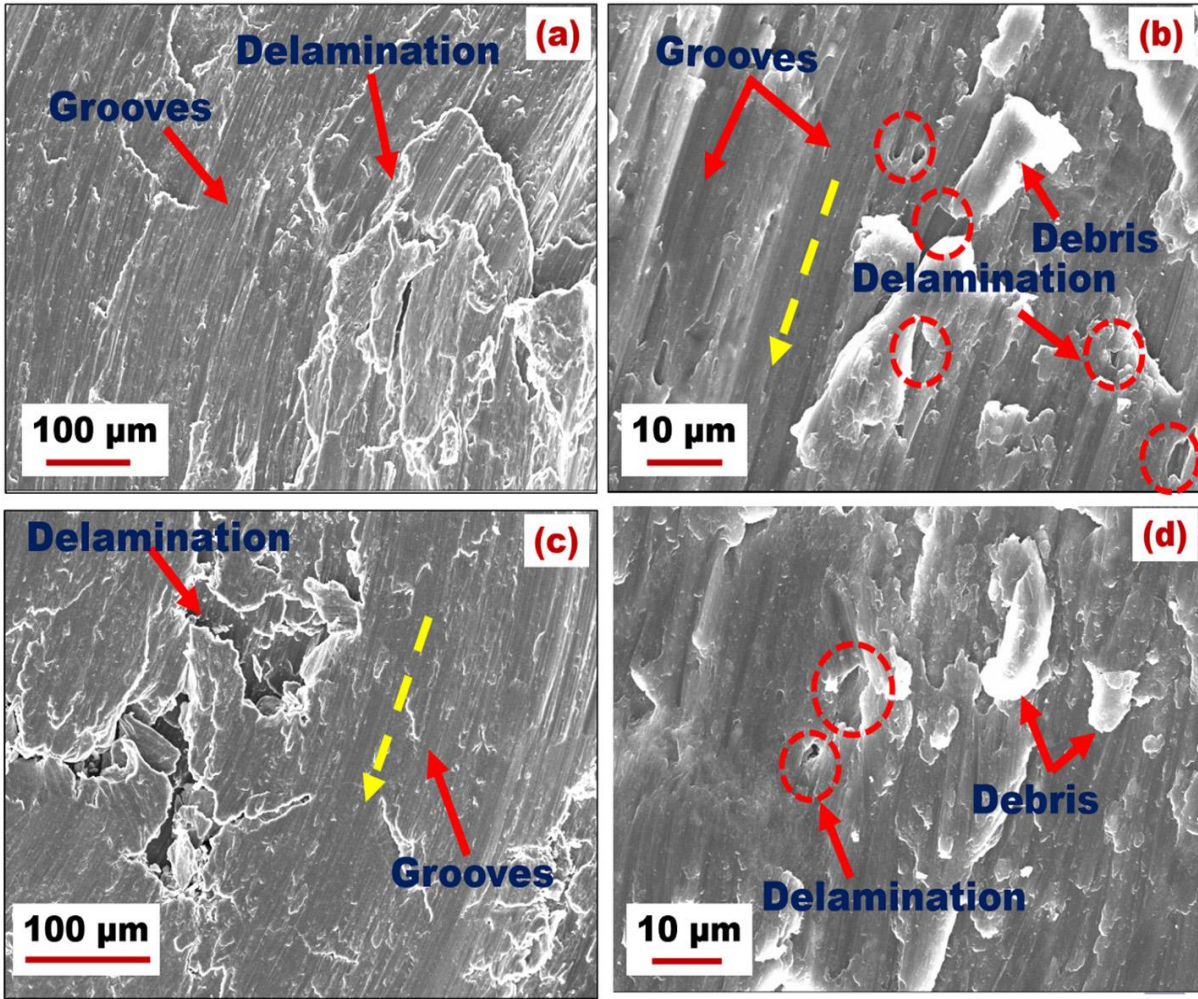
Figure 5.28: Worn out Surfaces of Sample-1 and Sample-2 pins

Table 5.13 presents the information on the width of the wear track observed on the samples at different operating conditions. It is observed that the width of the track increases with increase in speed at a given load. Initially at 50N load, the track width of the sample-1 pins has been measured as 4.180 mm. Whereas in case of sample-2 pin it is measured as 4.101 mm. As the speed increase from 53 RPM to 160 RPM, at a given load the track width increases from 4.180 mm to 5.337 mm in sample-1 pins. Similarly in the case of sample-2 pins, the track width has been increased from 4.101 mm to 4.465 mm. Similar trend has been observed at 75N load as well as 100N load where track width increased with increase in RPM. However, the track width observed in sample-2 pins are smaller than that observed in sample-1 pins. Approximately 5-10 % smaller values have been observed in the case of sample-2 pins as compared to sample-1 pins.

Table 5.13: Track width on the sample at various operating conditions

Sr. No	Operating Condition		Track Width (mm)		Weight loss (gm.)	
	Load (N)	Speed (RPM)	Sample-1	Sample-2	Sample-1	Sample-2
1	50	53	4.180	4.101	0.0043	0.0067
2	50	106	4.102	4.521	0.0061	0.0099
3	50	160	5.337	4.465	0.0065	0.0077
5	75	53	4.054	4.101	0.0038	0.0048
4	75	106	4.202	3.311	0.0058	0.0095
6	75	160	4.676	4.165	0.0126	0.0113
7	100	53	5.380	4.689	0.0112	0.0092
8	100	106	5.384	5.121	0.0113	0.0169
9	100	160	5.454	5.421	0.0156	0.0156

<div align="right">**CHAPTER-6**</div>

CONCLUSIONS AND SCOPE FOR FUTURE RESEARCH WORK

In the present research work, the application and capability of friction stir processing as an innovative surface engineering technique has been investigated.

6.1. Conclusions

In the present research work, Al5086-GRN-ηSiC hybrid surface composite has been developed using friction stir processing technique. A detailed microstructural characterization, mechanical properties analysis, and tribological properties were studied. The major conclusions can be drawn as below:

- The rotation speed (1800 RPM) and feed/transvers speed (40 mm/min) were found the best optimal condition to synthesis best quality and defect free Al5086-GRN-ηSiC hybrid surface composite. The GRN and ηSiC reinforcements were homogeneously distributed in the Al-matrix.

- The grain size of has been drastically reduced in the processed zone from 23 to 6 µm. The SEM and TEM morphology analysis revealed that the diphasic nano-mixture cluster of ηSiC and GRN in the range (100-200 nm) were formed.

- HR-TEM investigated showed that GRP co-exist in multi-layer of atoms in Al-matrix owing to mechanical exfoliation of graphite, which improved the mechanical properties of composite. The Al5086-GRN-ηSiC hybrid composite exhibit hardness value 198 HV, tensile strength 209 MPa (385±5 MPa as an exceptional result in case of APF-FSP), and elastic modulus (172 GPa).

- Therefore it has been observed that the hardness value has increased by 135.71% and tensile strength initially decreased by 14.69%, then increased up to 57.14% with APF-FSP (as an exception) and elastic modulus has increased by 129.33%.

6.2. Scope for Future Research Work

Analysis of the results acquired from the current work advocates quite a few possible extensions to the research. A few of them are listed:

1. Very little work has been reported yet to explore the effect of shape of friction processing tool tip on the surface integrity of materials.

2. Apart from the use of microsized and nano-scale alloyed powder as reinforcement can be used to improve the surface properties of materials.

3. Coating/cladding of functionalized layer can be developed by friction stir processing on Magnesium and titanium-based materials for biomedical applications.

4. Finite element modeling and analysis for friction stir processing can be done in order to understand the stress developed during processing. There is ample scope for the modeling and simulation of FSP process.

References

[1] Nagavally RR. Composite materials-history, types, fabrication techniques, advantages, and applications. Int. J. Mech. Prod. Eng. 2017;5(9):82-7.

[2] Khalifa TA, Mahmoud TS. Elevated temperature mechanical properties of Al alloy AA6063/SiCp MMCs. InProceedings of the world congress on engineering 2009 Jul 1 (Vol. 2, pp. 1-3). WCE 2009 London, UK.

[3] Clyne TW, Hull D. An introduction to composite materials. Cambridge university press; 2019 Jul 11.

[4] Found MS, editor. Experimental Techniques and Design in Composite Materials 4: Proceedings of the 4th Seminar on Experimental Techniques and Design in Composite Materials, Sheffield, UK, 1-2 September 1998. Balkema; 2002.

[5] Krawczak P, Maffezzoli A. Advanced thermoplastic composites and manufacturing processes. Frontiers in Materials. 2020 Jul 9;7:166.

[6] Adamson MJ. Thermal expansion and swelling of cured epoxy resin used in graphite/epoxy composite materials. Journal of materials science. 1980 Jul;15:1736-45.

[7] Drzal LT. The effect of polymeric matrix mechanical properties on the fiber-matrix interfacial shear strength. Materials Science and Engineering: A. 1990 Jun 15;126(1-2):289-93.

[8] Madhukar MS, Drzal LT. Fiber-matrix adhesion and its effect on composite mechanical properties. III. Longitudinal (0) compressive properties of graphite/epoxy composites. Journal of composite materials. 1992 Mar;26(3):310-33.

[9] Subramanian SU. Effect of fiber/matrix interphase on the long term behavior of cross-ply laminates. Ph. D. Thesis. Virginia Polytechnic Inst. and State Univ., Blacksburg, VA (United States); 1994 Jan 1.

[10] Liu XH, Moran PM, Shih CF. The mechanics of compressive kinking in unidirectional fiber reinforced ductile matrix composites. Composites Part B: Engineering. 1996 Jan 1;27(6):553-60.

[11] Shen CH, Springer GS. Moisture absorption and desorption of composite materials. Journal of composite materials. 1976 Jan;10(1):2-0.

[12] Miracle DB, Donaldson SL. Introduction to composites. ASM handbook. 2001;21:3-17.

[13] https://nptel.ac.in/content/storage2/courses/105108124/pdf/Lecture_Notes/LNm1.pd

[14] https://onlinelibrary.wiley.com/doi/pdf/10.1002/9781118985960.meh110#:~:text=Co mposites%20are%20usually%20classified%20by cmcCtCn.

[15] Strong AB. Fundamentals of composites manufacturing: materials, methods and applications. Society of manufacturing engineers; 2008.

[16] https://www.modorplastics.com/plastics-learning-center/thermoset-vs-thermoplastics/.

[17] Krenkel W, Reichert F. Design objectives and design philosophies, interphases and interfaces in fiber-reinforced CMCs.

[18] Chawla KK, Chawla KK. Metal matrix composites. Springer New York; 1998.

[19] Bunsell AR, Joannès S, Thionnet A. Fundamentals of fibre reinforced composite materials. CRC Press; 2021 Mar 28.

[20] Staab G. Laminar composites. Butterworth-Heinemann; 2015 Aug 11.

[21] Withers PJ. Elastic and thermoelastic properties of brittle matrix composites.

[22] https://123dok.com/document/zw13r10q-komposit-matrix-logam-metal-matrix-composite.html.

[23] Wang R-M, Zheng S-R, Zheng Y-P. 2 - Reinforced materials. In: Wang R-M, Zheng S-R, Zheng Y-P, editors. Polymer Matrix Composites and Technology: Woodhead Publishing; 2011. p. 29-548.

[24] Drzal LT, Rich MJ, Lloyd PF. Adhesion of graphite fibers to epoxy matrices: I. The role of fiber surface treatment. The Journal of Adhesion. 1983 Jul 1;16(1):1-30.

[25] Ghorbel I, Valentin D. Hydrothermal effects on the physico-chemical properties of pure and glass fiber reinforced polyester and vinylester resins. Polymer Composites. 1993 Aug;14(4):324-34.

[26] Breiman U, Aboudi J, Haj-Ali R. Semianalytical compressive strength criteria for unidirectional composites. Journal of Reinforced Plastics and Composites. 2018 Feb;37(4):238-46.

[27] Quigley B, Abbaschian G, Wunderlin R, Mehrabian R. A method for fabrication of aluminum-alumina composites. Metallurgical Transactions A. 1982;13(1):93-100.

[28] Wallenberger FT, Nordine PC. Strong, small diameter, boron fibers by LCVD. Materials Letters. 1992 Aug 1;14(4):198-202.

[29] Johnson SM, Brittain RD, Lamoreaux RH, Rowcliffe DJ. Degradation mechanisms of silicon carbide fibers. Journal of the American Ceramic Society. 1988 Mar;71(3):C-132.

[30]   Wang YY, Wei QH, Wang HS, Shao CT, Cheng HH, Zhang QL. Preparation and Properties of Acupuncture Quartz Fiber Reinforced Quartz-Based Composites. Key Engineering Materials. 2016 Aug 11;697:419-22.

[31]   Kainer KU. Basics of metal matrix composites. Metal Matrix Composites: Custom-made Materials for Automotive and Aerospace Engineering. 2006 Jan 9:1-54.

[32]   Fu SY, Feng XQ, Lauke B, Mai YW. Effects of particle size, particle/matrix interface adhesion and particle loading on mechanical properties of particulate–polymer composites. Composites Part B: Engineering. 2008 Sep 1;39(6):933-61.

[33]   https://www.pacificaerospacecorp.com/what-are-the-pros-and-cons-of-composite-materials/.

[34]   https://www.intechopen.com/chapters/63509.

[35]   Gay D. Composite materials: design and applications. CRC press; 2022 Aug 31..

[36]   Dahal RK, Acharya B, Saha G, Bissessur R, Dutta A, Farooque A. Biochar as a filler in glassfiber reinforced composites: Experimental study of thermal and mechanical properties. Composites Part B: Engineering. 2019 Oct 15;175:107169.

[37]   Minsch N, Herrmann FH, Gereke T, Nocke A, Cherif C. Analysis of filament winding processes and potential equipment technologies. Procedia CIRP. 2017 Jan 1;66:125-30.

[38]   Quanjin M, Rejab MR, Kaige J, Idris MS, Harith MN. Filament winding technique, experiment and simulation analysis on tubular structure. InIOP conference series: materials science and engineering 2018 Apr (Vol. 342, No. 1, p. 012029). IOP Publishing.

[39]   https://www.tranpak.com/faq/what-is-compression-molding/.

[40]   Kendall KN, Rudd CD, Owen MJ, Middleton V. Characterization of the resin transfer moulding process. Composites Manufacturing. 1992 Jan 1;3(4):235-49.

[41]   Mallick PK. Thermoset matrix composites for lightweight automotive structures. InMaterials, Design and Manufacturing for Lightweight Vehicles 2021 Jan 1 (pp. 229-263). Woodhead Publishing.

[42]   Advani SG, Hsiao KT, editors. Manufacturing techniques for polymer matrix composites (PMCs). Elsevier; 2012 Jul 18.

[43]   Aynalem GF. Processing methods and mechanical properties of aluminium matrix composites. Advances in Materials Science and Engineering. 2020 Sep 18;2020:1-9.

[44]   Whittaker D. Powder processing, consolidation and metallurgy of titanium. Powder Metallurgy. 2012 Feb 1;55(1):6-10.

[45]   Lee H-S. 10 - Diffusion bonding of metal alloys in aerospace and other applications. In: Chaturvedi M, editor. Welding and Joining of Aerospace Materials (Second Edition): Woodhead Publishing; 2021. p. 305-27.

[46]   Dini JW. Electroplating, electroless plating and electroforming. Lawrence Livermore National Lab., CA (USA); 1990 Feb 1.

[47]   Alam SN, Kumar L. Mechanical properties of aluminium based metal matrix composites reinforced with graphite nanoplatelets. Materials Science and Engineering: A. 2016 Jun 14;667:16-32.

[48]   Seetharaman S, Gupta M. Fundamentals of metal matrix composites.

[49]   Singh L, Singh B, Saxena KK. Manufacturing techniques for metal matrix composites (MMC): an overview. Advances in Materials and Processing Technologies. 2020 Apr 2;6(2):441-57.

[50]   Ma ZY, Mishra RS, Mahoney MW. Superplastic deformation behaviour of friction stir processed 7075Al alloy. Acta materialia. 2002 Oct 9;50(17):4419-30.

[51]   Mishra RS, Mahoney MW, McFadden SX, Mara NA, Mukherjee AK. High strain rate superplasticity in a friction stir processed 7075 Al alloy. Scripta materialia. 1999 Dec 31;42(2):163-8.

[52]   Mishra RS, Ma ZY, Charit I. Friction stir processing: a novel technique for fabrication of surface composite. Materials Science and Engineering: A. 2003 Jan 20;341(1-2):307-10.

[53]   Ma ZY. Friction stir processing technology: a review. Metallurgical and materials Transactions A. 2008 Mar;39:642-58.

[54]   Thomas WM, Nicholas ED, Kallee SW. Friction based technologies for joining and processing. InTMS friction stir welding and processing conference 2001 Nov 4 (pp. 1-8).

[55]   Powell HJ, Wiemer K. Joining technology for high volume manufacturing of lightweight vehicle structures. In29th International Symposium on Automotive Technology & Automation 1996 Jun (pp. 1-6).

[56]   Thomas WM, Nicholas ED. Friction stir welding for the transportation industries. Materials & design. 1997 Dec 1;18(4-6):269-73.

[57]   Mishra RS, Mahoney MW. Friction stir processing: a new grain refinement technique to achieve high strain rate superplasticity in commercial alloys. InMaterials Science Forum 2001 Jan 15 (Vol. 357, pp. 507-514). Trans Tech Publications Ltd.

[58]   Mishra RS, Ma ZY, Charit I. Friction stir processing: a novel technique for fabrication of surface composite. Materials Science and Engineering: A. 2003 Jan 20;341(1-2):307-10.

[59]   Thomas WM, Nicholas ED. Emerging friction joining technology for stainless steel and aluminium applications"Productivity beyond 2000': IIW Asian Pacific Welding Congress. Auckland, New Zealand. 1996 Feb.

[60]   Rhodes CG, Mahoney MW, Bingel WH, Calabrese M. Fine-grain evolution in friction-stir processed 7050 aluminum. Scripta materialia. 2003 May 1;48(10):1451-5.

[61]   Cabibbo M, Meccia E, Evangelista E. TEM analysis of a friction stir-welded butt joint of Al–Si–Mg alloys. Materials Chemistry and Physics. 2003 Aug 28;81(2-3):289-92.

[62]   Sato YS, Urata M, Kokawa H, Ikeda K, Enomoto M. Retention of fine grained microstructure of equal channel angular pressed aluminum alloy 1050 by friction stir welding. Scripta Materialia. 2001 Jul 13;45(1):109-14.

[63]   Reynolds AP, Tang W. Alloy, tool geometry, and process parameter effects on friction stir weld energies and resultant FSW joint properties. Friction stir welding and processing. 2001 Nov:15-23.

[64]   Kwon YJ, Shigematsu I, Saito N. Mechanical properties of fine-grained aluminum alloy produced by friction stir process. Scripta materialia. 2003 Oct 1;49(8):785-9.

[65]   Charit I, Ma ZY, Mishra RS. High strain rate superplasticity in friction stir processed aluminum alloys.

[66]   Berbon PB, Bingel WH, Mishra RS, Bampton CC, Mahoney MW. Friction stir processing: a tool to homogenize nanocomposite aluminum alloys. Scripta Materialia. 2001 Jan 5;44(1):61-6.

[67]   Thomas, W.M., Nicholas, E.D., Smith, S.D., "Friction stir welding- tool developments", Aluminum Joining Symposiums, 2001 TMS Annual Meeting, 11-15. R. A.

[68]   Prado RA, Murr LE, Soto KF, McClure JC. Self-optimization in tool wear for friction-stir welding of Al 6061+ 20% Al2O3 MMC. Materials science and engineering: A. 2003 May 25;349(1-2):156-65.

[69]   Mishra RS, Mahoney MW, McFadden SX, Mara NA, Mukherjee AK. High strain rate superplasticity in a friction stir processed 7075 Al alloy. Scripta materialia. 1999 Dec 31;42(2):163-8.

[70]   Ma ZY, Mishra RS, Mahoney MW. Superplastic deformation behaviour of friction stir processed 7075Al alloy. Acta materialia. 2002 Oct 9;50(17):4419-30.

[71]   Charit I, Mishra RS, Mahoney MW. Multi-sheet structures in 7475 aluminum by friction stir welding in concert with post-weld superplastic forming. Scripta Materialia. 2002 Nov 1;47(9):631-6.

[72]   Ma ZY, Mishra RS, Mahoney MW, Grimes R. High strain rate superplasticity in friction stir processed Al–Mg–Zr alloy. Materials Science and Engineering: A. 2003 Jun 25;351(1-2):148-53.

[73]   Mahoney, M; Mishra, R.S; Nelson, T; Flintoff, J; Islamgaliev, R and Hovansky,Y. "High strain rate, Thick section superplasticity created via friction stir processing", Friction Stir welding and Processing, , 2001, Pages 183- 194

[74]   Chow KK, Chan KC. The cavitation behavior of a coarse-grained Al5052 alloy under hot uniaxial and equibiaxial tension. Materials Letters. 2001 Jun 1;49(3-4):189-96.

[75]   Chow KK, Chan KC. Effect of stress state on cavitation and hot forming limits of a coarse-grained Al5052 alloy. Materials letters. 2002 Jan 1;52(1-2):62-8.

[76]   Moustafa EB, Khalil AM, Ahmed HM, Hefni M, Mosleh AO. Microstructure, hardness, and wear behavior investigation of the surface nanocomposite metal matrix reinforced by silicon carbide and alumina nanoparticles. J. Miner. Met. Mater. Eng. 2021;7:57-62.

[77]   Hari D, Devi NN, Prabhakaran R, Sutharsan M, Balamurugan KG. Microstructural Analysis of Friction Stir Processed Al5083 Alloy. InRecent Advances in Manufacturing, Automation, Design and Energy Technologies: Proceedings from ICoFT 2020 2022 (pp. 245-252). Springer Singapore.

[78]   Ajani A, Gilani H, Islam S, Khandoker N, Mazid AM. Fabrication of CNT-Reinforced 6061 Aluminium Alloy Surface Composites by Friction Stir Processing. Jom. 2021 Dec;73(12):3718-26.

[79]   Maji P, Nath RK, Karmakar R, Madapana D, Meitei RB, Ghosh SK. Wear and corrosion behavior of Al7075 matrix hybrid composites produced by friction stir processing: Optimization of process parameters. Jom. 2021 Dec;73:4397-409.

[80]   Shaik B, Gowd GH, Prasad BD, Ali PS. Parametric optimization by using friction stir processing. InAIP Conference Proceedings 2021 Oct 18 (Vol. 2395, No. 1). AIP Publishing.

[81]   Liew KW, Chung YZ, Teo GS, Kok CK. Effect of Tool Pin Geometry on the Microhardness and Surface Roughness of Friction Stir Processed Recycled AA 6063. Metals. 2021 Oct 25;11(11):1695.

[82]   Akbari M, Asadi P. Effects of different cooling conditions on friction stir processing of A356 alloy: numerical modeling and experiment. Proceedings of the Institution of Mechanical Engineers, Part C: Journal of Mechanical Engineering Science. 2022 Apr;236(8):4133-46.

[83]   Boopathi S, Thillaivanan A, Pandian M, Subbiah R, Shanmugam P. Friction stir processing of boron carbide reinforced aluminium surface (Al-B4C) composite: Mechanical characteristics analysis. Materials Today: Proceedings. 2022 Jan 1;50:2430-5.

[84]   Patel V, Li W, Andersson J, Yang X. A novel approach to measure three-dimensional surface topography for stationary shoulder friction stir processing. Journal of Materials Research and Technology. 2021 Nov 1;15:5608-14.

[85]   Raja R, Jannet S, Allen Varughese LG, Ratna S. Tensile Behaviour of Aluminium Oxide and Zirconium Dibromide Reinforced Aluminum Alloy 6063 Surface Composites.

[86]   Mostafavi M, Taghiabadi R, Jafarzadegan M. Optimizing the mechanical properties of Al-4.5 Cu-xSi alloys through multi-pass friction stir processing and post-process aging. Archives of Civil and Mechanical Engineering. 2021 Nov 17;22(1):11.

[87]   Ross PJ. Taguchi techniques for quality engineering: loss function, orthogonal experiments, parameter and tolerance design.

[88]   Pradeep S, Jain VK, Muthukumaran S, Kumar R. Microstructure and texture evolution during multi-pass friction stir processed AA5083. Materials Letters. 2021 Apr 1;288:129382.

[89]   Basak AK, Pramanik A, Prakash C. Deformation and strengthening of SiC reinforced Al-MMCs during in-situ micro-pillar compression. Materials Science and Engineering: A. 2019 Aug 19;763:138141.

[90]   Podržaj P, Jerman B, Klobčar D. Welding defects at friction stir welding. Metalurgija. 2015 Apr 1;54(2):387-9.

[91]   Kim YG, Fujii H, Tsumura T, Komazaki T, Nakata K. Three defect types in friction stir welding of aluminum die casting alloy. Materials Science and Engineering: A. 2006 Jan 15;415(1-2):250-4.

[92]   Rodriguez RI, Jordon JB, Allison PG, Rushing T, Garcia L. Microstructure and mechanical properties of dissimilar friction stir welding of 6061-to-7050 aluminum alloys. Materials & Design. 2015 Oct 15;83:60-5.

[93]   Al-Moussawi M, Smith AJ. Defects in friction stir welding of steel. Metallography, Microstructure, and Analysis. 2018 Apr;7:194-202.

[94]   Dialami N, Cervera M, Chiumenti M. Defect formation and material flow in friction stir welding. European Journal of Mechanics-A/Solids. 2020 Mar 1;80:103912.

[95]   Mallick PK. Thermoset matrix composites for lightweight automotive structures. InMaterials, Design and Manufacturing for Lightweight Vehicles 2021 Jan 1 (pp. 229-263). Woodhead Publishing.

[96]   Mabuwa S, Msomi V. Review on friction stir processed TIG and friction stir welded dissimilar alloy joints. Metals. 2020 Jan 17;10(1):142.